The Connectivity Framework as a Tool to plan Nature Restoration Measures

A graph-theory approach to assess aquatic habitat connectivity of the Sliedrechtse Biesbosch

MSc Thesis

D.L. van Leeuwen

TU Delft Delft University of Technology

Iv-Groep

The Connectivity Framework as a Tool to plan Nature Restoration Measures

A graph-theory approach to assess aquatic habitat connectivity of the Sliedrechtse Biesbosch

by

D.L. van Leeuwen

to obtain the degree of Master of Science
at the Delft University of Technology,
to be defended publicly on Thursday March 23, 2023 at 16:00.

Student number:	4488490	
Project duration:	June 1, 2022 – March 23, 2023	
Thesis committee:	Dr. ir. B.C. van Prooijen,	TU Delft (chairman)
	Dr. ir. E. Mosselman,	TU Delft, Deltares
	Dr. ir. C.J. Sloff,	TU Delft, Deltares
	Dr. ir. L.M. Stancanelli,	TU Delft
	Ir. A.C. Briele,	Iv-Infra

TU Delft Delft University of Technology

Iv-Groep

Abstract

This study assesses the application of graph theory to examine the connectivity of aquatic habitat in the Sliedrechtse Biesbosch and preserve or improve the area's ecological value. The study addresses the relation between hydrodynamics and ecology, and evaluates different definitions of connectivity. Graph theory provides a novel and promising approach to assess connectivity in aquatic environments. With increasing availability of data, more accurate and informative analyses can be carried out, resulting in more effective designs of restoration measures. The application of graph theory in such research has, as one of its main strengths, its visual accessibility to laypersons or others without expertise in interpreting numerical model results. Furthermore, graph theory can offer both a holistic system view of a water network by evaluating the system as a whole, as well as a local view which is possible by looking at the single nodes and edges in the graph. This enables investigation of the role of individual channels within the system and the identification of vulnerable spots within the network, limiting the availability of aquatic habitat.

Graph theory is applied in various fields of research. As numerous metrics exist to examine the properties of a graph, an introduction to the most important metrics is given in this study. Adequacy of metrics is dependent on the questions posed and parameters relevant for the specific topic to be investigated. It is shown that in aquatic habitat connectivity, metrics such as betweenness centrality and bridges are indicative to obtain a general view of the network. When temporal variations play a role, as is the case in a tidal area, metrics as the number of components (NOC), the order of the largest component and the length of connected pathways (LOCOP) of the largest component are suitable to determine the connectivity. Whereas these metrics show useful in studying aquatic habitat connectivity, they may be less appropriate in connectivity studies of the same water system aiming at other fields of application, e.g. sediment connectivity.

Results show that graph theory provides a useful instrument in analyzing the aquatic habitat connectivity of the Sliedrechtse Biesbosch, which is investigated in a case study. The ease at which key nodes and edges are identified offer great possibilities for the design of nature restoration measures. In the present layout of the study area, large variation of aquatic habitat connectivity occurs based on a flow velocity fragmentation threshold of 0.3 m/s, corresponding to the maximum tolerable flow velocity for the European flounder (Platichthys flesus). Due to tidal influences in the study area, flow velocities vary continuously and the threshold flow velocity is exceeded during part of the tidal cycle. Considering the available habitat of other species gives different results depending on the tolerable flow velocities of the specific species. As is shown in this research, a combination of graph theory and numerical modelling enables the design and simulation of different nature restoration measures and system layouts to improve the aquatic habitat connectivity of the area.

The method presented in this research can be particularly useful to ecologists investigating suitable habitats for specific fish species. Also for engineers and others involved in the design of nature restoration measures, the method can be helpful since the designs of restoration measures can be evaluated considering the effect on habitat availability. The research provides an informed basis for subsequent applications of graph theory and numerical modelling to aquatic habitat connectivity. By selecting the most suitable design parameters and improvements of the network schematization, a justified decision can be made on the most effective restoration measures concerning the improvement of available habitat. Especially considering a combination of habitat preferences, such as flow velocity, water depth and turbidity, can provide proper insight in the aquatic habitat connectivity of an area for specific species.

Preface

It is with due pride and joy that I present this thesis, which marks the end of my academic career. This thesis is the final part to conclude the Master of Science studies in Hydraulic Engineering at the faculty of Civil Engineering and Geosciences of Delft University of Technology. For the past ten months I have been working on this project and it has taught me a lot, not only about the thesis topic, but also about myself. I would like to use this occasion to reflect on the past time and to thank a number of important and committed people.

I had the opportunity to conduct my graduation research at Iv-Infra, where I was supervised by Carolin Briele. Her time and commitment helped me tremendously during my research. Besides the substantive work, I was also able to experience what it is like to work at an engineering company. I would like to thank all of my colleagues at Iv for sharing their experiences and introducing me to working at an engineering firm. The pleasant working environment really contributed to the great time I had as an intern.

Furthermore, I would like to express my gratitude to the other committee members, Bram van Prooijen, Erik Mosselman, Kees Sloff and Laura Stancanelli. Although such a large committee introduced some scheduling issues considering the joint meetings, your willingness and flexibility led to a smooth process. Your insight and criticism took the research to a higher level, both during the committee meetings and the one-to-one meetings. Additionally, I would like to thank Erik and Kees for inviting me to carry out part of my research in their department at Deltares. This enabled me to solve any modelling issues quickly and accelerated the overall progress.

Finally, I would like to thank my family, my friends and my girlfriend for their support and interest during the past period. They motivated me and kept me on the right track towards graduation.

My student life in Delft has come to an end. I look back to seven and a half wonderful years and I am curious to what the future will bring!

David van Leeuwen
Utrecht, March 2023

Contents

List of Figures

List of Tables

List of Abbreviations

AHN Actueel Hoogtebestand Nederland.

CI Connectivity Index.

DCI Dendritic Connectivity Index.

FM Flexible Mesh.

GIS geographic information system.

HW high water.

LOCOP length of connected pathways.
LW low water.

NAP Normaal Amsterdams Peil.
NOC number of components.

RMM Rijn-Maasmonding (Rhine-Meuse estuary).
RMSE Root Mean Square Error.

SWE shallow-water equations.

1 Introduction

1.1 Background and relevance

Over the last couple of centuries, human population growth and migration have driven urbanization all around the world. Although the relation between urban development and biodiversity is poorly understood, a negative correlation between the two is generally assumed. Especially in developing countries, the distance between cities and protected areas is shrinking. Research on trends in global eco-regions, rare species and protected areas suggests significant biodiversity degradation associated with current and upcoming urbanization (McDonald, Kareiva, & Forman, 2008). In the more developed countries, the effects are already recognized and a movement towards nature restoration can be discerned.

An example of this trend is found in the Netherlands, where historically people migrated towards the western part of the country because of the connection to sea and rivers. Facilitated by e.g. trade and agriculture the region grew and the population increased rapidly. Nowadays the most populated area is roughly the area enclosed by Rotterdam, Amsterdam and Utrecht and is also known as the 'Randstad'. When in 1953 a combination of a heavy storm and spring tide caused a major flooding, which led to almost 2000 casualties, it was decided that flood-prone areas, including the Randstad, should be protected heavily. In the past century, many embankments and other flood defenses have been built to prevent the densely populated area from flooding. Although these structures are very effective from a safety point of view, it introduced adverse effects on ecological issues. In particular the construction of the Haringvliet sluices had major impact on nature. In the Biesbosch, a national park around 50 km upstream of the Rhine and Meuse river mouth, a tide-induced water level variation of 2 m used to be present. After the construction of this dam, the water level fluctuations reduced to only 20 to 30 cm in the Brabantse Biesbosch, while 60 to 70 cm in the Sliedrechtse Biesbosch remained because of the open connection with the sea via the Nieuwe Waterweg (Figure 1.1). The ancient tidal movement was halted, inducing many changes in nature. Fish that used to swim from the sea upstream into the Biesbosch area to spawn, were hindered because of the hard barrier of the Haringvliet sluices. Also the gradual transition between salt and fresh water disappeared. Species as salmon and sturgeon made way for freshwater species as perch and pike. The bird population was impacted since many mudflats, essential feeding areas for waterfowls, drowned permanently. The birds of prey population on the other hand increased as mice and rabbits found better living environments. Additionally, the tranquility of the area decreased because of a better accessibility for humans.

In order to improve the biodiversity in urban areas near the sea, a trend in giving space back to nature for ecological improvements is found. This leads to the nature rehabilitation projects such as the construction of tidal parks. Also, habitat rehabilitation measures are designed, to improve the living environment for fish and other organisms. Concerning the Rhine-Meuse estuary, Rijkswaterstaat (the Dutch executive agency of the Ministry of Infrastructure and Water Management) and several other parties are investigating multiple locations to be appointed as tidal parks. Tidal parks imply the restoration of tidal action in the water system and hence the need to know more about the feasibility and the sustainability of such systems. One of the intended locations of a tidal park is the Sliedrechtse Biesbosch (Rijkswaterstaat, n.d.-b, 2021b). To create tidal nature various interventions can be implemented, such as the construction or restoration of creeks and channels, making space for flood plains or taking measures to reduce ship waves to create shelter for fish. Although from 2009 to 2010 a number of measures was already taken

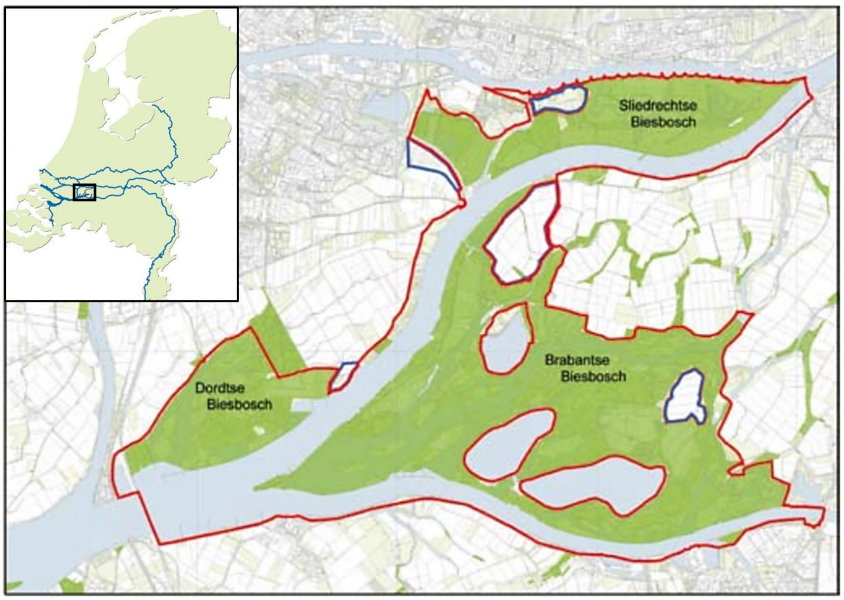

Figure 1.1: Location and different parts of the Biesbosch National Park (Sluiter & Veenhuizen, 2008).

(Bureau Waardenburg, 2007), the area was recently appointed again as subject for new restoration measures (PAGW, 2022). Since this area is one of the few freshwater tidal areas in the world, its ecological coherence is of great interest.

In the search for ecological coherence, an effective but relatively new method is to apply the connectivity framework. In the field of hydrology, the term 'connectivity' refers to the water-mediated transfer of matter, energy or organisms between elements of the hydrological cycle (Pringle, 2003). Ecological integrity of landscapes is dependent on this hydrological connectivity and, consequently, reduction of the connectivity of an area can have major impact on biodiversity. The link between hydrological connectivity and changes of (aquatic) ecosystems is given in Figure 1.2 (Zhang et al., 2021). Also in ecology the connectivity framework is applied, and refers to the structural and functional connectivity of landscapes that facilitate suitable habitats for flora and fauna (Mohammad & Saiful, 2010). In general, the concept of connectivity can be applied in many different fields of research and can be approached in multiple ways. Zhang et al. (2021) state that "the index of hydrological connectivity and numerical models are the most significant approaches to assess the changes in hydrological connectivity." Changes in hydrological connectivity can be found e.g. after natural processes have reshaped an area or after nature restoration measures have been executed. So far, connectivity assessment has primarily been applied to assess the present state of an area. However, the framework can also be deployed to assess the efficacy of measures taken, or with a more predictive character, to propose (the optimal location of) new measures. In such comparisons between two different states of an area, it is useful to express the connectivity in a value. One way to do this is by means of a Connectivity Index (CI). Various CI expressions exist and generally expressions are based on a specific area. It is therefore questionable if existing CI expressions are satisfactorily applicable to the Sliedrechtse Biesbosch. Another method that enables clear comparison is graph theory. Graph theory has become a popular tool for studying habitat connectivity in recent years because of its ability to represent complex systems in a simple and intuitive way. In a graph-theory model, the different habitats in an ecosystem are represented as nodes, and the connections between them are represented as edges. By analyzing the properties of the graph, such as the number of edges, the number of nodes, and the 'connectedness' of the nodes, researchers can gain a better understanding of the overall structure of the ecosystem and how it is affected by external factors.

In this research, a graph-based method is developed to assess the connectivity of a water network. The purpose of the method is to evaluate the connectivity of an area and to identify vulnerable locations where nature restoration measures should be regarded in the future. The method can be used to compare a

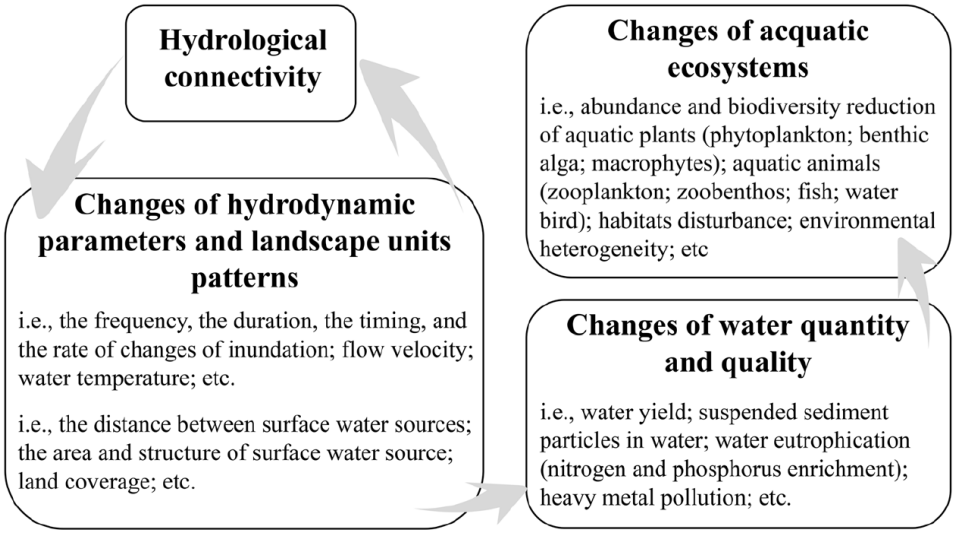

Figure 1.2: Links between hydrological connectivity and health of aquatic ecosystems (Zhang et al., 2021).

system's connectivity state at different moments in time. This enables one to objectively judge the efficacy of formerly executed restoration measures as well as to predict certain measures' potential. The Sliedrechtse Biesbosch, as was introduced above, serves as a case study. Present weak links in the channel network are identified and connectivity improving measures are proposed and researched. This way, the validity of the developed method is proven by comparing the area's present state to various fictive future states, after nature restoration measures are implemented.

1.2 Research aim and objectives

This study consists of a research aim and four accompanying research objectives. Here, the research aim describes the main goal and overarching purpose of the research. This focuses on what the research project is intended to achieve. The objectives divide the research aim into smaller parts, each treating a specific aspect of the aim.

1.2.1 Research aim

The aim of this research is to use a graph theory approach to study the connectivity of aquatic habitats in the Sliedrechtse Biesbosch. This involves constructing a graph that represents the individual creeks and channels in the area, and analyzing the connectivity of the graph to determine the strengths and weaknesses of the area in accommodating a diverse ecosystem. The results of this research provide valuable information for conservation efforts in the Sliedrechtse Biesbosch, and can also be applied to other aquatic ecosystems around the world. In summary, the aim of this research is expressed as:

> *Apply and evaluate the use of graph theory to objectively identify vulnerable locations in a water channel network that limit the aquatic habitat connectivity of a freshwater tidal area, in order to propose adequate nature restoration measures and preserve or improve the area's ecological value.*

1.2.2 Research objectives

To achieve this aim, a number of objectives are formulated that individually contribute to the aim by addressing specific aspects. The objectives are treated in the different chapters of this report. Finally, the aim and objectives are discussed in the conclusion.

1. Examine the relation between hydrodynamics and ecology in a freshwater tidal wetland.
2. Investigate the different applications of connectivity and discuss the various approaches besides graph theory.

3. Discuss the various metrics in graph theory and identify the most useful metrics for an aquatic habitat connectivity study.

4. Review the added value of graph theory over solely numerical modelling.

1.3 Methodology

The method consists of various aspects, such as a literature study, in which background information on the study area is gathered. Also different views and approaches to connectivity are investigated. When the fundamental concepts are clear, the required data is gathered to be able to carry out a quantitative study of the area. This is done by performing a numerical modelling study. Based on the output of this modelling study, the connectivity of the case study area is assessed and nature restoration measures are proposed. A schematic summary of the connectivity study process is given in a flow chart in Figure 1.4.

1.3.1 Literature review

The concise description of the approach of this research consists of different phases. First a literature review is carried out. Since the aim of this research implies a thorough understanding of the relationship between hydrodynamics and ecology, background information is gathered and reference is made to similar nature restoration measures. The concept of connectivity can be applied in nature restoration projects so the different views and approaches to connectivity are investigated. Concerning graph theory, a range of applications can be discerned. In this research, only the basic principles of graph theory are applied, requiring knowledge of the fundamentals of this theory and the metrics to interpret a graph. Finally, since the developed method is applied in a case study, site-specific information on the study area is required. Since the study area is located in a freshwater tidal delta, the unique hydrodynamic situation in the area is investigated and the area properties are examined.

1.3.2 Data collection and preparation

In order to build an accurate numerical model and to obtain representative results from simulations, the model input parameters need to be determined. The relevant data is gathered by literature review, consulting (public) data sources such as the database of Rijkswaterstaat and Deltares and by processing data in open-source software such as geographic information system (GIS) QGIS and programming language Python. With these tools, input files are created which are required in the numerical model.

1.3.3 Numerical modelling

A detailed analysis of hydrodynamics is carried out by applying a schematized model. Numerous simulation software systems are available in the field of hydrodynamic modelling but different models come with different fields of application. In the complex Biesbosch freshwater delta, many different processes play a role. Here, Delft3D Flexible Mesh (FM) is selected since this modelling software offers one modelling environment for the simulation of multiple processes such as coastal and river flows, with detailed local flows, water levels, sediment transport and morphology. Besides, it is capable of handling the interactions between the processes and evaluates, among other things, water quality and ecology. Delft3D FM provides optimal modelling flexibility by handling curvilinear and irregular grids whilst performing well in terms of computational speed and accuracy. 1D- and 2D grids can be combined and resolution can be increased locally (Melger, 2019).

In order to obtain accurate and realistic simulation results, an accurate model is set up. Important parameters are the bed topography of the area, boundary conditions and physical parameters. As can be seen in Figure 1.3, bed topography data of the study area is known (Rijkswaterstaat, 2021a). On behalf of Rijkswaterstaat, bed level measurements have been carried out, expressed in meters above Normaal Amsterdams Peil (NAP).

Data on river discharge, tidal constituents, water levels and properties such as bed roughness and composition are gathered. With this information a reference case is defined with a constant discharge and tidal regime. After thorough investigation of the reference case, the connectivity state of the area is evaluated

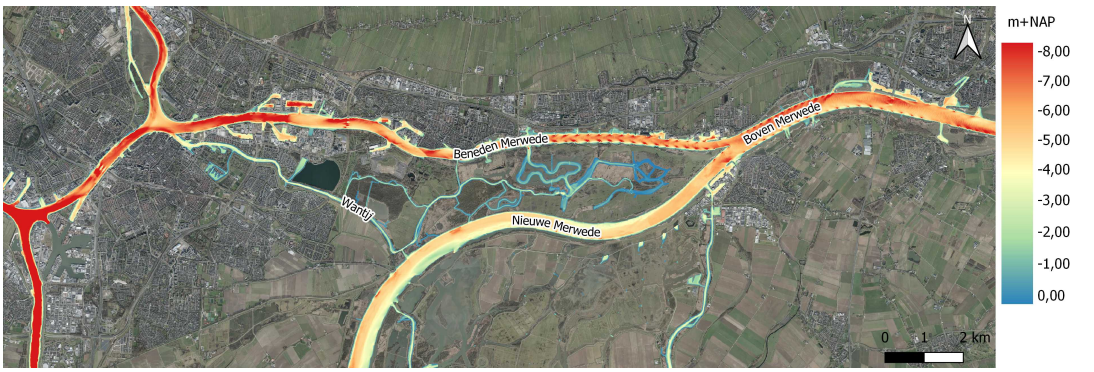

Figure 1.3: Most recent bed topography of the Sliedrechtse Biesbosch and the adjacent rivers (Rijkswaterstaat, 2021a).

and multiple nature restoration measures are proposed and simulated. Also, different climate scenarios can be applied such as sea level rise and larger discharge seasonality (greater differences between high and low river discharges). These influence the discharge and sediment distribution in the area and may limit the extent to which the proposed measures are future proof. However, these long-term effects on connectivity are not discussed in this report.

1.3.4 Connectivity analysis

As was stated in the introduction, the aim of this research is to develop and apply a method to objectively identify vulnerable locations in a water channel network, that limit the connectivity of an area. The proposed method can be divided into three components, each consisting of multiple steps. A schematic overview of this process is given in Figure 1.4 and is clarified here.

First of all, the area under consideration is schematized into a graph consisting of nodes and edges. This process is called spatial graph development and gives the basis to apply graph theory. The next step is to determine what hydrodynamic properties of individual edges are of interest for determining the area's connectivity. Since in this research no physical hydrodynamic measurements are available, the hydrodynamic data is gathered from a numerical model. In order to obtain accurate model output, a representative model is built. Relevant input parameters are the boundary conditions, initial conditions and bed topography. After building and calibrating the model, different cases are simulated. Initially, the reference case is modelled and the relevant hydrodynamic data is collected and used as edge weight in the graph. Now a weighted graph is constructed and the connectivity is analyzed by applying a threshold. This threshold limits the existence of an edge depending on a minimum or maximum requirement to weight of the individual edges. By applying a threshold value of a parameter in a dynamic system, edges disappear from the graph and the network becomes fragmented. This process is interpreted finally in the connectivity analysis, by means of various metrics. Here the vulnerable locations or channels in the water system are identified and restoration measures are designed.

1.4 Limitations and boundaries

Inevitably, a number of assumptions is made. Assumptions are simplifications that come at the expense of how realistic the system is described. They are however required to make the system more manageable and be able to analyze the system's response to changes. The most important assumptions are discussed here.

The ecological connectivity study is based on the continuity of water, such that the channel network is fully connected if no specific requirements are imposed. If requirements are imposed, the network fragments in the sense that specific channels are not accessible for a considered species. This however does not imply that there is no flow through the channel. To limit the amount of work, the effects of one parameter on connectivity are investigated, being flow velocity. The same approach could be followed for numerous other parameters (e.g. water depth, discharge, tidal range, wave action, water quality, etc.),

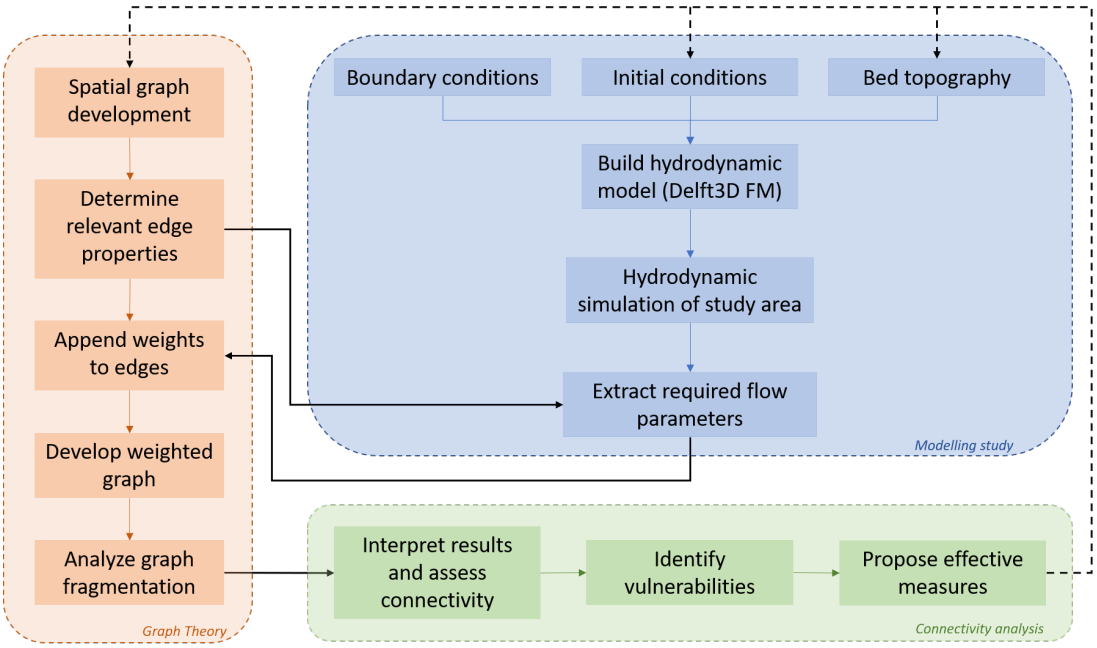

Figure 1.4: A flow chart of the three different components in the proposed connectivity analysis method, including steps and dependencies.

but this is not included in this research.

The research only takes into account hydrodynamic effects. As is explained in a later stage of this report, morphodynamic processes would induce higher uncertainties. That is why it is decided to exclude this from the research. In a connectivity study for which accurate data on sediment transport and morphological processes are available, it could be opted to include this component into the research to make it more realistic.

Since the channel network is schematized into a graph with nodes and edges, all individual channels are represented by an edge. The edge weights (flow velocity in this research) are determined from a numerical simulation and specifically apply to the observation points determined in the model, located at a fixed interval along the channel. This means that the weights in fact only represent the values that correspond to the exact observation point locations, and are not necessarily constant along the width and length of the entire channel. Limiting the edge length justifies to a certain extent this approach, and in an ideal case the graph edge lengths should be minimized. Since this would lead to extensive modelling and graph-theory efforts beyond the actual scope of this research, it is decided to neglect this effect and assume that the maximum flow velocity found at one of the observation points in the channel is governing in the entire channel. Since the flow velocity changes in time because of the tide, the observation point determining the limiting flow velocity can change in time as well.

1.5 Thesis outline

To have a clear overview of the content of this thesis, the outline is given in Figure 1.5. The thesis consists of seven chapters, divided into three parts. The first part contains the introduction (Chapter 1) which is concluded with this thesis outline. The research aim and objectives are introduced, as well as the general methodology for the research. This chapter can be used to identify the different tools and steps that are used within the research. Furthermore, in the first part the literature review is carried out and the case study area is introduced (Chapter 2), to provide the necessary background knowledge. The second part dives into the approach and application of the connectivity study of the Sliedrechtse Biesbosch. First the approach to the case study is explained, containing the model set-up and graph development (Chapter 3). The connectivity results of the case study are discussed in a separate chapter (Chapter 4). Finally,

the second part also contains the implementation of restoration measures to the case study area and the discussion of the efficacy of these measures (Chapter 5). The third part is the synthesis of this research report. First, the limitations and implications of the approach and results are discussed (Chapter 6). Finally, the main findings and key take-aways of the research are given in the conclusion (Chapter 7). Also, suggestions on future research and on the use of the method are given in this chapter.

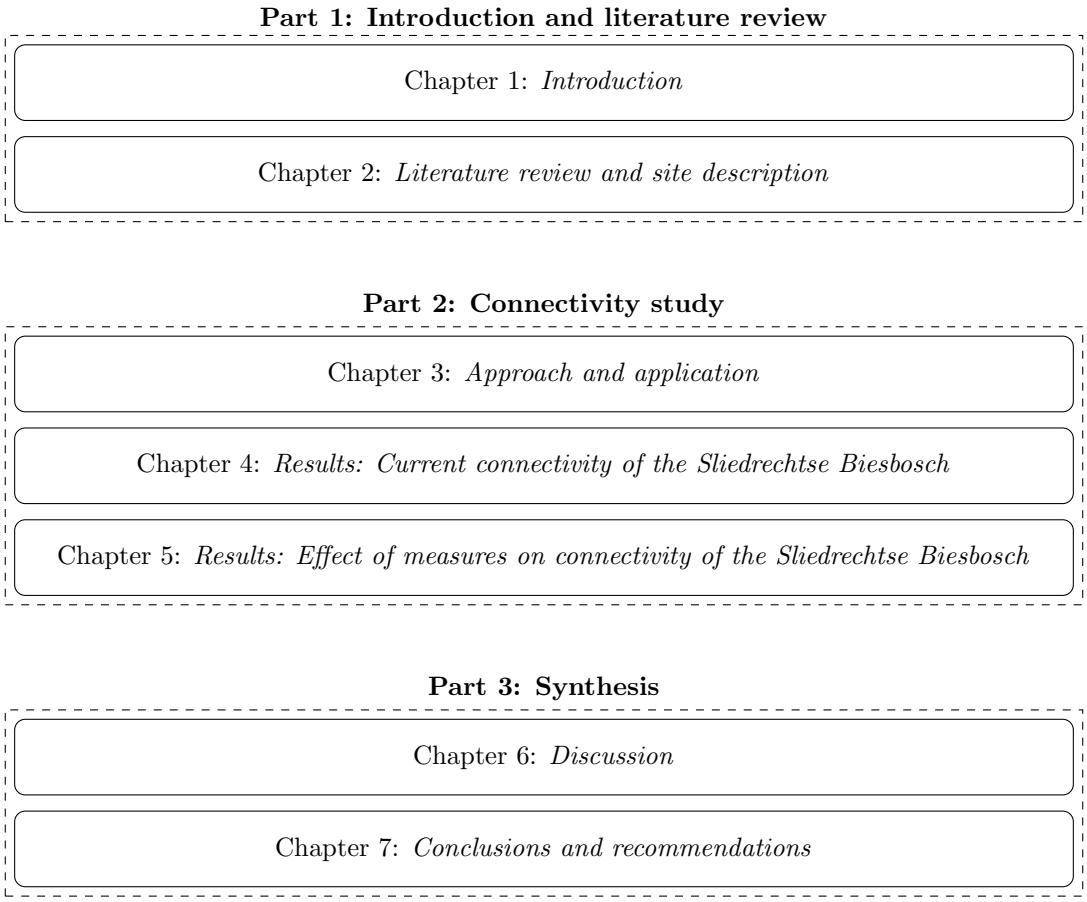

Figure 1.5: Thesis outline, indicating the different parts and chapters of this report.

2

Literature review and site description

This chapter reviews the available literature on the connectivity framework, graph theory and the application of graph theory in the analysis of connectivity in former research. First of all, the great variety of connectivity definitions and applications is denoted. Then, the background and basic concept of graph theory are introduced and its usefulness is illustrated by listing various fields of application. This theoretical part is concluded with discussing the most relevant knowledge on the application of graph theory in analyzing habitat connectivity. Furthermore, this chapter includes a description of the study area, the Sliedrechtse Biesbosch. The location of the area is described, just as site-specific characteristics such as the bed topography, bed composition and hydrodynamic forcing which acts on the water system. Since this research aims to include the relationship between hydrodynamics and ecology, also the ecological condition of the area is discussed. As in the Sliedrechtse Biesbosch a unique combination of fresh water and tidal influences is present, variation in time plays an important role.

2.1 Introduction to connectivity

2.1.1 Background

In general, connectivity refers to the state or quality of being connected. It is the degree to which something is connected or the ability to connect with other things. This concept can be applied in many different contexts, such as in computer science, networking, sociology, and mathematics. In each of these fields, connectivity has a specific meaning and is used to study or analyze different aspects of the systems or phenomena being considered. Also in ecology the concept of connectivity can be applied, e.g. by considering the connectivity of aquatic habitats. Here, it refers to the ways in which the different bodies of water are connected and interact with each other. This can include connections between rivers, streams, ponds, and other bodies of water, as well as the connections between the water body and the surrounding land. The connectivity of these habitats plays a crucial role in the health and functioning of aquatic ecosystems, as it allows the exchange of water, nutrients, and organisms between different parts of an area. This can help to maintain a diverse and healthy ecosystem and support the survival of a wide range of species.

When habitats are connected, they are able to support a greater diversity of species and provide more opportunities for organisms to interact and thrive. This can help to maintain the overall health of the ecosystem and support the survival of a wide range of species. In addition, connectivity can also play a role in the resilience of aquatic ecosystems, allowing them to better adapt to changes and disturbances. For these reasons, it is important to study and understand the connectivity of aquatic habitats in order to protect and manage these valuable ecosystems.

2.1.2 Definitions

Although the concept of connectivity itself is not new, its applicability to water systems and channel networks was introduced relatively recently. Multiple interpretations were given to the concept of con-

nectivity, as can be seen from Table 2.1.

Table 2.1: The widespread used principle of connectivity applied to many different processes and with different definitions according to various authors.

Definition	Reference
Hydrologic connectivity is the water-mediated transfer of matter, energy, or organisms within or between elements of the hydrologic cycle.	Bracken et al. (2013); Freeman, Pringle, and Jackson (2007); Pringle (2001)
Hydrological connectivity: the passage of water from one part of the landscape to another and is expected to generate some catchment runoff response.	Bracken and Croke (2007)
Hydrological connectivity operates on the four dimensions of fluvial hydrosystems: longitudinal, lateral, vertical and temporal. Here lateral connectivity refers to the links between a river and the waterbodies in the alluvial floodplain. Vertical connectivity includes exchanges between the surface and groundwater. The temporal dimension relates to changes occurring on both annual and historical scales.	Amoros and Bornette (2002)
Hydrological connectivity describes the physical coupling (linkages) of different elements within a landscape regarding (sub-)surface flows.	Masselink et al. (2017)
Structural connectivity: the physical adjacency of landscape elements, i.e. the spatial arrangement of the landscape that controls patterns in flux pathways.	Bracken et al. (2013); Passalacqua (2017)
Functional connectivity: the way the physical adjacency of landscape elements translates into fluxes of water, sediments and solutes, i.e. the environmental processes that produce the magnitude and direction of fluxes.	Bracken et al. (2013); Passalacqua (2017)
Ecological connectivity: the exchange pathways of water, resources and organisms between the channel, the aquifer and the floodplain, although interactions with adjacent uplands must also be considered.	Ward and Stanford (1995)
Habitat connectivity describes the spatial continuity of a habitat or cover type across a landscape. Terrestrial landscape connectivity is manifested in two dimensions, as animals in one patch can often cross a gap to another patch, usually following one of several alternate paths. In aquatic systems, longitudinal connectivity is used since movement between habitat patches is longitudinal along the river channel.	Cote, Kehler, Bourne, and Wiersma (2009)
Sediment connectivity: the transfer of sediment and some pollutants that attach to sediment.	Xie et al. (2020)
Sediment connectivity: the physically integrated status of a system at the meso- and macro-scale, i.e. the combined effect of lateral and longitudinal linkages between system components.	Heckmann and Schwanghart (2013)
Sediment connectivity: the physical transfer of sediments and attached pollutants through the drainage basin and may vary considerably with, amongst other components, particle size.	Bracken and Croke (2007)
Sediment connectivity: the degree of linkage which controls sediment fluxes throughout landscape, and, in particular, between sediment sources and downstream areas.	Cavalli, Trevisani, Comiti, and Marchi (2013)

Table 2.1 continued on next page

Table 2.1 continued from previous page

Definition	Reference
Landscape connectivity: the physical coupling of landforms (e.g. hillslope to channel) within a drainage basin.	Bracken and Croke (2007)
Connectivity refers to the degree to which matter (water, solutes, sediment, organic matter) and organisms can move among patches in a landscape or ecosystem, where patches are arbitrarily defined areas that vary depending on time and space scales under consideration. Connectivity can be characterized as gradational, from fully disconnected to fully connected, such that natural systems typically have differing degrees of connectivity that vary significantly in time and space.	Wohl et al. (2019)

Connectivity, considered as the state of being (inter)connected, can be applied in various contexts. For example in transport, connectivity can be used to describe how well two cities are connected by different means of transport. In computer science, connectivity is used to say something about the extent to which hardware or software is able to communicate or interact with other systems or programs. Within this research the concept of connectivity is applied to mainly hydrology and ecology. According to Pringle (2003) hydrological connectivity can be defined as the water-mediated transfer of matter, energy or organisms between elements of the hydrological cycle. This can be applied to different scales, ranging from entire river networks from source to sink to only specific creek systems. Hydrological connectivity can be described in four dimensions of fluvial systems: longitudinal, lateral, vertical and temporal (Amoros & Bornette, 2002). Here, the vertical component, covering the exchange between surface and groundwater, is not considered. Ecological connectivity refers to the connectivity of landscapes that facilitate suitable habitats for flora and fauna (Mohammad & Saiful, 2010) and is heavily dependent on the hydrological connectivity of the considered area (Figure 1.2). Ecology is a broad term consisting of multiple components. This requires assessment of multiple contexts of connectivity such as landscape and habitat connectivity.

Regardless of the context in which connectivity is used, two elements are often identified: structural connectivity and functional connectivity. Structural connectivity deals with spatial patterns of elements in landscapes, i.e. the physical links between elements such as connection channels and creeks. Functional connectivity on the other hand, refers to the effect of these spatial patterns, e.g. how a creek contributes to a high biodiversity. Where structural connectivity is quantifiable relatively conveniently by evaluating e.g. maps, aerial photos or flow data, functional connectivity is not so straightforward to assess because of its intrinsic dynamic nature and the complexity and variability of the interactions that define it (Lexartza-Artza & Wainwright, 2009).

Structural connectivity in the field of hydrology and ecology describes the physical links between elements. Numerous formulations exist, each referring to a specific area with specific properties. An accurate way to express habitat connectivity in a river environment is by looking at the longitudinal connectivity. Cote et al. (2009) formulate the structural component of this connectivity in terms of the Dendritic Connectivity Index (DCI), that provides an analogous means of quantifying aquatic habitat connectivity. The DCI represents the ease at which organisms are able to move freely between two random points of a river network, taking into account man-made barriers (e.g. sluices and weirs) as well as natural barriers (e.g. waterfalls) for both freshwater and saltwater fish species.

Tian, Yin, Bai, Yang, and Zhao (2021) proposed a quantitative method to evaluate efforts to improve wetland connectivity and to restore and protect wetland ecosystems. The paper introduces seven structural connectivity indicators and their relative weight and combines these in one structural connectivity index. The method proved particularly effective in accounting for connectivity characteristics of small elements in the river system network of the Baiyangdian wetland (China), which have been ignored by other methods and research in the area.

Functional connectivity relates to the effect of structural connectivity on e.g. biodiversity. In habitats, for example, structural habitat connectivity describes the physical links between habitat patches, while functional habitat connectivity gives the extent to which organisms actually move through the landscape. In this context, one can imagine that structural connectivity is particularly useful in the planning and design nature restoration measures, while functional connectivity is useful to evaluate the efficacy of measures after the measures are actually implemented. Each separately gives an indication of the connectivity of an area, but a combination of structural and functional connectivity gives the most complete view.

2.1.3 Methods and applications

The inexhaustible list of definitions of connectivity has led to a wide range of research methods to investigate connectivity. An incomplete but indicative list of previous research can be seen in Table 2.2.

Table 2.2: The different methods of connectivity assessment and their application in various research. The type of connectivity under consideration is shown in bold.

Method	Application	Reference
Graph theory	Review of applications of network theory to **habitat** patches in landscape mosaics, including (1) the conceptual model underlying the applications; (2) formalization and implementation of the graph model; (3) model parameterization; (4) model testing, insights, and predictions available through graph analyses; and (5) potential implications for conservation biology and related applications.	Urban, Minor, Treml, and Schick (2009)
	Study to explore the network structure of coarse **sediment** pathways in a central alpine catchment. Numerical simulation models for rockfall, debris flows, and (hillslope and channel) fluvial processes are used to establish a spatially explicit graph model of sediment sources, pathways and sinks. The raster cells of a digital elevation model form the nodes of this graph, and simulated sediment trajectories represent the corresponding edges.	Heckmann and Schwanghart (2013)
	An application of graph theory and connectivity metrics to coastal **sediment** dynamics, exemplified using the Ameland Inlet in the Netherlands. Quantification of sediment transport between nodes is determined by numerical modelling.	Pearson, van Prooijen, Elias, Vitousek, and Wang (2020)
	Application of graph theory to quantify the **structural** and **dynamical** connectivity of multi-directional estuarine channel networks, based on satellite imagery.	Hiatt, Addink, and Kleinhans (2022)
Indices	Evaluation of the **structural** connectivity for a source **habitat** (i.e., forest) with particular consideration of the roles of ecotones, small habitats, and barriers. A multi-buffer mapping procedure based on vector data is applied to two comparative test sites for mapping ecological networks (econets) which are composed of forest patches, ecotones, corridors, small habitats, and barriers. On this basis, several indices are proposed for quantitative evaluation of structural connectivity of econets.	Hou, Neubert, and Walz (2017)
	Evaluation of the potential **hydrological** connectivity dynamics between the tidal channel network and its surroundings using an index of connectivity in the whole Yellow River Delta.	Xie et al. (2020)

Table 2.2 continued on next page

Table 2.2 continued from previous page

Method	Application	Reference
	A proposed method for grading the evaluation of **structural** connectivity of river system networks, based on seven structural connectivity evaluation indicators. The method was applied to the Baiyangdian Wetland, China	Tian et al. (2021)

2.2 Introduction to graph theory

2.2.1 Background

Graph theory is a field in mathematics concerning the study of graphs. In this context, graphs are mathematical structures used to model pairwise relations between objects consisting of vertices (also referred to as nodes) which are connected by lines (also known as edges or links). Graph theory dates from the 18^{th} century when it was first described by Leonhard Euler and his famous paper on the Seven Bridges of Königsberg. For extensive information on the genesis of graph theory, the reader is referred to Biggs, Lloyd, and Wilson (1986). Whereas Euler applied a graph to a logistical problem, nowadays graph theory is applied in a wide range of fields such as computer science, biology, transportation, physics and chemistry. Also in the field of hydraulic engineering, the application of graph theory has proven its strengths in various connectivity studies.

In the context of aquatic habitat connectivity, graph theory can be used to represent the connections between different bodies of water as a network of nodes and edges. This allows researchers to analyze the structure and properties of the network, such as its connectivity, centrality, and resilience. This can provide valuable insights into the ways in which different habitats are connected and how these connections may be affected by various factors, such as the presence of barriers or changes in the flow of water. By using graph theory to study aquatic habitat connectivity, researchers can better understand the complex interactions within these ecosystems and how they may be affected by environmental changes.

2.2.2 Definitions

Graph theory contains a number of technical terms, indicating the type of system that is represented or its properties. The most important definitions are given in this section. Distinction is made between graph types and graph properties.

Graph types

The required type of graph depends on the structure of the graph that is to be represented. The four main distinctions between graphs are:

1. *Directed versus undirected graphs:* A directed graph, also known as a digraph, is a graph in which the edges have a direction associated with them. In other words, the edges in a directed graph can be traversed in only one direction, from the starting vertex to the ending vertex. This means that the edges in a directed graph are ordered pairs of vertices, rather than unordered pairs as in an undirected graph. An undirected graph is a graph in which the edges do not have a direction associated with them. In other words, the edges in an undirected graph can be traversed in either direction, from the starting vertex to the ending vertex or from the ending vertex to the starting vertex. This means that the edges in an undirected graph are unordered pairs of vertices.
2. *Weighted versus unweighted graphs:* A weighted graph is a graph in which each edge has a numerical value associated with it, called the weight of the edge. The weight of an edge represents the cost, distance, or some other value associated with traversing the edge. This allows the graph to model complex systems in which the relationships between the objects have different strengths or costs. An unweighted graph is a graph in which the edges do not have weights associated with them. In an unweighted graph, all the edges are considered to have the same weight, which is typically taken

to be 1. This simplifies the analysis of the graph and makes it easier to work with, but it may not accurately reflect the real-world relationships between the objects being modeled.

3. *Simple graphs versus multigraphs:* A simple graph is a graph that does not allow multiple edges between the same pair of vertices. In other words, a simple graph connects two nodes by at most one edge. A multigraph is a graph that can have multiple edges connecting the same pair of vertices. Simple graphs are the most basic type of graph, and they are often used as a starting point for more complex graph analysis. They are useful for modelling systems in which the relationships between the objects are simple and do not have multiple strengths or costs.

4. *Connected versus disconnected graphs:* A connected graph is a graph in which there is a path between every pair of vertices. This means that, for any two vertices in the graph, there is a sequence of edges that can be traversed to go from one vertex to the other. A disconnected graph is a graph in which there are two or more vertices that are not connected by a path. This means that there are one or more isolated subgroups of vertices that are not connected to the rest of the graph. The 'connectedness' of a graph is an important property because it determines whether or not information or resources can flow freely throughout the system represented by the graph. A connected graph represents a system in which all the objects are connected to one another, whereas a disconnected graph represents a system in which there are isolated subgroups of objects that are not connected to the rest of the system. A connected graph is different from a complete graph, since a complete graph implies an edge between every pair of vertices while a connected graph implies a path of one or more adjacent edges between every pair of vertices.

Graph properties and analysis metrics

The properties of a graph are characteristics or attributes of the graph that are used to describe and analyze its structure and behaviour. These properties can be defined in various ways, depending on the specific problem being studied and the goals of the analysis. A powerful attribute of graph theory is the wealth of analytical measurements that can be used to examine a network as a whole and its individual nodes and edges. Several metrics that are relevant in this research are given in Table 2.3.

Table 2.3: Various graph theory metrics and the level on which they provide information. Note that this is an incomplete list of all available metrics.

Metric	Definition	Level
Size	The size of a graph is the total number of vertices and edges in the graph. This is often represented as $G = (V, E)$, where V is the number of vertices and E is the number of edges in graph G. The size of a graph is an important property because it provides information about the overall complexity of the graph.	System
Order	The order of a graph is the number of vertices in the graph.	System
Connected components	The number of connected subgraphs in a graph, where a connected subgraph is not part of any larger connected subgraph.	System
Diameter	The diameter of a graph is the maximum of the shortest distance between any pair of vertices in the graph. In graph-theory terms, it is the length of the longest shortest path between any two vertices in the graph. The diameter of a graph is an important property because it represents the minimum distance that needs to be travelled between the two furthest separated nodes in the graph.	System
Bridge	A bridge or cut-edge is an edge that, when removed from the graph, increases the number of components in the graph. In other words, a cut-edge is an edge whose removal disconnects the graph. Cut-edges are important because they represent the minimum number of edges that need to be removed in order to disconnect a graph.	Edge

Table 2.3 continued on next page

Table 2.3 continued from previous page

Metric	Definition	Level
Centrality	Centrality refers to a set of metrics that measure the relative importance or influence of a node in a network. The concept of centrality is used to identify the most influential nodes in a network, based on various criteria. The choice of centrality metric depends on the type of network and the specific problem being studied. Common centrality applications are: - Closeness centrality: Measures the average length of the shortest path between a node and all other nodes in the graph. - Betweenness centrality: Measures the number of times a node acts as a bridge along the shortest path between two other nodes. - Degree centrality: Measures the number of connections a node has to other nodes in the graph.	Node
Density	The density of a graph is the number of occurring edges with respect to the number of possible edges. For undirected graphs, the mathematical formulation for the density $d(G)$ of a graph can be given as: $$d = \frac{2m}{n(n-1)} \quad (2.1)$$ or for directed graphs: $$d = \frac{m}{n(n-1)} \quad (2.2)$$ where m is the number of edges in graph G and n is the number of nodes.	System
Degree	The degree of a vertex in a graph is defined as the number of edges incident on the node. In a simple graph, where edges are not directed and there is at most one edge between any two vertices, the degree of a vertex is equal to the number of its neighbors. In a directed graph, there is a separate definition for in-degree (the number of incoming edges) and out-degree (the number of outgoing edges).	Node
Strength	The strength of a node is defined as the sum of the weights of its incident edges. If the graph is unweighted, the weight of each edge can be taken as 1, and the strength of a node is simply its degree (number of neighbors).	Node
Shortest path	The shortest path is a path between two vertices (nodes) in a graph such that the sum of the weights of its constituent edges is minimized.	System

In this research, the applicability of various parameters on both system level and node level is examined, resulting in a recommendation of a set of metrics for specific research topics.

2.2.3 Visual representation

The visual representation of a graph is an important tool for understanding and analyzing its properties. There are several ways to visually represent a graph, each with its own advantages and disadvantages. Some of the most common visual representations of graphs include:

- *The adjacency matrix:* This is a square $(n \times n)$ matrix that shows the connections between n vertices. In undirected and unweighted graphs, the entry in the i^{th} row and j^{th} column of the matrix is 1 if there is an edge between the i^{th} and j^{th} vertices, and 0 otherwise. The bi-directionality of the links in an undirected graph result in a symmetrical adjacency matrix. Directed and weighted graphs are represented by adjacency matrices with non-binary values in the matrix cells. This representation

is compact and easy to work with, but it can be difficult to interpret for large graphs. An example of a graph visualized as an adjacency matrix is given in Figure 2.1.

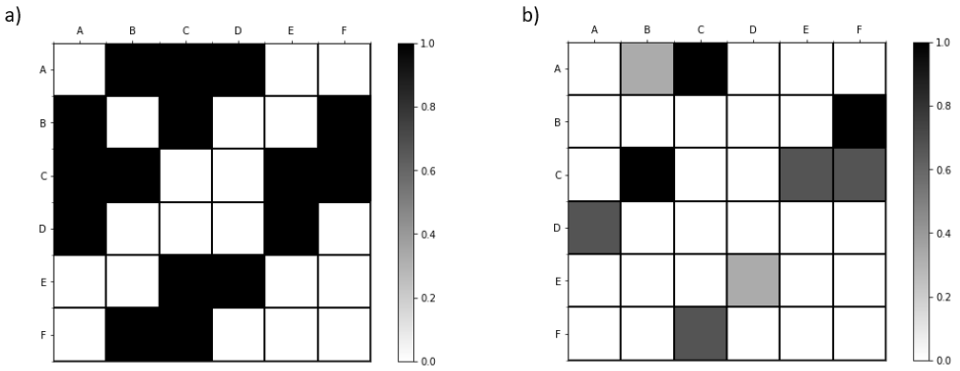

Figure 2.1: The 6×6 adjacency matrix corresponding to the network diagrams of Figure 2.2. Matrix (a) represents the simple undirected and unweighted graph (Figure 2.2a). In such graph, graphs are either connected or not, represented by black and white matrix cells, respectively. As can be seen, directed graphs lead to symmetrical adjacency matrices. Matrix (b) on the other hand is a visualization of the more complicated directed and weighted graph (Figure 2.2b), resulting in a non-binary adjacency matrix. Here the "strength" of the link between two nodes is indicated on a scale of 0 (white cells) to 1 (black cells), representing no connection and optimal connections, respectively. Since values between 0 and 1 are possible in this case, these in-between values are visualized on a gray scale.

- *The adjacency list:* This is a list of the vertices in the graph, along with the vertices that are connected to each vertex. This representation is more intuitive and easier to interpret than the adjacency matrix, but it can be less efficient to work with.
- *The edge list:* This is a list of the edges in the graph, along with the vertices that the edges connect. This representation is simple and easy to work with, but it does not provide as much information about the structure of the graph as the other representations.
- *The network diagram:* This is a visual representation of the graph in which the vertices are represented as points and the edges are represented as lines or curves connecting the points. Directionality is often indicated by an arrow, while weight can be visualized in multiple ways, e.g. by line thickness, colors or a written value next to the link. This representation is intuitive and easy to interpret, but it can be difficult to draw graphs accurately and efficiently, especially for large graphs. Network diagrams are particularly useful in indicating connectivity of an area. Nodes and links can then be drawn on top of a base map, giving a clear view of the location of nodes and where the most important links can be found. An example of a simple network diagram graph representation can be seen in Figure 2.2.

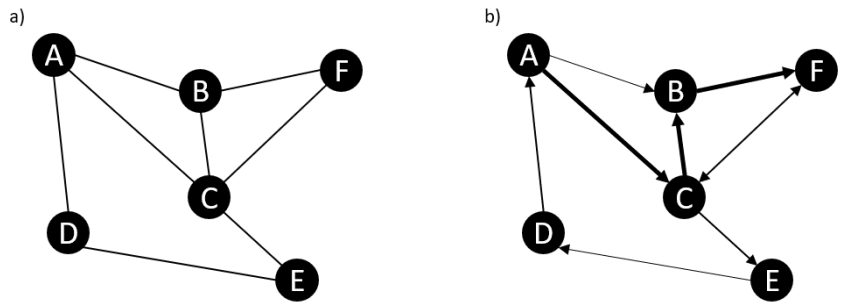

Figure 2.2: Example of a network diagram with six nodes (A-F) and eight or nine edges for (a) and (b), respectively. On the left-hand side (a) a simple undirected and unweighted graph. On the right-hand side (b) a directed and weighted graph. The direction is indicated by the arrow and the line thickness represents the weight of the link. Note that the bidirectional edge connecting nodes C-F are counted as two separate unidirectional edges.

Each of these visual representations has its own strengths and weaknesses, and the choice of representation depends on the specific problem being studied and the goals of the analysis. In general, the adjacency matrix is useful for working with algorithms that manipulate the connections between vertices, the adjacency list is useful for understanding the structure of the graph, and the network diagram is useful for visualizing the graph and identifying patterns.

2.3 Site description: The Sliedrechtse Biesbosch

2.3.1 Location and characteristics

The Sliedrechtse Biesbosch is part of the Rhine-Meuse estuary and is enclosed by two rivers on the northern and southern side of the area, the Beneden Merwede and the Nieuwe Merwede, respectively. On the upstream side of the area, these two rivers bifurcate from the Boven Merwede at the Kop van de Oude Wiel near Werkendam. The Boven Merwede on its turn is the continuation of the river Waal, which is the largest arm of the river Rhine. On the downstream side of the Sliedrechtse Biesbosch, the Wantij creek marks the border of the area and reaches far into the park since it connects to the several creeks in the area (see Figure 2.3 and Figure A.1).

Figure 2.3: The location of the Sliedrechtse Biesbosch and the enclosing rivers; the Wantij, Beneden Merwede and Nieuwe Merwede. ©OpenStreetMap contributors

The area has been subject of several projects in the past years. Rijkswaterstaat is investigating the possibility of permanently taking out of service three monumental locks. Two of those are located in the Sliedrechtse Biesbosch, the Helsluis and the Ottersluis. The locks are relatively small and are only used by recreational vessels in summer, making maintenance and operating staff relatively costly. Besides preserving the operational state of the locks, two general strategies can be distinguished: permanent opening of the locks and permanent closing of the locks. Both strategies have been investigated in the past years (Schuurman, 2012; Sloff & van Zetten, 2010)

2.3.2 Hydrodynamic conditions

The hydrodynamics occurring in the Rhine-Meuse estuary are dependent on various parameters, originating from tidal influences, river discharges, density differences and wind forces (Nijhuis, 2021). Additionally, the presence of the Haringvliet sluices make the hydrodynamics not so trivial. The sluicing programme of the Haringvliet sluices enables migratory fish to swim into the Haringvliet while preventing freshwater intakes from loss of quality.

Water level and flow velocity

The effect of the closure of the Haringvliet on the penetration of the tide into the Rhine-Meuse estuary is

clearly visible in Figure 2.4 (Vellinga et al., 2014). Only via the Nieuwe Waterweg the tidal wave can enter and propagate inland. At the North Sea shore at Hoek van Holland, tide-induced water level variations of 1.50 m are regularly observed, while the tidal amplitude has decreased further upstream at Dordrecht, to an amplitude of 0.80 m. Considering water level fluctuations even further inland, at Vuren, the tidal influence decreases to a difference of 0.40 m between high and low water levels. This tidal damping is attributed to two factors: bed friction and river discharge. Although the Sliedrechtse Biesbosch is under tidal influence, the water level variations are relatively small. As is visualised in Figure 2.4, the water level at Dordrecht and in the Beneden Merwede is solely influenced by the tidal constituent travelling through the northern and eastern part of the system (Nieuwe Maas and Noord) although the distance via the southern part of the system (Oude Maas) is of similar length.

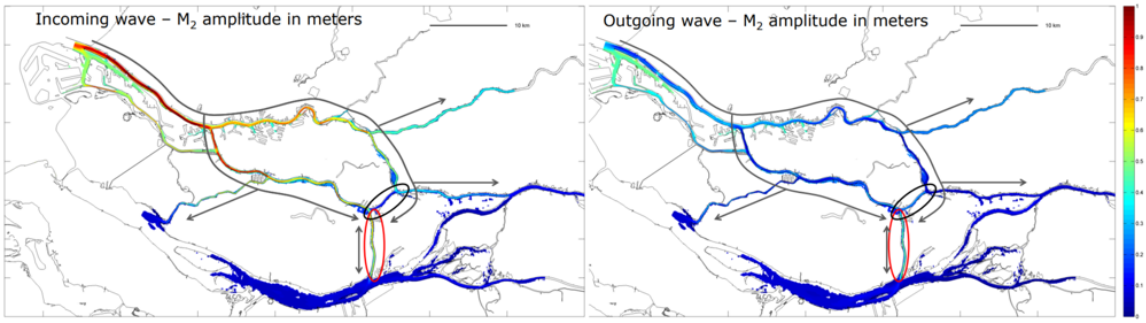

Figure 2.4: Incoming and outgoing tidal wave amplitude in the Rhine Meuse Delta, varying from 0 m to 1 m in dark blue and dark red, respectively. In grey arrows the propagation of the tidal waves is visualised, indicating that the junction between the Oude Maas and the Dordtsche Kil forms a tidal divide in the network (Vellinga et al., 2014).

Because of the closure of the Haringvliet, water level variations are minimal. It is due to the tidal wave entering the Nieuwe Waterweg and propagating via the Spui and Dordtse Kil rivers that minor variations are present. The Haringvliet sluices also affect the discharge distribution at the Kop van de Oude Wiel. During high tide, the penetration of the tide causes higher water levels in the northern part of the Rhine-Meuse estuary, reducing the river discharge in the Beneden Merwede. The major part of the Boven Merwede discharge then flows through the Nieuwe Merwede. During low tide, the water levels in the northern part of the estuary lower significantly, causing more water to flow through the Beneden Merwede. Although a quantitative analysis of the variation in discharge distribution at the Kop van de Oude Wiel during a tidal cycle is not known, it is known that on average the Boven Merwede discharge is distributed for 60 % through the Nieuwe Merwede (Frings, 2005).

Bed topography and composition

Sediment transported by the Boven Merwede is of a relatively wide grain size distribution. At the Kop van de Oude Wiel, the Boven Merwede splits up into the Beneden Merwede and the Nieuwe Merwede. In Figure 2.5 (Frings, 2005), the grain sizes along the channel width are plotted. Since just upstream of the bifurcation the Boven Merwede has a bend, it can clearly be seen that the transported sediment separates. In the inner bend, where flow velocities are smaller, fine particles settle. In the outer band on the other hand, the flow velocity is relatively large and settlement of larger particles is found. This lateral variation in grain sizes also determines the grain size of the sediment intake of the Beneden Merwede and the Nieuwe Merwede. As can be seen from Figure 2.5 the Nieuwe Merwede contains only relatively fine particles (ca. 0.4 mm), whereas the Beneden Merwede contains relatively large particles (ca. 0.7 mm).
During the 20th century, heavy metals and other pollutants have contaminated the soil in the creeks of the Sliedrechtse Biesbosch. Multiple investigations after the pollution have distinguished two ways of resuspension of the pollutants, via (horizontal) channel flow and via (vertical) ground water flow. If the flow velocity exceeds a threshold, surface water is contaminated which may further distribute the material into the surrounding area. In the Sliedrechtse Biesbosch, the risks of spreading contaminated material are mainly determined by erosion and resuspension due to currents. Spread initiated by wind waves can be excluded as a source of spread. Erosion caused by shipping is not expected, given the low draught of the passing recreational vessels (Snippen, Van der Heijdt, & Van Zetten, 2002). A flow criterion of 0.3 m/s is determined, to prevent erosion and resuspension of contaminated material. However, this criterion is

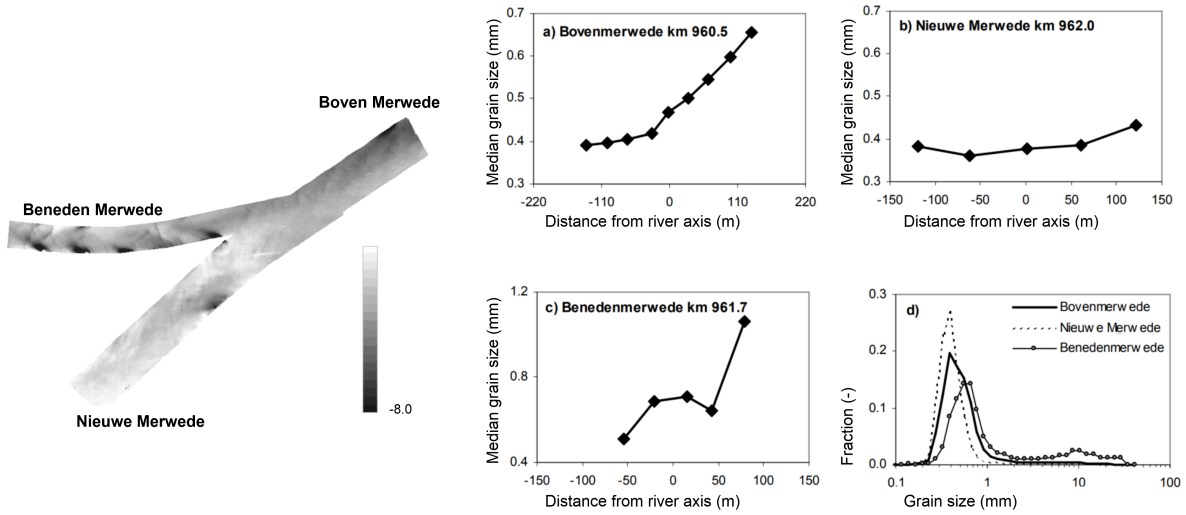

Figure 2.5: On the left-hand side the river bifurcation and bed topography. On the right-hand side the lateral variation of median grain size in the (**a**) Boven Merwede, (**b**) Nieuwe Merwede and (**c**) Beneden Merwede, as determined from samples taken in January 2004. In figure (**d**) the mean grain size distributions of the sediment in the three river branches are compared (Frings, 2005).

exceeded in a large part of the creeks in the Sliedrechtse Biesbosch. Exceptions to this are the Sneepkil, creeks along the Huiswaard and Oude Kat polder, the Houweningswater and parts of the Gat van Den Hengst. In these creeks, flow velocities are so low that erosion and resuspension of contaminated material can be excluded (Snippen et al., 2002). Remediation plans are made to remove contaminated soil layers. Because the creeks will be deepened during the remediation, the velocities at the site will be relatively low and a lot of sediment is expected to settle in the creeks (Visser, Snippen, & de Gelder, 2005).

2.3.3 Ecological value and biodiversity

Different species and vegetation have different preferences and ecological requirements. In nature restoration projects, various components should be taken into account to consider the area's suitability for a diverse group of fish and plants. Amongst other components the flow velocity, water depth, substrate, water quality and turbidity are factors that contribute to the habitat quality for specific species (Morrow Jr & Fischenich, 2000). Marijs et al. (2020) discuss the ecological design requirements for various species of aquatic and riparian plants, macro-fauna, fish, and amphibians and is therefore a useful reference in a restoration project aiming at a specific species. Among the treated species, the European flounder (Figure 2.6) is listed. This species is a flatfish which is usually found in coastal areas but it is the only flatfish species that occurs in freshwater areas in the Netherlands as well. Juvenile flounder migrates up the fresh water of rivers and lives in shallow waters. Once mature, flounder live in salt water in the Dutch coastal zone usually at depths of less than 50 meters. Substantial areas of rearing habitat for juvenile flounder have been lost due to the construction of the Delta Works and the Afsluitdijk. As a result, the density of flounder has greatly decreased. The creation of shallow, sheltered zones in the lower river area can increase the surface area of the juvenile area for flounder. The Kierbesluit of the Haringvliet sluices, an agreement that describes the partial opening of the sluices during high tide, provides partial restoration of tidal movement in the upstream rivers (Rijkswaterstaat, n.d.-a), allowing flounder to potentially increase in numbers. Ideal habitat has a flow velocity between 0 and 0.3 m/s.

Stoffers, Buijse, Verreth, and Nagelkerke (2022) highlights that the overall functioning of a habitat patch as nursing area is largely dependent on the size of the nursery area as this plays an important role in the distribution and spatial connectivity of habitat patches. Connectivity can be considered between patches within a certain area, but also the importance of permanent lateral connections between floodplains and the river is emphasized (Stoffers, 2022).
Between 2009 and 2010 a project has been carried out in the Sliedrechtse Biesbosch in which polders

Figure 2.6: The European flounder (Platichthys flesus) is a flatfish that spends part of its life cycle in fresh water (Marijs et al., 2020).

were connected to the tidal creeks. To enhance the tidal fluctuation in the area, an open connection with the Beneden Merwede was constructed. Dynamics of water flow was the starting point of this project to develop freshwater tidal nature. Flow in the creeks prevents undesired grow of vegetation while stagnant water outside the creeks initiates development of vegetation at places it is wished for (Bureau Waardenburg, 2007). The four main interventions are given below and are visualised in Figure 2.7. The names of the creeks and polders in the area are specified in Figure A.1.

1. Creating an open connection between the Beneden Merwede and the polder Kort- en Lang Ambacht.
2. Creating an open connection between the polder Kort- en Lang Ambacht and the creek Gat van Den Hengst.
3. Local widening the creek Gat van Den Hengst to create a better connection with the polder Aart Eloyenbosch.
4. Creating an open connection between the polder Aart Eloyenbosch and the creek Sneepkil.

2.3.4 Numerical modelling

For the evaluation of the hydrodynamics in the Sliedrechtse Biesbosch, a three-dimensional Delft3D Flexible Mesh model is used. This is a hydrodynamic model, implying that only the hydrodynamics are considered and that the associated transport of sediment is not included. Hydrodynamic modelling is a computational process approximating reality. Trade-offs have to be made since on the one hand, an accurate result is desired, while on the other hand a more accurate model requires more calculations and computational time. An optimal balance is to be found between the two. Delft3D FM is helpful in finding this balance since it enables users to define regions with higher resolution to locally increase the accuracy.

In fluid dynamics any problem starts with the conservation laws for mass and momentum. These conservation laws can be expressed mathematically by the three-dimensional Navier-Stokes equations, consisting of the continuity equation and the momentum equations. In Delft3D FM the 2D (depth-averaged) or 3D non-linear shallow-water equations (SWE) are solved. The depth-averaged continuity equation is acquired by integrating the three-dimensional continuity equation over depth for incompressible fluids. For more information on the SWE and the supporting assumptions, the reader is referred to Deltares (2022a).

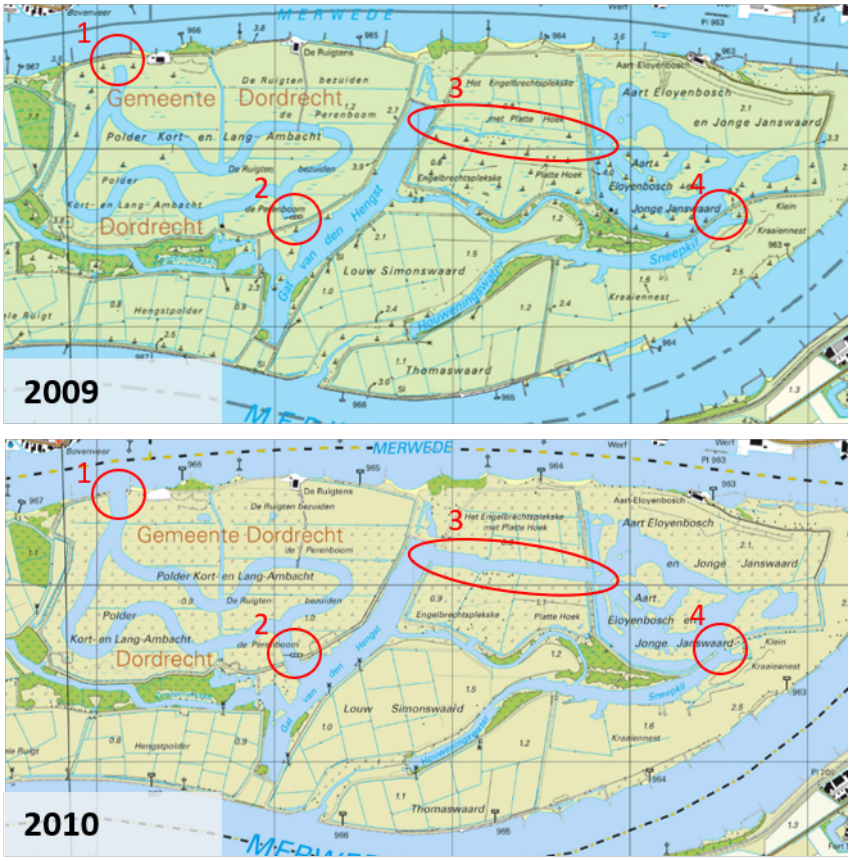

Figure 2.7: Restoration measures in the Sliedrechtse Biesbosch, observed by comparing a map of the area from 2009 and 2010 Kadaster (n.d.).

3

Approach and application

This chapter serves as a detailed description of the different steps taken to carry out a connectivity study in a channel network, such as the Sliedrechtse Biesbosch. First, the approach to hydrodynamic modelling is discussed and a numerical model is set up for the study area. All relevant considerations in this procedure are treated. Then, the application of graph theory is carried out and the graph for the study area is developed. Finally, this chapter discusses the expected results and how to interpret the different figures.

3.1 Hydrodynamic modelling

3.1.1 Simulation approach

The first section of this chapter discusses the importance of a modelling study in this research, just as the position of the modelling study within the work. The choice for modelling in Delft3D Flexible Mesh is clarified, considering the advantages of this software compared to other modelling software.

A detailed analysis of effects is to be carried out by applying a schematized model. Numerous simulation software is available in the field of hydrodynamic modelling but different software come with different fields of application. In the complex Biesbosch freshwater delta, many different process play a role. Here, Delft3D FM is selected since this modelling software offers one modelling environment for the simulation of multiple processes such as coastal and river floods, with detailed local flows, water levels, sediment transport and morphology. Besides, it is capable of handling the interactions between the processes and evaluate amongst other components water quality and ecology. The big advantage of Delft3D FM above Delft3D 4, is that Delft3D FM provides more modelling flexibility by handling curvilinear and irregular grids whilst performing well in terms of computational speed and accuracy (Melger, 2019). As especially perpendicular bends are more accurately followed by FM, this software allows higher flexibility in areas with less regular layouts, such as the study area considered in this research.

Another interesting property of Delft3D FM is that it supports local mesh refinements. To handle computation time efficiently, it is often beneficial to apply relatively low but sufficient resolution along the study area, while locally increasing the resolution at specific areas of interest to capture details of flow processes. Again, this property comes in particularly convenient since the large enclosing rivers and narrow creeks and channels in the Sliedrechtse Biesbosch differ in size drastically.

Instead of building a new model of the study area from scratch, another possibility is to use the Rijn-Maasmonding (Rhine-Meuse estuary) (RMM) model, which is available through Deltares. The Sliedrechtse Biesbosch is included in this RMM model in 1D, 2D and 3D with a model resolution of 40 m (Sloff, 2022). Although this is too coarse to simulate the flow through the narrow creeks in the area, the model might still be useful since Delft3D FM offers the possibility to refine the grid locally. In combination with the detailed bed topography, this can result in an accurate model output. Although this approach is probably the most accurate, it is chosen to build a new model. This decision is mainly based on the fact that the entire RMM model is too extensive for the application in this research. Computation time would not weigh up to the result accuracy. Also calibration is not based on the RMM model.

3.1.2 Simulation goal and method

In order to be able to objectively assess connectivity of the area and the effect of nature restoration measures on it, insight must be gained into hydrodynamic parameters such as water depth, flow velocity and conveyed discharge. The lack of this hydrodynamic data for the Sliedrechtse Biesbosch in the form of physical measurements, can be partly compensated for by carrying out a modelling study. Model output in this case replaces measurements and serves as the main source of input to assess the connectivity. The goal of the modelling study is therefore to obtain accurate hydrodynamic data for parameters at multiple locations in the study area at different moments in time, both before and after the restoration measures.

The relative position of the modelling study in this research is given with respect to the flow chart discussed in the research design (Figure 1.4). The modelling component of the research is highlighted in the blue box of this figure. As can be seen from the figure, the simulation output is required for the graph theory analysis of the water system, finally leading to a connectivity assessment of the considered area.

3.1.3 Model set-up

This section elaborates the construction of the model. A step-by-step approach is used to build an indicative model starting from scratch and aiming for a representative model of the study area. The first step is to draw the land boundaries, following the land contours of the area. Although the land boundaries are not considered in running the model, they are helpful in constructing the grid, as will be explained below. Next to the grid, determining model components are the bed level, boundary conditions and physical parameters. In the remainder of this chapter, each of these components is clarified, building towards the final model.

Grid construction

The grid is at the basis of the hydrodynamic model, since this determines to a large extent the accuracy and computation time of the model. Delft3D FM allows for unstructured grids, consisting of triangles, quadrangles, pentagons and hexagons, which is beneficial in an area of irregular geometry. An accurate grid complies with the orthogonality and smoothness considerations. Non-orthogonality is measured as the cosine of the angle between the line connecting two flow nodes (line between the circumcentres of two grid cells) and the line connecting two grid cells corners (edge of two adjacent grid cells). Perfect orthogonality is thus obtained when this angle is 90°, such that the non-orthogonality is 0. The smoothness is defined as the ratio between the areas of two adjacent grid cells. As a guideline, the criteria for the two considerations are: non-orthogonality < 0.02 and $1 \leq$ smoothness < 1.2. Note that these are guidelines for an efficient grid, but not strict requirements. For more information on Delft3D FM grid construction and properties is referred to Deltares (2022b). The constructed grid and an example of a local grid refinement can be seen in Figure 3.1.

Bed level

Part of the model input is bed level information. This can be divided in two components: topography and bed topography. Here topography implies the elevation of land forms above water level, while bed topography entails the elevation of land below water level. Considering the topography, detailed information is openly available via the Actueel Hoogtebestand Nederland (AHN). This is a digital elevation map for The Netherlands obtained by laser technology. For this model the most recent version of this data set is used (AHN4), which dates from 2020 to 2022 and has a point density of on average 10-14 elevation points per squared meter (AHN, 2022). The elevation map is subdivided into map sheets which can be downloaded individually. For this research, eight elevation maps covering the area of interest are imported in QGIS 3.16 (2020). This geographic information system (GIS) enables to create and analyze all types of data such as elevation maps. By first merging the eight map sheets and then drawing a frame around the area of interest, the specific elevation data for the Sliedrechtse Biesbosch can be extracted (Figure 3.2a). Similarly, the relevant bed topographic data is extracted from a larger data set in QGIS (Figure 3.2b). The data is made publicly available by Rijkswaterstaat and is obtained by multibeam echosounding Rijkswaterstaat (2021a). The resolution of this bed level data set is 1 m. By merging the topographic elevation map and the bed topographic elevation map, a total bed elevation profile of the

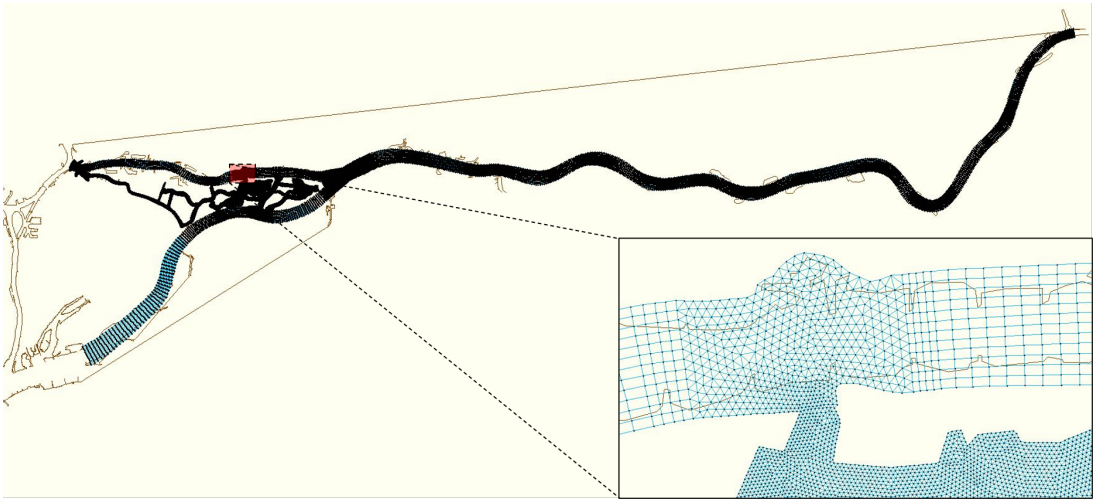

Figure 3.1: Entire grid and local refinement at a bifurcation.

area of interest is created (Figure 3.2c). Finally, the empty points in the data set have to be filled. As can be seen from Figure 3.2c, there is a number of spots where neither topographic nor bed topographic data is available. Therefore these points are considered as 'no data' and should be filled. This is done in QGIS by means of interpolation over the nearest points and results in a completely filled elevation data set (Figure 3.2d). Note that the bed level data displayed in Figure 3.2 contains only the study area, whereas the grid covers a longer reach of the river. For clear visualisations, only part of the bed level data is given here, but the same method as described above is followed to construct the bed level file for the entire grid.

Both the topography and the bed topography data set are delivered as a TIF-file. This file type is usually applied for storing raster or image graphics. Also the merged and filled bed level file that is made by the operations in QGIS result in a TIF-file. Delft3D FM requires an XYZ-file, which is one of the most common types of files to store coordinates of location points. Therefore a file-type conversion is executed to translate the TIF-file into an XYZ-file.

The constructed bed level file has a resolution of 1 m, since this is the lowest resolution of the constituents. However, since the constructed grid has a much lower resolution, the high bed level resolution is not used. This is because the bed level is clipped on the grid and bed level values are interpolated onto each grid cell. Therefore, the bed level resolution is decreased to 5 m, still containing the shape of the bed level but having a much more effective file size. Finally, the bed level is interpolated onto the grid, resulting in the bed given in Figure 3.3.

Boundary conditions

The domain of the model is chosen such that the study area is fully enclosed. This implies that three hydrodynamic boundary conditions have to be imposed, one for each river included (Boven Merwede, Beneden Merwede and Nieuwe Merwede). Boundary conditions consist of a location specification and a hydrodynamic forcing at that location. Since the river bifurcates from one river into two tributaries, one upstream boundary condition and two downstream boundary conditions are imposed. These are selected as follows:

1. *Upstream boundary condition:*
   At the upstream area of the domain, a discharge boundary condition is imposed. Although the area of interest ends just upstream of the bifurcation from Boven Merwede into Beneden Merwede and Nieuwe Merwede, the boundary condition is imposed around 40 km upstream of the bifurcation, near Tiel. This has three advantages. First of all, this location of the boundary condition corresponds to the location of a discharge measuring station of Rijkswaterstaat. Since continuous discharge measurements have been carried out here, a large amount of data is available and can be used for calibration of the model. Secondly, by extending the model domain in upstream direction, tidal

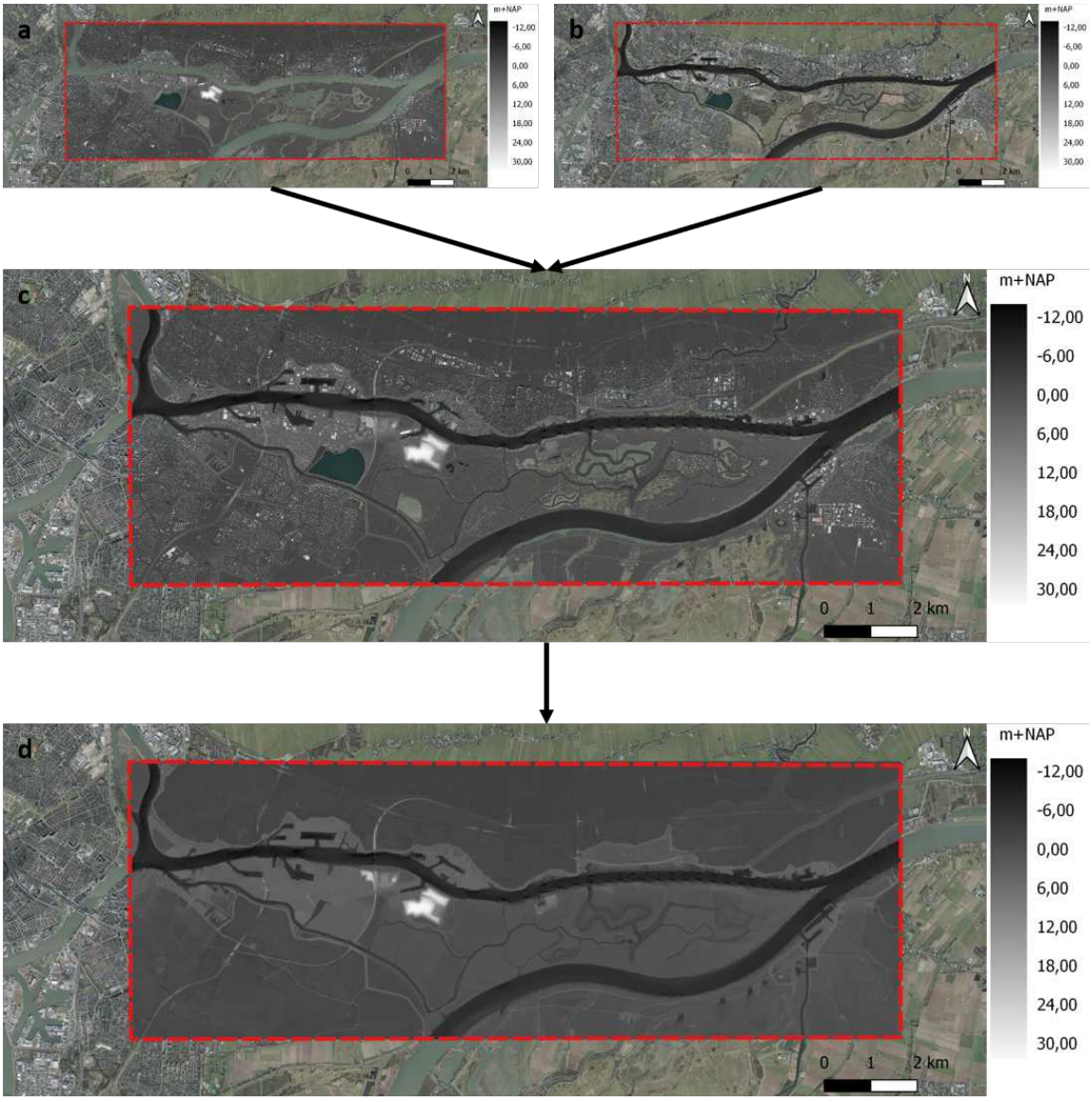

Figure 3.2: The extracted topographic elevation data (**a**) (AHN, 2022) combined with the extracted bed topographic data (**b**) (Rijkswaterstaat, 2021a) result in the total bed level representation (**c**). A closer look to **c** shows that some points in the study area are not represented in the elevation data. By interpolation the missing data points are replaced by elevation points which results in a complete elevation data set (**d**).

forcing travelling through the Beneden Merwede river can dampen gradually, whereas a boundary condition at the bifurcation would suppress the tidal effects at that location. Finally, upstream extension of the model covers two additional water level measuring stations which are useful in the calibration phase. The discharge imposed in the simulation is derived from discharge measurements in prior years (Table 3.1). A representative value of $Q = 1500$ m^3/s is chosen.

2. *Downstream boundary condition (Beneden Merwede):*
The first downstream boundary condition is a water level boundary condition and is imposed at the most western part of the domain, where the Beneden Merwede bifurcates into the rivers Old Meuse and Noord. This is located at Dordrecht and corresponds to a location of a water level measuring station. The water level imposed in the simulation is derived from water level measurements in prior years (Table 3.2). A representative value of $h = 0.53$ m is chosen. Since the location of Dordrecht is under tidal influence, also a representative tide needs to be imposed. Water level time series analysis shows that the average tide has a period of approximately 12 hours and 25 minutes, with

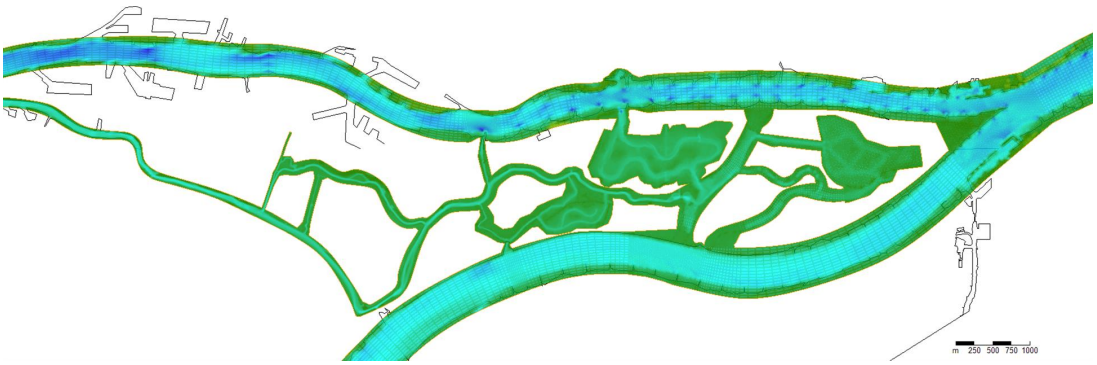

Figure 3.3: Bed level interpolated on the grid.

an amplitude of around 40 cm. This corresponds to the principal lunar semi-diurnal tide (M2-tide) with amplitude $a = 0.40$ m. Although other tidal constituents are most likely also present (e.g. K1 and S2), their relative contribution to the total water level is limited. Therefore other tidal components are neglected in this research. The magnitude of the tidal wave amplitude is consistent with earlier research by Vellinga et al. (2014) (Figure 2.4).

3. *Downstream boundary condition (Nieuwe Merwede):*
The second downstream boundary condition also is a water level boundary condition and is imposed at the south-western part of the domain, in the Nieuwe Merwede. In this case, the model is extended downstream approximately 10 km. This makes water level measurements from the Moerdijk measuring station more accurate and useful during calibration. Following the same reasoning as for the boundary condition at Dordrecht, the water level boundary condition at Moerdijk is chosen as a mean water level of $h = 0.48$ m with an M2-tide with amplitude $a = 0.18$ m. This corresponds to Figure 2.4. Also from this figure it can be seen that the same tidal wave arriving at Moerdijk, passes Dordrecht first. This implies that there is a phase lag between the two locations. Analysis of water levels at the two measurement stations indicates that the average time lag amounts to 2 hours and 43 minutes, which corresponds to a phase lag of roughly 80°.

For both downstream water level boundary conditions, a time series is generated reproducing the fluctuating water level at the edge of the domain. This time series is created according to equation (3.1). With this general equation, multiple tidal astronomical constituents can be taken into account. In this case however, only the M2-tide is included.

$$H(t) = A_0 + \sum_{i=1}^{k} A_i \cdot cos\left(\frac{2\pi}{T(c_i)} \cdot t + \phi_i\right) \tag{3.1}$$

Where:

$H(t)$	water level at time t [m+NAP]
A_0	water level offset [m]
k	number of relevant astronomical components
c_i	astronomical component i
t	time [s]
A_i	amplitude of astronomical component i [m]
$T(c_i)$	period of astronomical component i [s]
ϕ_i	phase of astronomical component i [rad]

Wave nonlinearity

At open sea, a symmetrical tidal signal can be identified. Here bed and wall friction don't play a role in the water level variations. Where the tidal wave reaches shallow regions or encounters an opposing current, e.g. at the coast or propagating inland, friction is no longer negligible and its effects can be observed in the shape of the tidal signal. Nonlinear waves are asymmetrical in height or duration of crest and trough. Two categories of wave nonlinearity are wave skewness and wave asymmetry. Skewed waves

are distorted in symmetry around the horizontal axis. This indicates a deviation between the wave crest and wave trough in both height and duration. Generally, skewed waves have a short and high wave crest and a long and flat wave through (Figure 3.4b). Asymmetric waves on the other hand are defined as waves that are asymmetric along the vertical axis. This indicates that there is a difference between the steepness of the wave front and the wave and can be recognized as the leaning forward or backward of a wave (Figure 3.4c). This results in a larger acceleration between trough and crest and smaller acceleration between crest and trough. The height and duration of the crest and trough of an asymmetric wave are not necessarily asymmetric.

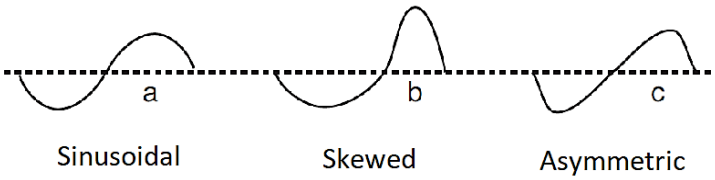

Figure 3.4: Wave nonlinearity (Raap, 2021).

Since both downstream boundaries are located a significant distance inland, it can safely be assumed that the tidal signal is nonlinear. Therefore, imposing a simple sinusoidal varying water level such as was described in Equation (3.1) would be unrealistic. The linear wave is transformed by means of equation (3.2).

$$y = cos\left(\omega t + \phi + \frac{y}{n}\right) \tag{3.2}$$

Where:

y	water level at time t [m+NAP]
ω	angular frequency [rad/s]
t	time [s]
ϕ_i	phase offset [rad]
n	asymmetry parameter [m/rad]

By taking an infinitely small time step t and imposing an initial value for y, the equation can be made explicit and results in Equation (3.3). Analyzing measured water level fluctuations at Dordrecht and Moerdijk indicates that the average period during which the water level is rising is around 3 hours and 25 minutes. The average period during which the water level falls is around 9 hours. By combining Equation (3.1) and Equation (3.3) and optimizing for n, the results of the boundary conditions at the two downstream locations is found (Figure 3.5). The best fit is found at $n = 0.57$ m/rad.

$$y_t = cos\left(\omega t + \phi + \frac{y_{t-1}}{n}\right) \tag{3.3}$$

Hydrodynamic constants

Considering hydrodynamic constants of the model, default Delft3D FM values are used. The most relevant constants are the gravitational acceleration term ($g = 9.813$ m/s^2) and the water density ($\rho_w = 1000$ kg/m^3). Other parameters such as air density, temperature and salinity are not adjusted since the corresponding processes (wind, salinity and temperature fluctuations, respectively), are not taken into account in this modelling study. It should however be noted that in future scenarios with sea level rise and decreased summer discharges, salinity might become an interesting process to consider in assessing the ecological value of the Sliedrechtse Biesbosch.Calibration and validation Calibration is based on data from three water level measuring stations along the Boven Merwede and Nieuwe Merwede, located at Zaltbommel, Vuren and Werkendam looking in downstream direction. Here real-world measurements can be compared to model output. Since the boundary conditions consist of measurement time-series, the model can be calibrated by evaluating the development of the flow in the domain and comparing this to the measurement time-series at the measuring stations of Zaltbommel, Vuren and Werkendam. Measurements at one additional location are available, since Rijkswaterstaat (2010) carried out a measurement study

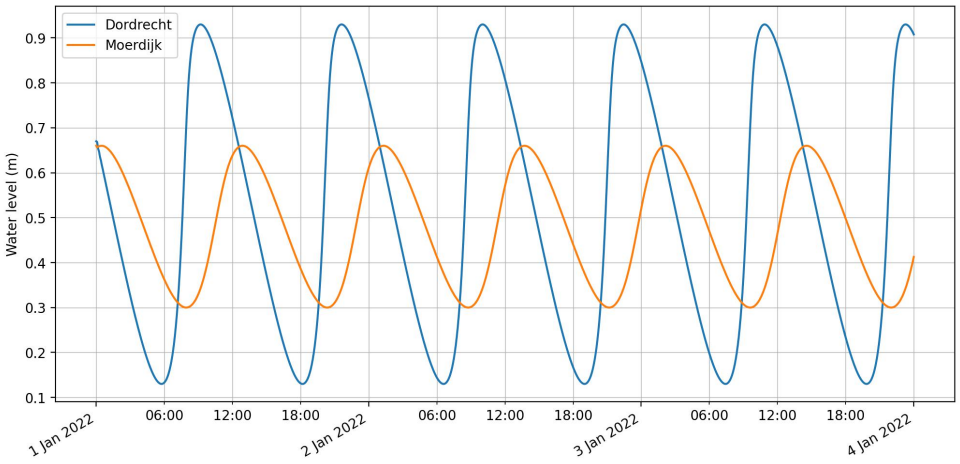

Figure 3.5: Downstream water level boundaries.

Table 3.1: Discharge measurements for various years.

Year	Summer discharge [m^3/s]			Winter discharge [m^3/s]		
	Mean	Minimum	Maximum	Mean	Minimum	Maximum
2013	1745.11	892.98	4428.96	1920.92	1095.07	4874.69
2014	1358.67	850.55	2208.09	1518.34	1059.74	2196.17
2015	1304.81	777.39	2522.47	1433.41	697.69	3141.67
2016	1708.73	876.57	3151.26	1460.82	718.83	3527.30
2017	1182.14	919.48	1499.42	1448.67	737.14	3400.83
2018	1104.18	624.13	1716.82	1647.64	542.71	5088.16
2019	1237.01	818.44	2057.11	1550.22	919.48	3453.00
2020	1038.38	755.62	1439.90	1670.79	844.09	4052.25
2021	1555.62	926.14	4600.63	1516.40	805.73	5001.95
Average	**1359.40**	**826.81**	**2624.96**	**1574.14**	**824.50**	**3859.56**

Table 3.2: Water level measurements for various years at Dordrecht.

Year	Summer		Winter	
	MWL [m+NAP]	Mean amplitude [m]	MWL [m+NAP]	Mean amplitude [m]
2013	0.47	0.395	0.57	0.417
2014	0.48	0.381	0.57	0.401
2015	0.48	0.391	0.59	0.405
2016	0.55	0.397	0.54	0.406
2017	0.48	0.374	0.59	0.403
2018	0.44	0.372	0.52	0.425
2019	0.46	0.383	0.64	0.399
2020	0.44	0.377	0.62	0.411
2021	0.52	0.384	0.60	0.378
Average	**0.48**	**0.384**	**0.58**	**0.405**

at the Helsluis while opening the lock for a full tidal cycle. In all, three time periods are chosen for calibration. Since at the Helsluis only a specific time-series is known, this is one of the selected periods for calibration. The other two are selected such that one covers a mild winter discharge, while the other covers a mild summer discharge. An overview of the availability of data is given in Table 3.4.

Table 3.3: Water level measurements for various years at Moerdijk.

Year	Summer		Winter	
	MWL [m+NAP]	Mean amplitude [m]	MWL [m+NAP]	Mean amplitude [m]
2013	0.40	0.179	0.51	0.216
2014	0.44	0.155	0.55	0.167
2015	0.42	0.163	0.54	0.186
2016	0.47	0.180	0.49	0.188
2017	0.44	0.139	0.54	0.188
2018	0.38	0.139	0.44	0.202
2019	0.42	0.152	0.58	0.194
2020	0.41	0.145	0.56	0.191
2021	0.47	0.172	0.55	0.165
Average	**0.43**	**0.158**	**0.53**	**0.189**

Table 3.4: Availability of water level measurements at different locations within the model domain.

Location	March 2010	January 2022	August 2022
Helsluis	x		
Werkendam	x	x	x
Vuren	x	x	x
Zaltbommel	x	x	x

The main property that determines the response of the flow is the bed friction. The bed topography exerts a shear stress on the passing flow. Large bed forms or vegetation decelerate the flow, while a smooth bed allows large flow velocities. By considering the simplified form of the continuity equation ($Q = u \cdot A$), one can immediately derive that this would cause a water level increase and decrease, respectively. The magnitude of the shear stress is often characterised by means of a roughness coefficient. Bottom roughness coefficients can be defined according to multiple formulations, i.e. by using a uniform Chézy value (C) or by applying the roughness formulations of Manning or White-Colebrook. Imposing a fixed Chézy value means that the friction coefficient is constant in time and space. Applying the Manning or White-Colebrook formulation implies an extra step, since the Chézy friction coefficient is calculated for every space and time step based on the local water depth H and a formulation-specific constant. The corresponding formulations for Manning and White-Colebrook are given in Equation (3.4) and Equation (3.5), respectively.

$$C = \frac{H^{\frac{1}{6}}}{n} \tag{3.4}$$

$$C = 18 \log\left(\frac{12H}{k_s}\right) \tag{3.5}$$

Where:

C	Chézy friction coefficient [$m^{1/2}/s$]
H	water depth [m]
n	Manning coefficient [$s/m^{1/3}$]
k_s	Nikuradse equivalent geometrical roughness [m]

For calibration, multiple simulations have been carried out applying different bed roughness formulations and values, after which the most corresponding formulation is selected. Initially, all three formulations discussed above have been applied. This results in a range of outcomes. Applying a uniform Chézy value gives relatively accurate results at the individual locations, however, one Chézy value that accurately

corresponds to the entire domain cannot be found.

Applying the White-Colebrook formulation for bottom roughness requires the Nikuradse roughness length (k_s). A generally applied formulation for this parameter is $k_s = 2 \cdot D_{50}$, where D_{50} is the median grain size. From Figure 2.5, it can be found that representative grain sizes are in the range of 0.4 to 0.7 mm. Simulations based on this roughness formulation continuously underestimated the water level and therefore was considered not applicable to this area. A possible explanation for this is that various grain size diameters are found within the domain (as can be seen from Figure 2.5), while the model only takes into account one single value for the Nikuradse roughness length (k_s).

The most accurate results were obtained by means of the Manning bed roughness formulation. As can be seen from Equation (3.4), the Manning coefficient (n) must be determined. A typical Manning value is $n = 0.02$ and higher values correspond to larger friction. Determining the most accurate Manning value applicable for the entire model is an iterative process. For the three different time periods (Table 3.4), simulations have been carried out and results are compared at the Helsluis and Werkendam. For each simulation a number of statistics is derived, i.e. the mean deviation, standard deviation, maximum deviation and R^2. The coefficient of determination (R^2) is a statistical way to describe the accuracy of a model fit with respect to reality. In this case, it is more informative than the Root Mean Square Error (RMSE) since it gives a percentage instead of an arbitrary value. The RMSE is a metric that tells the average distance between predicted values from the model and actual values from the data set. This implies that the dimension is equal to that of the actual data, which explains the importance of more information on the data set. A model with an RMSE of 0.1 m might be very accurate in describing a large river a mean water level of 10 m. The same model is probably considered to be poorly fitting a small creek with a mean water level of 0.5 m. Since the calibration locations in the model domain have different water depths, a more objective evaluation of the model quality can be given by means of R^2. The definition of the coefficient of determination is given in Equation (3.6).

$$R^2 = 1 - \frac{SS_{res}}{SS_{tot}}, \quad \text{with:} \qquad SS_{res} = \sum_i \left(h_i - \hat{h}_i\right)^2, \quad \text{and} \qquad SS_{tot} = \sum_i \left(h_i - \overline{h}\right)^2 \tag{3.6}$$

Where:

SS_{res}	sum of squares of residuals
SS_{tot}	total sum of squares
h_i	actual (measured) values for water level
$\hat{h}_i$	residuals of h, distance between actual value and prediction
$\overline{h}$	mean value of h

In case of a perfect fitting model, the residuals are 0 resulting in $R^2 = 1$. Lower values for R^2 indicate a lower accuracy and even negative values can be found. The results of the calibration simulations at various locations and periods in time can be found in Tables 3.5 to 3.8. Plots corresponding to the given tables are included Appendix C.

Table 3.5: Obtained error for different values of the Manning friction coefficient at the Helsluis (1 March 2010 until 3 March 2010).

Manning friction [s/m$^{1/3}$]	Mean deviation [m]	Standard deviation [m]	Maximum deviation [m]	R^2 [-]
0.020	0.0821	0.0613	0.2391	0.878
0.021	0.0773	0.0615	0.2417	0.887
0.022	0.0771	0.0616	0.2445	0.887
0.023	0.0825	0.0603	0.2473	0.879
0.024	0.0919	0.0597	0.2502	0.861
0.025	0.1033	0.0616	0.2535	0.832

Table 3.6: Obtained error for different values of the Manning friction coefficient at Werkendam (1 March 2010 until 3 March 2010).

Manning friction [s/m$^{1/3}$]	Mean deviation [m]	Standard deviation [m]	Maximum deviation [m]	R^2 [-]
0.020	0.0987	0.0507	0.1591	0.482
0.021	0.0674	0.0350	0.1217	0.758
0.022	0.0413	0.0183	0.0829	0.914
0.023	0.0278	0.0225	0.0841	0.946
0.024	0.0532	0.0278	0.1134	0.848
0.025	0.0921	0.0261	0.1553	0.615

Table 3.7: Obtained error for different values of the Manning friction coefficient at Werkendam (1 January 2022 until 5 January 2022).

Manning friction [s/m$^{1/3}$]	Mean deviation [m]	Standard deviation [m]	Maximum deviation [m]	R^2 [-]
0.020	0.0985	0.0598	0.1914	0.769
0.021	0.0855	0.0517	0.1717	0.826
0.022	0.0735	0.0423	0.1518	0.875
0.023	0.0618	0.0331	0.1315	0.914
0.024	0.0505	0.0258	0.1111	0.944
0.025	0.0402	0.0224	0.0959	0.963

Table 3.8: Obtained error for different values of the Manning friction coefficient at Werkendam (1 August 2022 until 5 August 2022).

Manning friction [s/m$^{1/3}$]	Mean deviation [m]	Standard deviation [m]	Maximum deviation [m]	R^2 [-]
0.020	0.0235	0.0150	0.0697	0.950
0.021	0.0233	0.0156	0.0682	0.949
0.022	0.0233	0.0170	0.0677	0.946
0.023	0.0234	0.0188	0.0700	0.941
0.024	0.0236	0.0208	0.0766	0.935
0.025	0.0243	0.0228	0.0827	0.928

Comparing the R^2 values from the different simulations results in the selection of a Manning friction parameter of $n = 0.023$ s/m$^{1/3}$. Depending on the location, this gives a mean water level deviation of roughly 2-7 cm. It should be noted that the calibration is mainly focused on flow in the rivers, and only one location in the entrance of the Sliedrechtse Biesbosch. Expecting that the same friction formulation also fits the various creeks and channels in the study area is a significant assumption which should be kept in mind in the evaluation of the results of the connectivity study. More measurements and characteristics of the area would increase reliability.

3.2 Spatial graph development

Crucial in the application of a graph theory is the schematization of the network. The way the system is divided into nodes and edges determines for a large part the metrics and thus governs the outcome of the connectivity assessment. Numerous methods have been used in the development of the spatial graph. Wohl (2017), for instance, describing connectivity as the degree to which matter and organisms can move among patches in a landscape or ecosystem, defines patches as arbitrarily defined areas that vary depend-

ing on the considered time and space scales. Molinari, Stewart-Koster, Malthus, and Bunn (2022) apply a less ambiguous procedure of defining nodes and edges, as inundation maps were used and each raster pixel containing surface water was defined as a node. Nodes were considered to be connected by edges if the node and its immediate neighbour had surface water. Finally, Pearson et al. (2020) start by splitting up the system into a number of sub-areas or distinct cells (nodes), based on properties such as depth contours, hydrodynamic forcing and sediment composition. Next, each individual cell is considered the source node and a simulation is carried out, tracking sediment particles departing from the source node. The cells where the sediment particles end up are characterized as receptor nodes. Edges are identified between a source node and a receptor node and the quantity of particles determines the weight of the link.

For this research it is opted to base the spatial graph development on the layout of channels and bifurcations. Nodes are located at junctions and the channels between the junctions are represented by the graph's edges. This approach leads to a graph consisting of 44 nodes and 64 edges. The graph can be drawn on top of a map, resulting in a relatable image (Figure 3.6), but it can also be drawn in a more schematic way, where the nodes are fixed at their geographical location while the edges are now straight lines between the nodes (Figure 3.7). The visualisation now loses the actual length of the channel. The length, and other properties of the individual channels, can be stored as a weight which can be appointed to an edge.

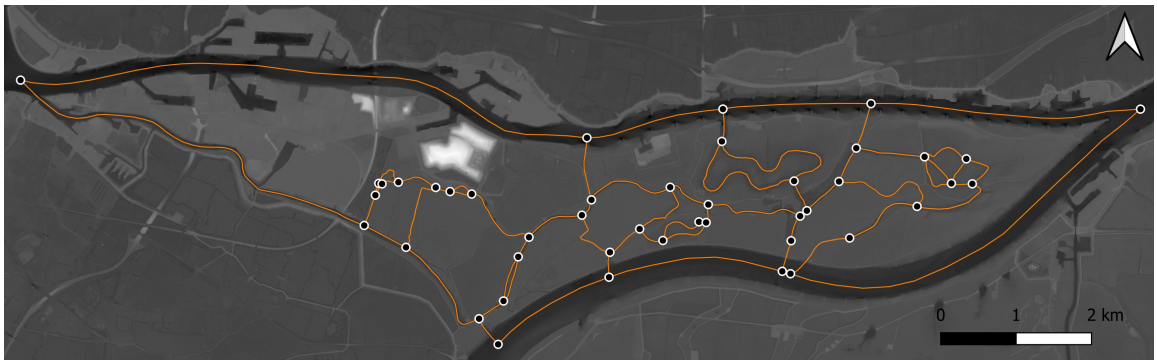

Figure 3.6: Spatial graph development of the Sliedrechtse Biesbosch, where all bifurcations are taken as nodes and the channels connecting the bifurcations are taken as edges.

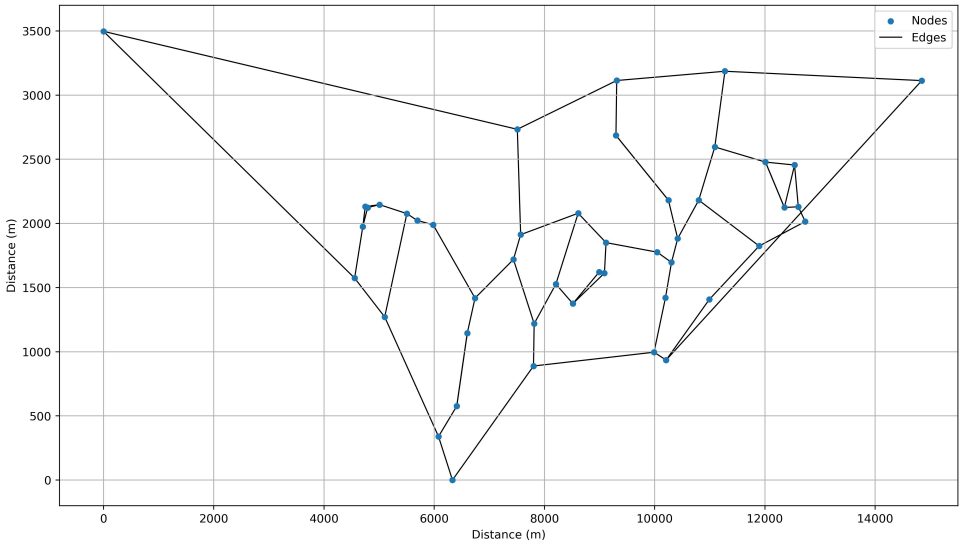

Figure 3.7: Schematized graph of the Sliedrechtse Biesbosch.

By composing graphs in a schematic manner, a clear visualisation of the connectivity of a system appears. As can be seen from Figure 3.7, the Sliedrechtse Biesbosch is fully connected implying that all nodes are connected via links. The system consists of 1 component consisting of 44 nodes. This means that an organism or particle, can in fact travel from a randomly selected point in the system to any other point. This statement only holds if the system is indeed undirected and the travelling subject imposes no specific requirements. However, organisms or particles often do impose requirements. Fish for example might require a maximum flow velocity, while particles or nutrients demand a minimum flow velocity since they can only travel by passive transport. In these cases a threshold can be imposed for a specific edge property. E.g. fish with limited swimming capacity impose a threshold to the maximum flow velocity in a channel. Since the flow velocity is different at any location in the graph, imposing such requirement causes a number of edges that exceed this limit to disappear from the graph. The area now fragments into a system of multiple components and isolated (unconnected) nodes, of which the largest components. The habitat connectivity of the area has decreased. In this research, the habitat connectivity is assessed by investigating the fragmentation and optimizing the available habitat at any point in time.

This approach for assessing the connectivity of an area can be applied for all parameters of interest. If an organism imposes multiple requirements, the analysis can be carried out for each parameter individually and then be placed on top of each other. By examing the fragmentation pattern and causes, weak links are quickly revealed and restoration measures can be designed effectively.

3.2.1 Edge weight

Relevant parameters in the suitability and reachability assessment of habitats are dependent on the considered species. While fish are independently able to determine their preferred living environment based on parameters such as water depth and flow velocities, other organisms or nutrients spread through diffusion and flow. In the latter case, the length of a link is of importance, while for fish the length of a channel might not be an obstruction. Another case where channel length is of importance, is determining the most cost-effective measure. Dredging 1 m of bed material of a 200 m long channel might be more economic than deepening a 150 m long channel by 2 m. In this research, the scope is on aquatic habitat connectivity and flow velocity is considered to be governing.

3.2.2 Spatial and temporal variability

Stationary hydrodynamic boundary conditions would, after some spin-up time of the model, lead to an equilibrium flow condition. This implies that the hydrodynamic conditions at all locations along the domain are constant in time. Practically this never occurs because of upstream water supply due to rainfall or melting ice, causing temporal discharge variations. Also, the penetration of the tide causes water level and flow velocity fluctuations, making the study area a non-stationary water body. In this study, temporal discharge variations at the upstream boundary are neglected. The imposed constant discharge boundary condition was described earlier in this chapter. Water level variations on the other hand are mainly influenced by the sea level. The further upstream an area is with respect to the sea, the less susceptible it is to water level variations of the sea. On the long-term this can be seen in sea level rise, while on a shorter time scale, water level variations can be seen by considering the tide. Since in this research momentary connectivity is to be analyzed, the former is not considered here. Tidal influences however cannot be neglected and, in fact, determine the hydrodynamic character of the Sliedrechtse Biesbosch.

Waves can be distinguished as either deep water waves or shallow water waves, depending on the wave length to water depth ratio. The main difference is that deep water waves are not affected by interaction with the bed while this is the case for shallow water waves. The transition to shallow water waves is usually chosen where the water depth is less than $1/20^{th}$ of the wave length. Tidal waves, with typically wave periods of several hours and wave lengths of several hundred kilometers, approaching the shore and propagating inland are classified as shallow water waves or long waves. The celerity of such waves can be found according to equation (3.7) and is dependent on the local water depth h. A water depth of 5 m, representative for some of the creeks in the Sliedrechtse Biesbosch, equation (3.7) results in $c = 3.50$ m/s. Because of the distance between the most downstream part of the study area, where the tidal wave enters the area, and the most upstream part, a phase difference is to be expected at locations within the domain.

This implies that high water (HW) and low water (LW) do not occur at all locations at the same time. Instead, when it is HW at Dordrecht, water levels upstream of Dordrecht are rising and HW is reached as the tide propagates. This tidal propagation is visualized in figure 3.8. Here, HW is defined as the maximum height reached by a rising tide and LW is defined as the minimum height reached by a falling tide.

$$c = 0.5 \cdot \sqrt{gh} \tag{3.7}$$

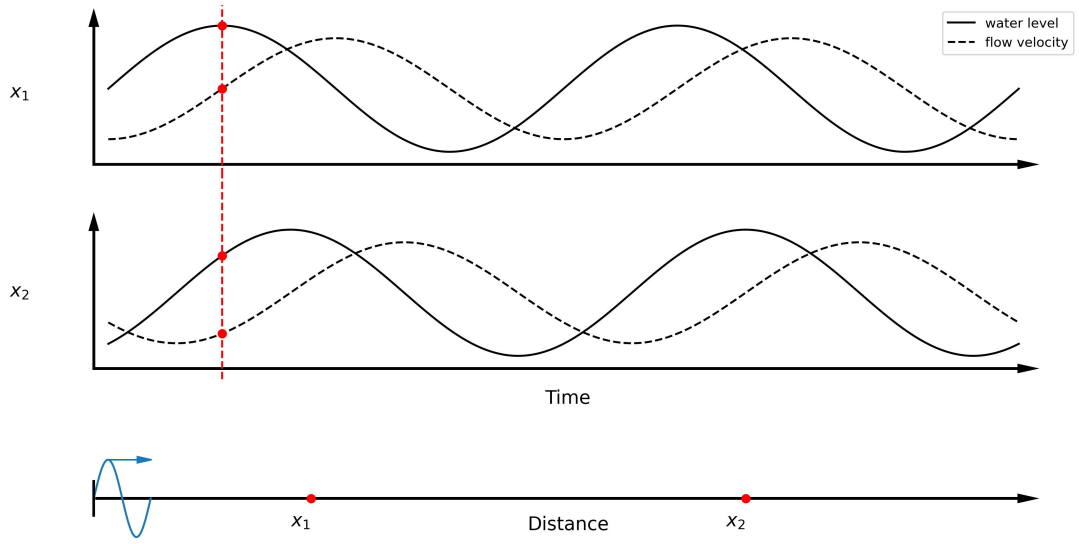

Figure 3.8: Propagation of a tidal wave, crossing two measuring stations at location x_1 and x_2. Since the tidal wave travels with celercity c and distance $x_1 < x_2$, there is a phase difference between the water levels and flow velocities at the two locations.

With respect to the connectivity of the area, this implies that one cannot simply assess the connectivity of the area at one moment in time. Because of the temporal and spatial variability, water depth and flow velocity extremes occur at different locations at different moments in time. On the other hand, a connectivity analysis considering only the extreme values is also not representative, since the tidal influence excludes the possibility of occurrence of extremes at every location simultaneously. Such analysis would inevitably result in a too conservative view of the connectivity, missing the goal of this research of targeted identification of weak channels in a network. Instead, it is decided to assess the connectivity at a fixed interval during a one tidal cycle. The time step for assessing connectivity is chosen at $\Delta\, t\, =\, 10$ minutes, such that one M2 tidal cycle (T =12 hr 25 min) is completely assessed with 75 steps. For each of these steps, a graph is developed, where nodes and edges are identical but instantaneous flow conditions are appended to the edges. This results in different edges to be decisive at each time step. Finally, the relative importance of the representative channels can be determined by analyzing the duration that each channel is decisive during one tidal cycle.

3.2.3 Assemblage

As illustrated in the sections before, spatial and temporal variability are to be included in the graph to obtain accurate results. These are included in the edge weight of all individual nodes. First of all, to take into account the spatial variation between the different channels and even the variation within each channel, a point is plotted along the channel at an interval of $\Delta x_p = 5$ m (Figure 3.9a). To prevent false results based on insufficient depth, it has to be guaranteed that these points are located on the deepest part of the channel cross-section. Therefore, a transect is plotted perpendicular to the channel at each point ($\Delta x_t = 5$ m). Next, points are plotted on each transects, with an interval of $\Delta x_{tp} = 1$ m. This creates a resolution of 5×1 m. Now, for each transect, the points are interpolated onto the topography (Figure 1.3), appending a depth value to every point x_{tp}. Filtering out the deepest point on each

transect, results in an array of points located at the deepest part of the channel cross-section (Figure 3.9b).

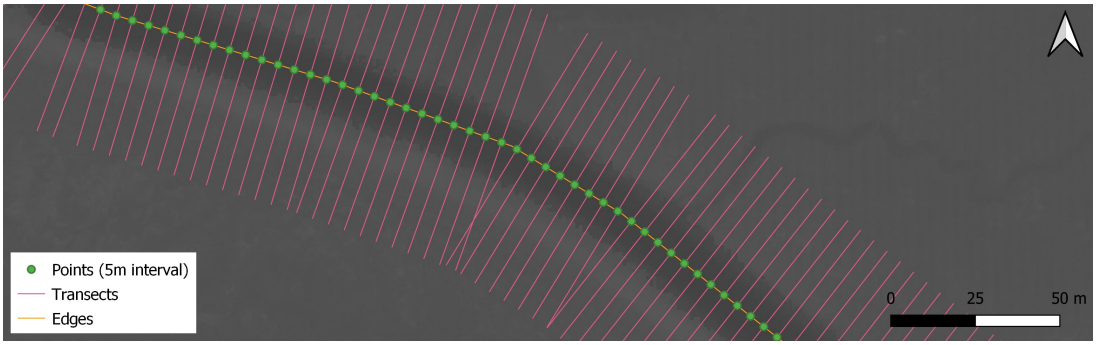

(a) Points and transects plotted along one of the edges of the graph, with interval $\Delta x_t = 5$ m.

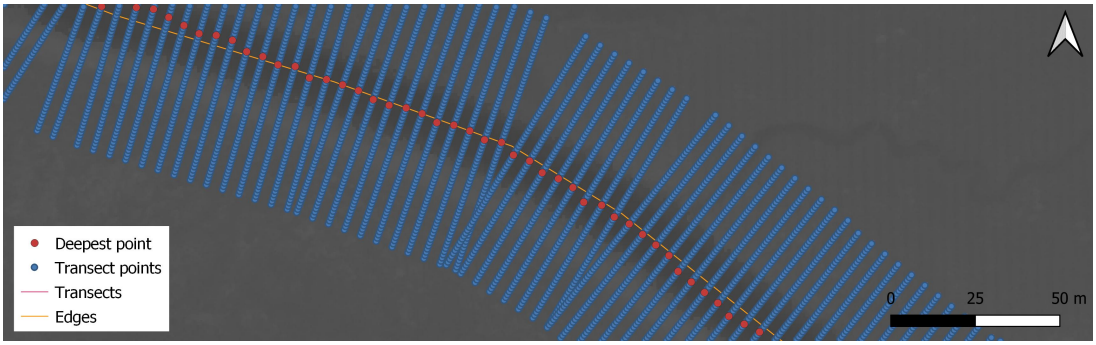

(b) Points plotted along transects with interval $\Delta x_{tp} = 1$ m and eliminating the shallowest points to remain with the deepest part per cross-section.

Figure 3.9: Incorporating spatial variability in the graph.

At the derived deepest points, the modelling output is analyzed. At every point along the edge, a time series for both the water depth and the flow velocity is plotted. Consequently, every edge contains as many time series for the water depth and flow velocity as it has transects. The number of data points per edge is thus different for each edge and can easily be approached by dividing the length of the channel by Δx_p of 5 m. An example of the flow velocities occurring at every 5 m cross-sections is given in Figure 3.10. All absolute flow velocity time series are plotted. This figure also gives the minimum and maximum flow velocity for each time step. This flow velocity envelope includes all other flow velocities found in the channel for each time. Note that the location of these extremes can differ per time step, to obtain the extreme values in the entire channel. Since the connectivity of the network is examined based on a maximum flow velocity, the extreme flow velocity time series (as indicated by the upper red line in Figure 3.10) is attributed as a weight to the graph.

3.3 Interpretation

3.3.1 Assessment metrics

A graph theory approach to connectivity allows the use of numerous metrics, of which an introduction was given in Table 2.3. Different levels of analysis can be applied. The graph can be studied purely looking at the location of nodes and edges, irrespective of their weight and time variability. This gives an initial impression of the graph. For this purpose, the bridges are identified and betweenness centrality is considered. Bridges are by definition weak spots in a graph, as deletion of these links causes immediate fragmentation. Centrality on the other hand can be used to identify the most important nodes in a graph. Betweenness centrality is the most appropriate centrality metric in this research since it measures the number of times a node acts as a bridge along the shortest path between two other nodes. Closeness centrality indicates the most centrally located nodes and degree centrality ranks the nodes by degree.

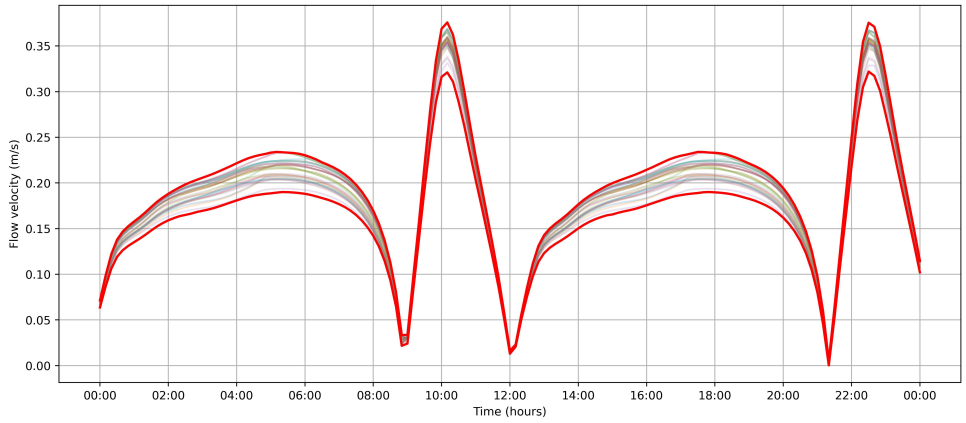

Figure 3.10: Flow velocity time series at individual cross-sections in a channel in the Sliedrechtse Biesbosch. All time series are enclosed by the flow velocity envelope, given in red.

Although these last two metrics can be very useful in studying a graph, they are less appropriate in this research.

A more detailed analysis takes into account the weights and their variation in time. This results in a more accurate view on the area's connectivity.The time-varying connectivity of the Sliedrechtse Biesbosch is assessed by means of three metrics. Since the hydrodynamic conditions in the channels change in time, it is likely that the connectivity metrics change as well. By evaluating the change of the metrics in time, the connectivity states become relative to each other and periods of high connectivity can be discerned from periods of low connectivity. Then assessing the variations in graphs, indicates which edges are most governing to connectivity, and which edges cause fragmentation of the area the most. The three metrics by which the connectivity is assessed, are:

1. *Number of components:* The number of components (NOC) represents the amount of connected subgraphs within graph G. In a connected graph, there is only one component since the entire graph is connected. When fragmentation occurs however, edges disappear and subgroups of connected vertices appear. The NOC in this case increases.

2. *Order of the largest component:* The order of the largest component is the number of vertices in the largest component. The largest component in this case is discerned based on the total channel length within the component, and not on the number of vertices.

3. *Length of connected pathways of the largest component:* The length of connected pathways (LOCOP) of the largest component is the cumulative length of all connected edges in the largest component of the graph, a metric that was introduced by Okin et al. (2009). A larger LOCOP represents a larger size of the available habitat.

3.3.2 Network diagrams

Since the connectivity is evaluated every 10 minutes, a network diagram can be drawn for every time step. This results in a series of figures. By comparing the diagrams for time steps where large changes in assessment metrics occur, one can observe what happens with the availability of the individual edges in the graph. Analysis of these changes leads to the identification of cut-edges and contribute to the selection of local nature restoration measures.

4

Results: Current connectivity of the Sliedrechtse Biesbosch

In this chapter, the results of the connectivity study are discussed for the current state of the Sliedrechtse Biesbosch. Literature on applications of graph theory to quantify connectivity, as treated earlier (Chapter 2), as well as the graph and hydrodynamic model (Chapter 3) provide the foundation of the conclusions on the area's connectivity. The magnitude of the introduced metrics vary in time and are visualized in a summarizing figure first. Then, this figure and associated metrics are thoroughly analyzed by elaborating on the most striking features. This enables a complete understanding of the connectivity time-state of the area and allows to recognize vulnerable locations that limit this connectivity. Finally, the sensitivity of the connectivity results to the imposed flow velocity threshold is investigated and various suggestions are done to prevent fragmentation of the area. These measures are further developed and implemented in the next chapter (Chapter 5) to emphasize the usefulness of this objective way of looking at connectivity and develop restoration measures on a local level.

4.1 Graph theory

The graph-theory approach to this connectivity study is best discussed in two steps. First the time evolution of the assessment metrics is visualized and remarkable changes are noted. Next, these changes can be explained by analyzing the time-specific graphs.

4.1.1 Connectivity results

Based on structural aquatic habitat connectivity one can say that the Sliedrechtse Biesbosch is fully connected or, in graph-theory terms, the system can be described as a connected graph. In other words, a random point in the water system can always be reached from any other point in the system, since all creeks and channels are somehow attached to each other. A visualization of the connected graph can be found in Figure 3.7. Functionally however, the 'connectedness' of the graph is not guaranteed and is dependent on the hydrodynamic properties of the flow. The flow velocity requirement ($u_{max} = 0.3$ m/s) results in fragmentation of the graph, forming several connected subgraphs. The tidal character of the area is expected to influence the connectivity continuously since water level and flow velocity change as a consequence of the tide.

4.1.2 Metric interpretation and evaluation

First the network is examined by means of identification of the bridges and betweenness centrality. As can be seen from Figure 4.1, the graph contains 16 bridges (represented by the thick lines in the figure). The color of the bridge indicates the impact of deletion of the corresponding edge on the size of the largest remaining component in the graph. This clearly illustrates the relative irrelevance of bridges located on the outside of the graph, while bridges located in the centre of the graph are crucial. In the case of the Helsloot and Zoetemelkskil, a relative fragmentation of around 35 % and 40 % can be observed, respectively.

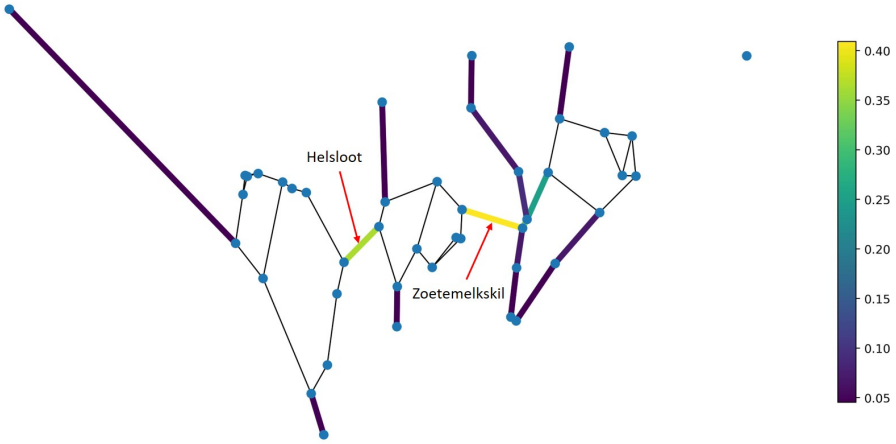

Figure 4.1: Bridges in the graph of the Sliedrechtse Biesbosch and the relative fragmentation after deletion of each individual bridge.

Quantifying the betweenness centrality of the individual nodes, results in a similar pattern. In Figure 4.2, the nodes located at the Helsloot and Zoetemelkskil again appear to be important to the graph. The color of the nodes indicates the relative number of times the nodes was passed in the shortest path between any two nodes in the graph. It makes sense that the nodes around bridges in the centre of the graph have high betweenness centrality, since the shortest path between any node on the left side of the graph and any node on the right side of the graph inevitably crosses the bridges. What can be observed as well is the relatively low betweenness centrality of the nodes on the outside of the graph. This can be explained by the fact that these nodes are crossed by fewer shortest paths.

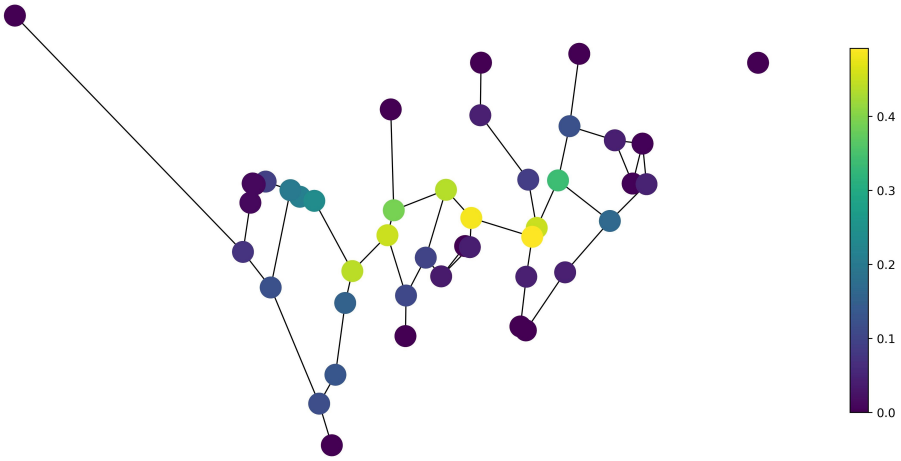

Figure 4.2: Betweenness centrality of the individual nodes in the graph of the Sliedrechtse Biesbosch.

The connectivity variation in time is described by the three metrics introduced in the previous chapter: the number of connected components in the graph, the number of nodes in the larges component in the graph (order), and the LOCOP of the largest component in the graph. The connectivity variation during 24 hours, accompanied by the water level variation at Dordrecht, can be found in Figure 4.3.

The variation of the connectivity metrics in time as given in Figure 4.3 is still quite abstract. However, some remarkable conclusions can be given. Particularly the reduction of the graph's LOCOP from roughly

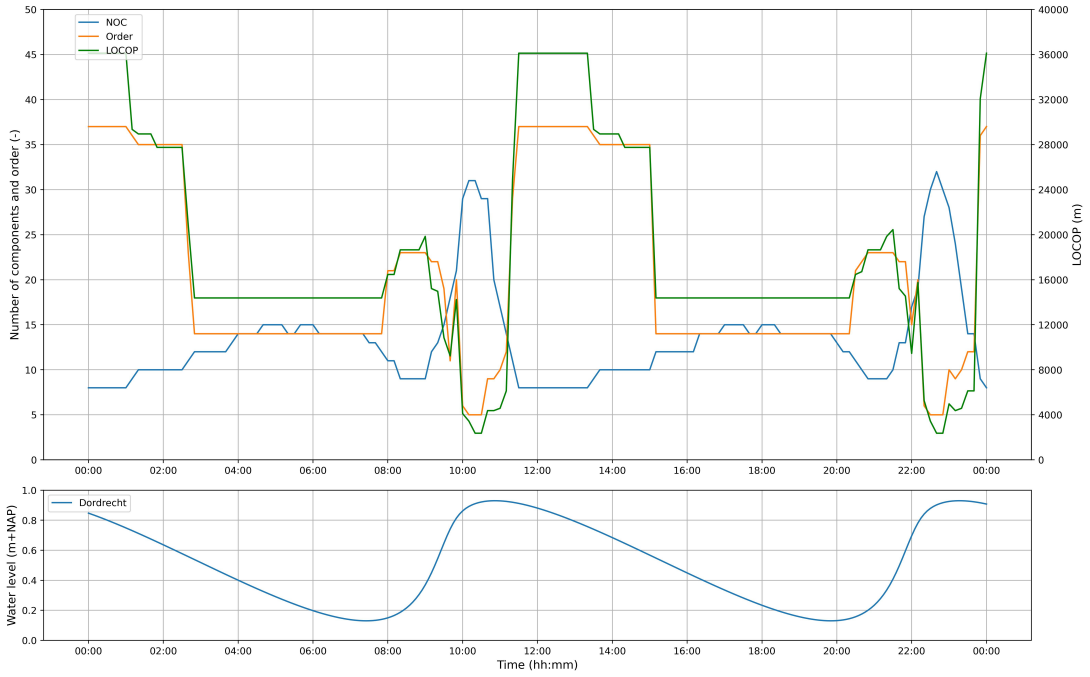

Figure 4.3: Evolution of connectivity of the Sliedrechtse Biesbosch during one day and a maximum tolerable flow velocity of $u_{max} = 0.3$ m/s, evaluated by means of three metrics: the number of components in the graph, the number of nodes in the largest component, and the LOCOP and length of connected pathways of the largest component. The bottom figure gives the water level variations in time at the most downstream location of the domain, at Dordrecht.

36 km to 14.5 km indicates that large connectivity variation is found. Relevant connectivity variations can be distinguished at times where one or more of the metrics change considerably, e.g. where there is a small instantaneous increase in the maximum number of components (blue line), a large and sudden drop of the maximum number of nodes in the largest component (orange line) and a large instantaneous decrease of the LOCOP of the largest component (green line). These three characteristics occur when the network suddenly fragments into two or more components. If a small increase of the NOC (small rise of the blue line) and a significant decrease in the number of nodes of the largest component (large drop of the orange line) is observed, this indicates that an edge in the middle of the component is removed since local flow velocities exceed the threshold value. This combination indicates that a new component splits off entailing multiple nodes. Such a combination can be found in Figure 4.3 from 03:10 to 03:20 and from 15:20 to 15:30. The time difference of roughly half a day is not coincidentally and can be attributed to the tidal period. After all, the same hydrodynamic situation occurs with an interval of approximately 12 hours and 20 minutes. By evaluating the difference between the graph at times just before and just after prominent changes in the metrics occur, the location of fragmentation can be identified.

The simulation results allows more detailed analysis of the flow velocity in the area, which can be used to explain the fragmentation pattern observed in Figure 4.3. This is given for one tidal cycle in Figure 4.4 with a time step of 30 minutes. As can be seen from the figure, the flow velocity in the Nieuwe Merwede is continuously larger than 0.30 m/s, while the flow velocity in (part of) the Beneden Merwede is only smaller than this value for short periods just before HW (10:00) and just after HW (00:00 to 01:00 and 12:30).

In the following, striking metric changes in Figure 4.3 are analyzed, while Figure 4.4 is referred to in some cases for additional explanation.

01:00 - 01:10

Between 01:40 and 01:50, Figure 4.3 indicates a major drop in graph LOCOP, from 36 km to 29 km. In the mean time, the NOC slightly increases from 8 to 9 and the number of nodes in the largest component

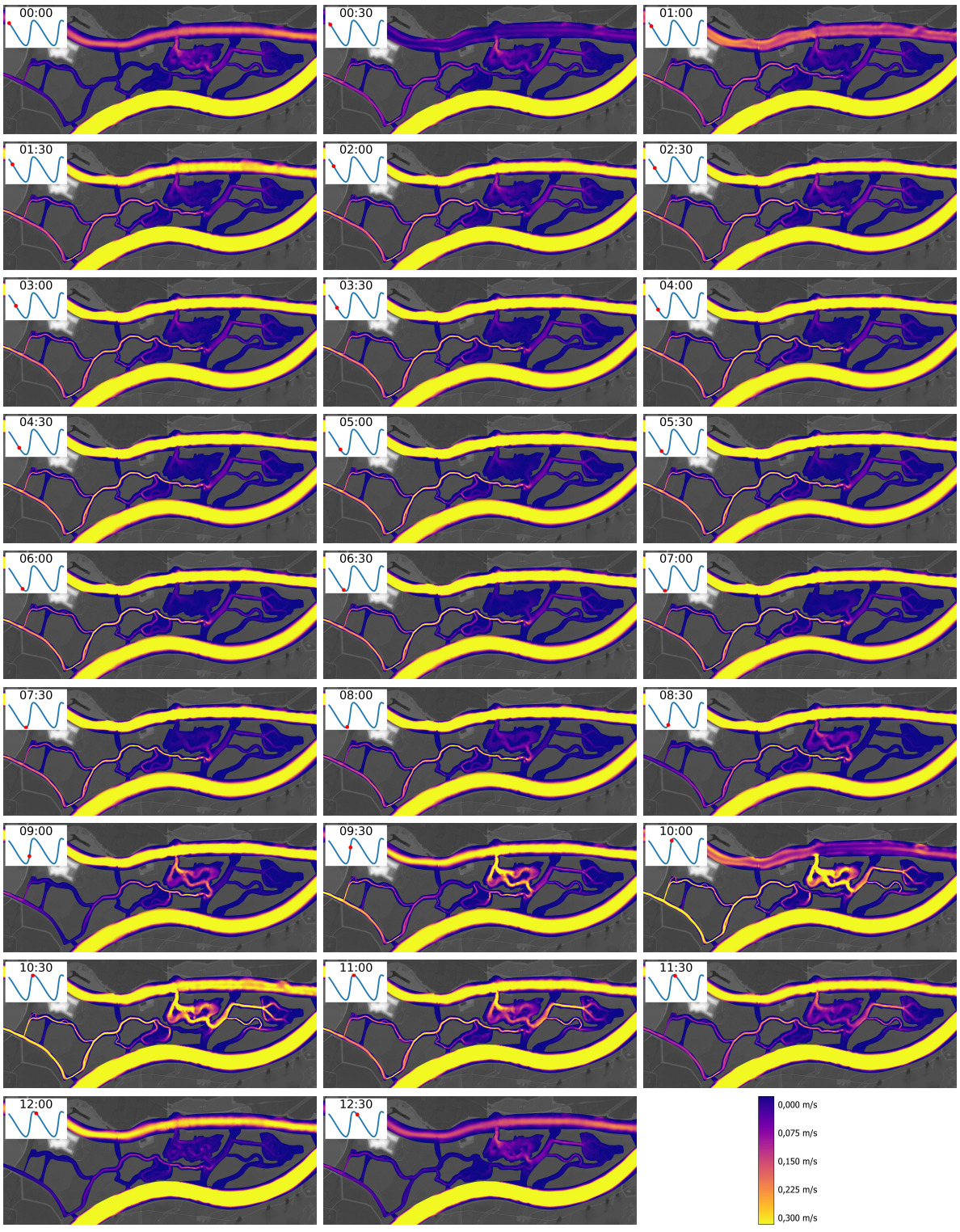

Figure 4.4: Flow velocities in the Sliedrechtse Biesbosch during one tidal cycle, given per 30 minutes and indicating the respective water level at the downstream end of the Beneden Merwede (at Dordrecht). Flow velocities of 0.30 m/s and larger are indicated in yellow.

reduces from 37 to 36. From these numerical changes, it can be deduced that initially the graph is quite connected (from a combination of low NOC, large number of nodes in the largest component and a large LOCOP of the largest component). Also one can derive that graph fragmentation is likely to occur on the

outer edges of the graph, since the number of nodes in the graph decreases with one, while the number of components increases with one (fragmentation of one single edge, leading to an isolated node). Finally it is expected that the disconnected edge has a large length, since the LOCOP decreases considerably. Evaluating Figure 4.5a and Figure 4.5b confirms all three hypotheses and shows that the disconnected edge is indeed a relatively long edge on the outside of the graph. The disconnected edge corresponds to the most downstream part of the Wantij.

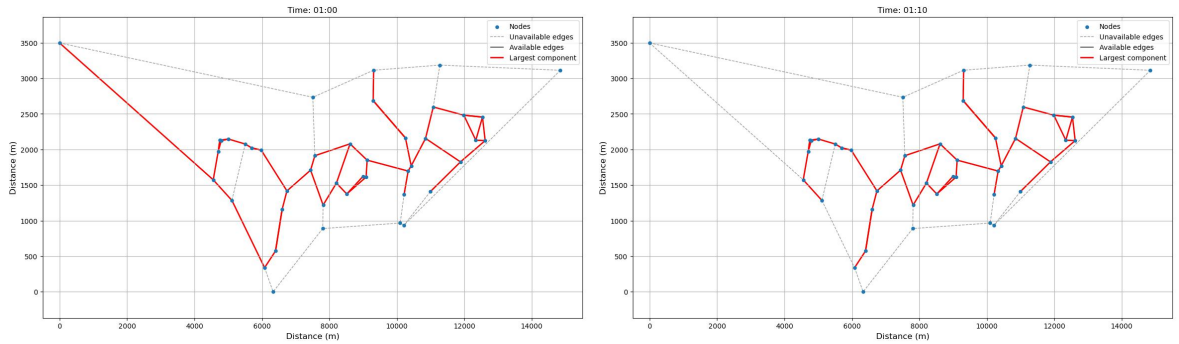

(a) Graph at t = 01:00.

(b) Graph at t = 01:10.

Figure 4.5: Evolution of the graph from 01:00 to 01:10.

02:30 - 02:40 - 02:50

Similarly to 01:00, a significant decrease in LOCOP is observed between 02:30 and 02:50. The clear difference however, is the fact that in this case also a large drop in the number of nodes in the largest component occurs (from 35 to 14). The increase in the number of components is not considerable (increase of 2). By reasoning, it can be suggested that this is a result of considerable fragmentation. Although the increase in the NOC is limited, the largest component shrinks significantly. Therefore it is likely that at least one of the edges in the centre of the graph disconnects and splits the graph into two or more smaller components. This is exactly what can be observed by considering the corresponding graphs (Figures 4.6a to 4.6c). The edges, corresponding to part of the Helsloot and Zoetemelkskil creeks, disconnect because of flow velocities exceeding 0.3 m/s. Their location in the centre of the graph and the fact that there is no diversion around the considered channels, result in fragmentation. As can be seen from Figure 4.3, this connectivity state lasts for more than 5 hours per tidal cycle (10 hours per day).

07:50 - 08:00

Unlike the first two considered time intervals, the interval from 07:50 to 08:00 shows an increase in both the LOCOP and the number of nodes in the largest component of the graph. Since the number of nodes increases with 7 and the LOCOP increases to about 16.5 km, a re-connection of the network takes place. The extent to which each re-connected node contributes to the LOCOP of the component is not clear. One possibility is that every re-connected node is located on edges on the outside of the graph and contributes to the LOCOP. Another possibility is that six of the seven re-connected nodes are located in the centre of the graph, while only one re-connected node corresponding to a long edge induces the entire increase of LOCOP. Finally, all possibilities in between can be considered. To gain insight in the exact cause of the increase in metrics, Figure 4.7a and Figure 4.7b are considered. Comparison of the graphs indicates that a significant part of the increased LOCOP can be attributed to the re-connection of the Wantij channel and that by the availability of the edge representing the Helsloot two components are merged.

09:00 - 09:10

The major decrease in LOCOP of the largest component in the graph between 09:00 and 09:10, largely matches the situation between 01:00 and 01:10 (see Figure 4.3). Again, the decrease in nodes with one, in combination with a decrease of almost 5 km in LOCOP, is likely to be caused by the disconnection of

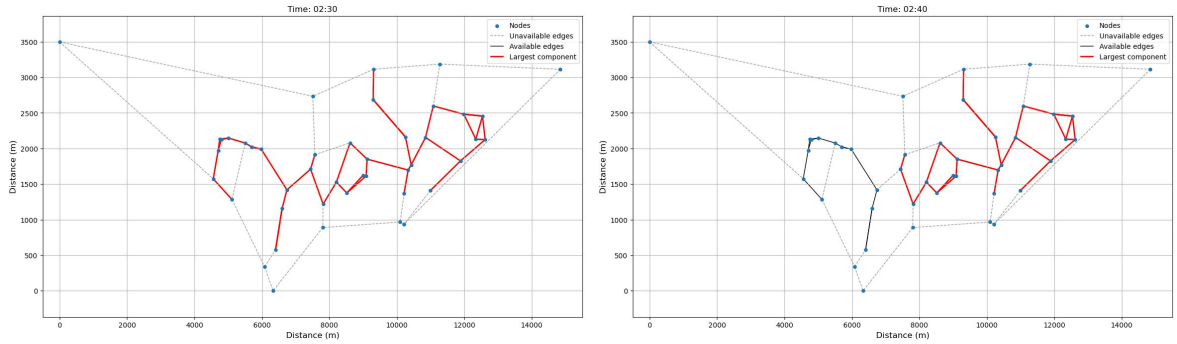

(a) Graph at $t = 02{:}30$.

(b) Graph at $t = 02{:}40$.

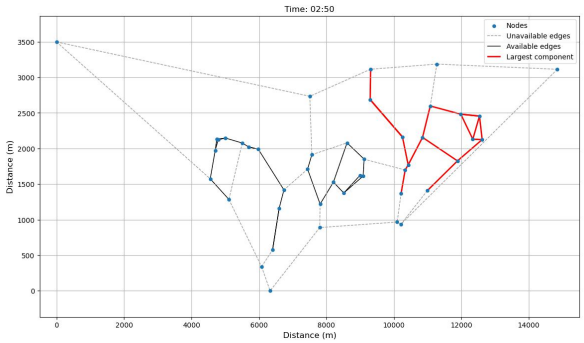

(c) Graph at $t = 02{:}50$.

Figure 4.6: Evolution of the graph from 02:30 to 02:50.

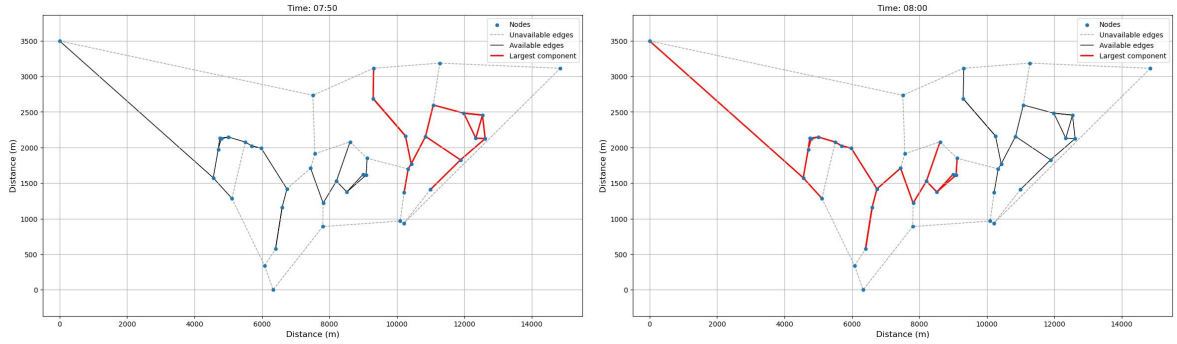

(a) Graph at $t = 07{:}50$.

(b) Graph at $t = 08{:}00$.

Figure 4.7: Evolution of the graph from 07:50 to 08:00.

a node on the outside of the graph and receiving a long edge. Figure 4.8a and Figure 4.8b confirm this assumption by showing the disappearance of the Wantij.

09:30 - 09:40 - 09:50 - 10:00

Around 09:30, the metrics in Figure 4.3 show a large variation within an interval of 30 minutes. In fact, the values change every ten minutes. Between 09:30 and 09:40, a decrease in both the LOCOP and the number of nodes is observed. From Figure 4.3 it is not possible to say what exactly is the cause of the change in metrics. From 09:40 to 09:50 as slight re-connection can be observed while between 09:50 and 10:00, a clear fragmentation pattern can be seen: a combination of decreasing LOCOP and number of nodes in the largest component with an increasing NOC in the graph. The evolution of the metrics can be attributed to the re-connection and disconnection of channels as given in Figures 4.9a to 4.9d. Again, the importance of the Helsloot and Zoetemelkskil creeks is emphasized, since these cause the fragmentation in Figure 4.9b. and the increase in LOCOP in Figure 4.9c.

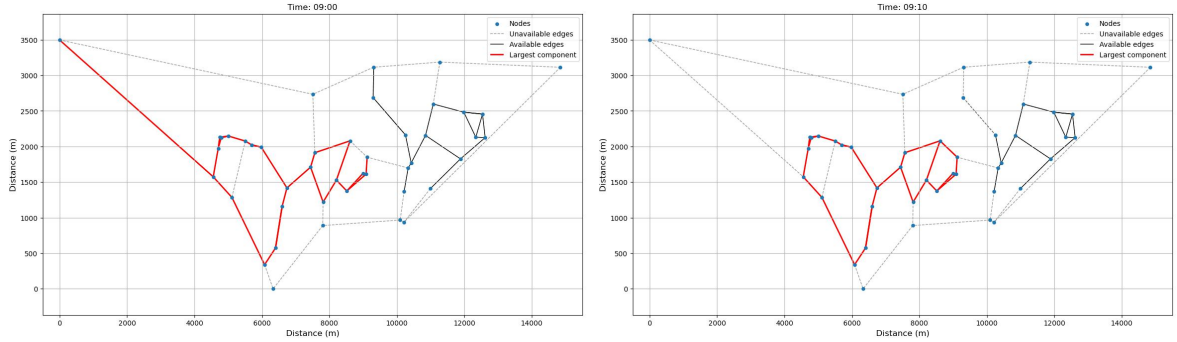

(a) Graph at $t = 09{:}00$. **(b)** Graph at $t = 09{:}10$.

Figure 4.8: Evolution of the graph from 09:00 to 09:10.

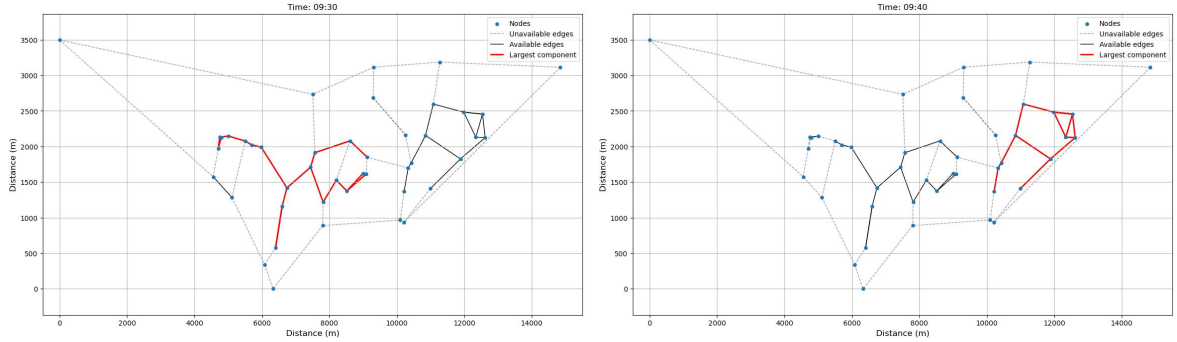

(a) Graph at $t = 09{:}30$. **(b)** Graph at $t = 09{:}40$.

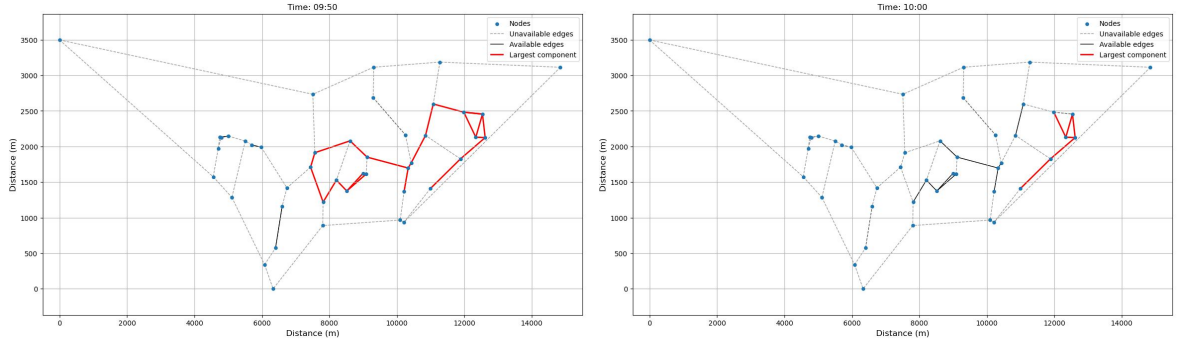

(c) Graph at $t = 09{:}50$. **(d)** Graph at $t = 10{:}00$.

Figure 4.9: Evolution of the graph from 09:30 to 10:00.

10:20

The network reaches its most fragmented state at 10:20. This is indicated by the minimum value for both the LOCOP and the number of nodes in the largest remaining component in combination with the maximum NOC in the graph. From Figure 4.10 it appears that only in the most upstream part of the Sliedrechtse Biesbosch the flow velocities do not exceed 0.30 m/s. This occurs around high water and from Figure 4.4 it can be observed that especially the flow velocities in the polder Kort- en Lang Ambacht (connected to the Beneden Merwede, see Figure A.1) are large. This is caused by the rising water level in the Beneden Merwede. During low water, the flow in the Beneden Merwede is directed downstream. However, when the downstream water level rises due to the tide, the flow is counteracted by a higher

water level, reducing the flow velocity and even changing the flow direction. Since the water level in the Beneden Merwede rises quicker than the water level in the Sliedrechtse Biesbosch (via the Wantij), the flow is diverted through the polder Kort- en Lang Ambacht. This results in the situation that water flows into the polder from two directions of the Beneden Merwede, as can be seen in Figure 4.11. Around 10:20, HW reaches the Zoetemelkskil and the the flow is directed further into the area, towards the polder Aart Eloyenbosch (the most upstream located creeks within the Sliedrechtse Biesbosch, see Figure A.1). Flow from the Wantij and flow from the Kort- en Lang Ambacht are now both directed into the Aart Eloyenbosch, resulting in relatively large flow velocities.

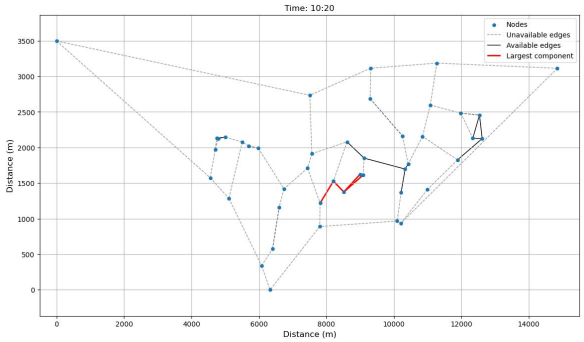

Figure 4.10: Graph at t = 10:20.

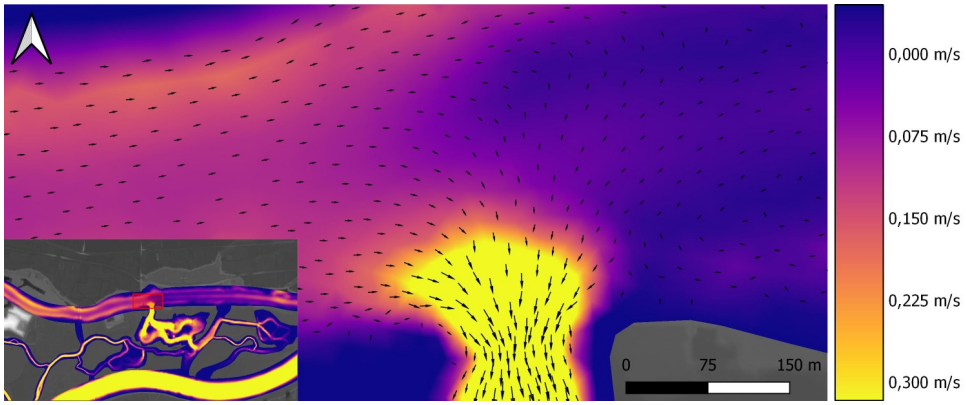

Figure 4.11: Flow direction and magnitude at the Kort- en Lang Ambacht inlet from the Beneden Merwede.

11:10 - 11:20 - 11:30

The final remarkable event in Figure 4.3 is the large increase in LOCOP and number of nodes which occurs between 11:10 and 11:30. This increase covers almost the entire range between the metrics' minima and maxima. This is likely to happen when a very fragmented graph re-connects and multiple small components merge into fewer large components. This is exactly what can be observed from Figures 4.12a to 4.12c. In the first ten minutes, the Wantij is re-connected, causing a large jump in the LOCOP of the largest component in the graph (Figure 4.12b). The LOCOP and number of nodes are further increased by re-connection of the Helsloot and Zoetemelkskil, as these edges attach three smaller components and form one large component (Figure 4.12c). Note that after 11:30 the state of connectivity remains more or less constant until 13:20. At 13:20 a similar connectivity evolution can be noticed, which is attributed to the tidal period of 12 hours and 25 minutes. The pattern as found in roughly the first half of Figure 4.3 is therefore repeated every 12.40 hours.

For the most noticeable changes in connectivity metrics (Figure 4.3) the source of the changes was described above. However, more (less significant) changes can be found in the metrics, of which the NOC

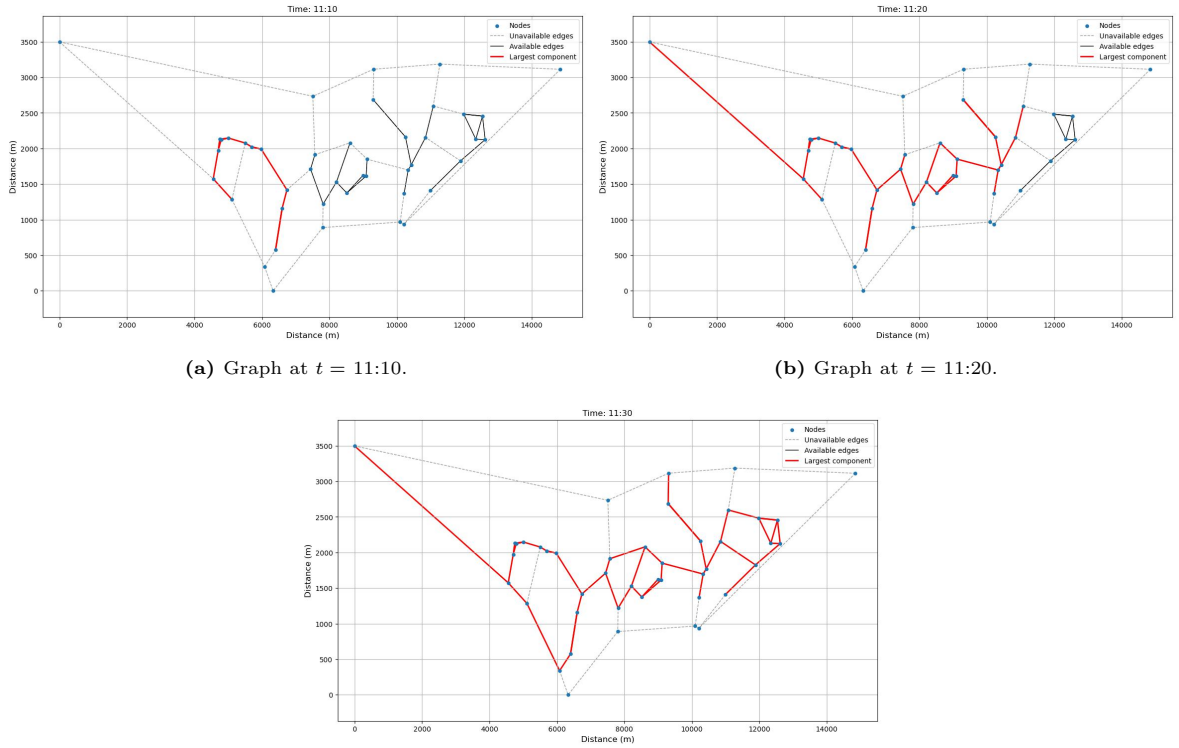

(a) Graph at $t = 11{:}10$.

(b) Graph at $t = 11{:}20$.

(c) Graph at $t = 11{:}30$.

Figure 4.12: Evolution of the graph from 11:10 to 11:30.

specifically changes continuously. For the sake of completeness, all temporary graphs can be found in Appendix C to derive the development of all individual metrics in time.

4.2 Conclusions

From the evolution of the metrics and the corresponding temporary graphs, two main conclusions can be drawn about the fragmentation of a graph:

1. The connectivity metrics used in this approach are very sensitive to the disconnection and reconnection of large edges on the outside of the largest component in the graph. In the case study of the Sliedrechtse Biesbosch this can especially be linked to the sensitivity of the metrics to the availability of the Wantij. Whenever this edge is available, it is almost always part of the largest component because of its relatively large length. This causes major fluctuations in the LOCOP of the graph as the channel's length is over 5200 m and the maximum graph LOCOP found throughout the entire tidal cycle is around 36 km. Although disconnection of the Wantij largely effects the metric evolution, it's impact on connectivity is relatively limited. As connectivity is defined as the extent to which the network is fragmented, the location of the channel on the outside of the graph reduces the impact on the network's connectivity.

2. The other situation that impacts the connectivity metrics most, is the situation in which edges in the centre of the graph disappear, given that these edges are bridges between two or more components. A bridge in this case is defined as an edge between two nodes that cannot be reached via another path in the graph. In the Sliedrechtse Biesbosch this is specifically the case for the Helsloot and the Zoetemelkskil. When (one of) these edges disappear(s) from the graph the LOCOP significantly reduces, as well as the number of nodes in the largest component. Also, the times at which this happens corresponds to the maximum values of the NOC within the graph. A larger NOC implies a more fragmented graph.

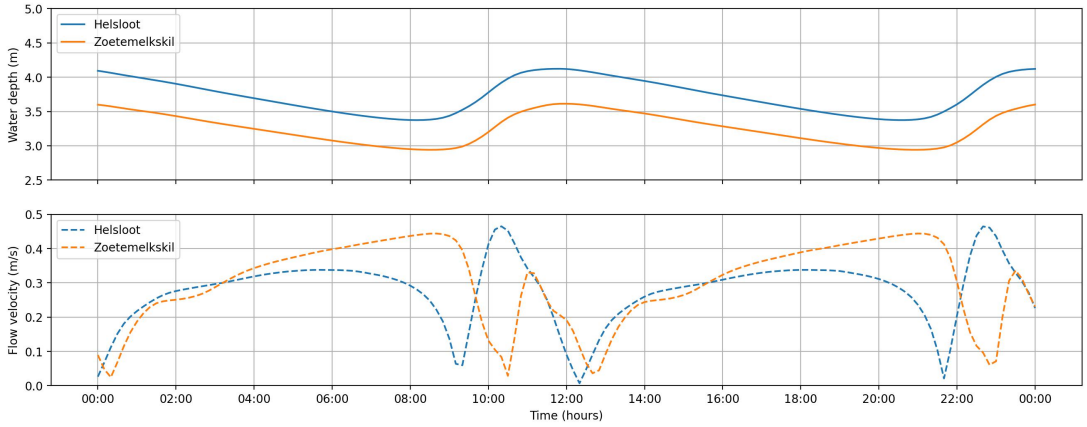

Figure 4.13: Water depth and flow velocity variations in time in the Helsloot and Zoetemelkskil creeks. Note that the absolute velocity in the channel is given, neglecting the direction of the flow. The flow direction changes when the flow velocity approaches zero.

4.3 Threshold sensitivity

The results discussed before are based on a flow velocity of 0.3 m/s. It is emphasized that this threshold is relevant for a particular species such that the aquatic habitat connectivity of that species is investigated. Different species come with other preferences which results in other threshold parameters and values. To indicate the effect of the flow velocity threshold on connectivity result, an analysis is carried out applying different threshold values. Weatherfish (Misgurnus fossilis, Figure 4.14a), for example, prefer only small flow velocities ranging from 0 to 0.1 m/s. Burbot (Lota lota, Figure 4.14b) on the other hand accept a larger range of flow velocities, between 0 and 0.5 m/s (Marijs et al., 2020).

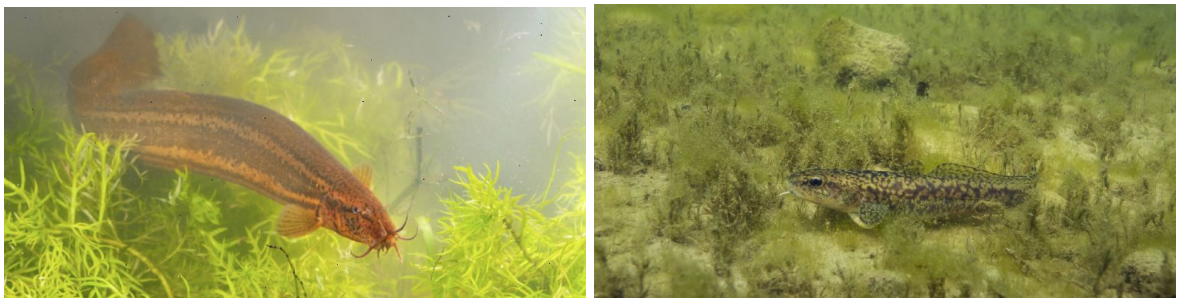

(a) Weatherfish (Misgurnus fossilis).

(b) Burbot (Lota lota).

Figure 4.14: Fish species with different habitat preferences (Marijs et al., 2020).

The results for different flow velocity thresholds are given in Figure 4.15. As can be observed, the available habitat for weatherfish is always smaller than the available habitat for flounder. This is explicable since weatherfish accept only limited flow velocities of maximum 0.1 m/s while flounder accept velocities up to 0.3 m/s. The available habitat for weatherfish is therefore always also available for flounder. The same observation can be found while considering the length of connected pathways of burbot. Since this species accepts larger flow velocities up to 0.5 m/s, the available habitat is also much larger than that of flounder and weatherfish. It can be noted that for burbot, the maximum LOCOP of around 36 km is available for almost 80 % of the tidal cycle (9.5 hours per tidal cycle). This implies that the flow velocity does not exceed 0.5 m/s in the largest part of the Sliedrechtse Biesbosch during this time. From the analysis it can be found that the definition of the threshold significantly impacts the available habitat. The proposed method is therefore particularly useful considering a specific (fish) species instead of the entire fish class.

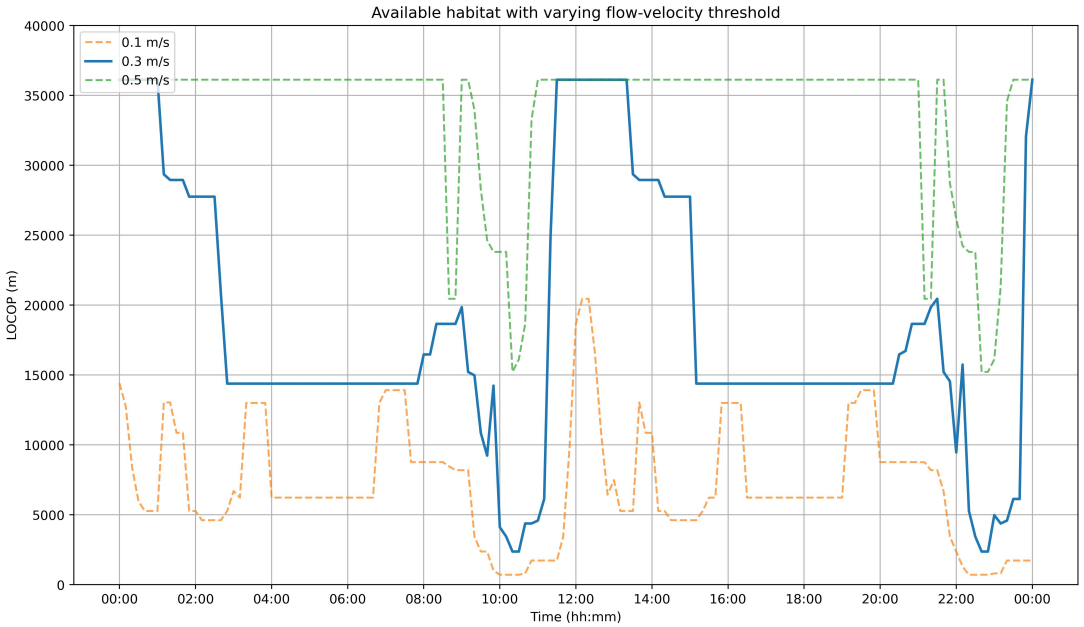

Figure 4.15: Available habitat expressed in the length of connected pathways (LOCOP) for different flow-velocity thresholds. This research is based on a threshold of 0.3 m/s.

4.4 Adequate measures

As stated in the conclusions of the connectivity analysis, disconnection of the Wantij largely impacts the LOCOP of the graph, but it doesn't impact the overall connectivity of the network significantly. Therefore recommendation is made to accept the decoupling of this edge and to give consideration to other crucial locations, such as the Helsloot and Zoetemelkskil creeks. These two edges determine the LOCOP of the graph for 5 hours per tidal cycle, which is over one third of the duration. Since the flow velocity u is selected to be the threshold parameter in the system, specific attention should be given to the flow velocities in the considered channels.

Various measures can be thought of to reduce the fragmentation of the Sliedrechtse Biesbosch. These can be subdivided into different hydraulic strategies, each with multiple interventions:

1. *Construct a bypass*
   The connectivity governing channels in the study area are the Helsloot and the Zoetemelkskil. These channels are crucial in the connectivity because they are the only link between two polders or sub-networks. One can think of their importance by considering an electric circuit, which can be series or parallel. In a series circuit, all components are connected end-to-end to form a single path for current flow, while in a parallel circuit all components are connected across each other with two or more different paths. In a series circuit, if a path is interrupted, the remaining components after the interruption are not in service any more. In a parallel circuit, if a path is interrupted, the remaining components are still reachable via other paths. Although the metaphor with electric circuits doesn't fully hold, it gives a clear illustration of the difference between in series connected systems and parallel connected systems. In the study area used here, the Helsloot and Zoetemelkskil creeks can be compared to in series connected links between nodes of a parallel connected network. To make the system more resilient to flow velocity fluctuations, a bypass around these channels can be constructed to create a parallel network instead of a partly series network.

2. *Locally reduce the flow velocity*
   Various factors influence the flow velocity in a channel. Among these are the volume of water (discharge), the shape of the channel, the slope of the channel and the friction exerted by the bed and vegetation in the channel. By changing (one of) these parameters, the flow changes. This implies that adjusting the channel properties such as the width, depth or the friction, influence the

flow velocity in the channel.

3. *Divert the flow out of the area*
   Similar to constructing a bypass within the considered area to prevent excessive flow through a specific channel, it could also be aimed to direct the flow around (part of) the area.

In order to prevent the flow velocity in the Helsloot and Zoetemelkskil from exceeding the threshold value, the current flow velocities have to be considered and lowered by means of measures. As can be seen from Figure 4.13, the flow velocity during falling tide in the Helsloot is slightly above the threshold value of 0.3 m/s, such that a small adjustment to the channel might already improve its availability. Based on the area's protected status, dredging measures are undesired. Therefore, roughening of the channel is proposed by means of adding vegetation to the channel banks and bed. The high water results in relatively high flow velocities ($u > 0.4$ m/s) but this is of short duration. Therefore the short period of fragmentation is accepted here.

For the Zoetemelkskil, the low water results in the highest flow velocities. Since the falling tide takes almost three times as long as the rising tide, a more profound measure is to be taken here. Although adjusting the channel dimensions might offer a solution here, the area layout is very suitable for the construction of a bypass. The Zoetemelkskil is located on the south of the Kort- en Lang Ambacht polder, as can be seen in Figure A.1, and a bypass could be constructed from this polder to the bifurcation of the Doode Kikvorschkil and Zoetemelkskil. This bypass could then take over part of the discharging capacity of the Zoetemelkskil or lead to a reduction in flow velocity in the channel.

Further details and implementation of the possible measures discussed above are specified in the following chapter.

5

Results: Effects of measures on connectivity of the Sliedrechtse Biesbosch

In this chapter various restoration measures are investigated. The approach is similar to the connectivity study of the present study area, but four adjustments to the area are implemented. First, a bypass is constructed around the Zoetemelkskil. This requires adjustment of both the graph and the numerical model. Then, cases are examined in which the two locks that are situated in the area are permanently opened. In these cases, the graph remains the same but the numerical model needs a small adjustment. Finally, a case in which all three measures are implemented is treated. For all cases the efficacy is assessed by means of the ***number of components****, the order of the largest component and the* ***length of connected pathways*** *of the largest component and comparing these results with the results from the present area connectivity.*

5.1 Implementing measures

To examine the effect of potential connectivity improving measures, such as elaborated in section 4.4, updated hydraulic data must be gathered. Since an adjustment in channel lay-out causes other flow velocities and water levels. Although in the assessment of present connectivity, an analysis based on physical measurements can be carried out (if available), this is not possible for studying the connectivity in a fictive area lay-out. One is now reliant on an accurate numerical model. As for the Sliedrechtse Biesbosch, a numerical model was already set-up for gathering hydraulic data of the original area lay-out, the proposed measure can simply be implemented in the numerical model to find the corresponding data relevant for the connectivity study. For any improvement measure, the numerical model needs to be adjusted to gather accurate data. However, dependent on the type of measure to be investigated, the network schematization (graph) also needs to be adjusted. Individual channel adjusting measures do have an effect on the hydraulic properties of a water system, but the graph remains unchanged. The connection between two present points already exists. Constructing a bypass on the other hand, implies a change in graph. In this case, a new connection is constructed between two points in the system, which should be represented by a new edge between two nodes.

To demonstrate the ease of forecasting connectivity by implementing measures, this process is carried out for the construction of a bypass. Although many other options are at one's disposal, this measure is selected because it requires a revision of the full connectivity assessment process, including the adjustment of both the network schematization and the numerical model. In section 4.2, the Zoetemelkskil was stated to be one of the connectivity limiting channels. Furthermore, a bypass around this channel was selected as a potential measure here looking at the location of the channel with respect to surrounding channels. Therefore, this location is chosen for implementing the bypass measure. Furthermore, the habitat connectivity effects of permanently opening the locks present in the area is examined. Also a case in which all three measures are considered is treated. The four restoration measures to be tested are listed below and are treated in the following sections of this chapter.

1. Constructing a bypass around the Zoetemelkskil.
2. Permanently opening the Helsluis to create an open connection between the Helsloot and the Beneden Merwede.
3. Permanently opening the Ottersluis to create an open connection between the Wantij and the Nieuwe Merwede.
4. Combination of the three measures listed above.

5.2 Bypass around Zoetemelkskil

5.2.1 Spatial graph development

The case study area is schematized into a graph in the same way as was done for the present lay-out, with nodes on the channel junctions and edges as the channels. In this case however, a bypass has been constructed (as can be seen by comparing Figure 5.1 with the original lay-out in Figure 3.6). As this bypass is an extra connection in the graph and a new junction is created, the number of nodes and edges increase. This area lay-out results in a graph consisting of 45 nodes and 66 edges.

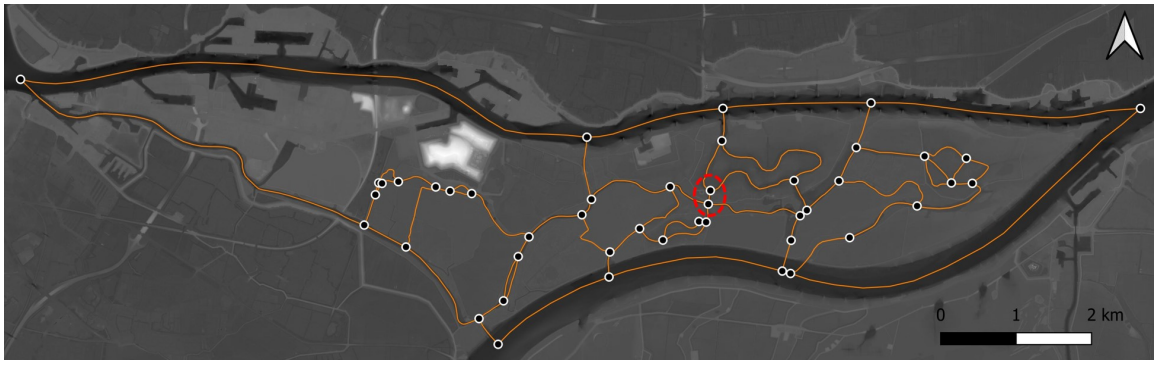

Figure 5.1: Spatial graph development of the Sliedrechtse Biesbosch, including a bypass around part of the Zoetemelkskil.

The proposed bypass has a length of 140 m and a width of approximately 30 m. The bed is located at -1.0 m+NAP. The cross-sectional shape of the bypass resembles a rectangular channel. The location and a cross-sectional view can be seen in Figure 5.2a and Figure 5.2b.

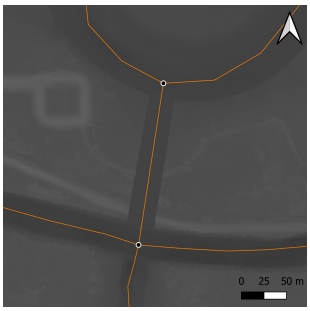

(a) Location of the bypass.

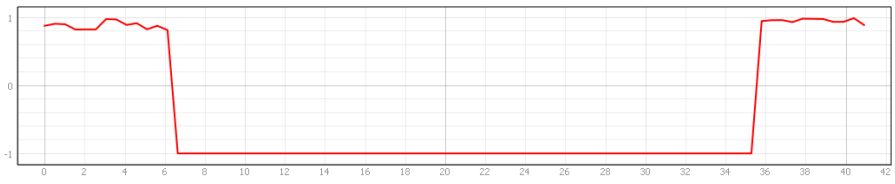

(b) Cross-section of the bypass.

Figure 5.2: Location and cross-section of the bypass.

5.2.2 Numerical model set-up

A numerical model representing the area incorporating the bypass measure is set-up by maintaining making small changes to the original model. As the bed topography is changed, the grid has to be changed correspondingly to capture information on the respective location. Concerning the boundary

conditions and physical parameters, identical settings are applied as in the original case. It must be mentioned that the numerical modelling applied here has a forecasting purpose and therefore cannot be calibrated or validated to any physical measurements.

5.2.3 Results and interpretation

As the graph is changed and a bypass is created around the Zoetemelkskil, the bridge here is downgraded to an ordinary edge. This enquires the re-identification of the bridges in the graph and their relative impact after deletion. As can be observed in Figure 5.3b, the Zoetemelkskil is indeed no longer identified as a bridge and therefore the weak spot in the system seems solved. The Helsloot on the other hand is still indicated as a relatively important bridge, leading to fragmentation of around 35 % after deletion.

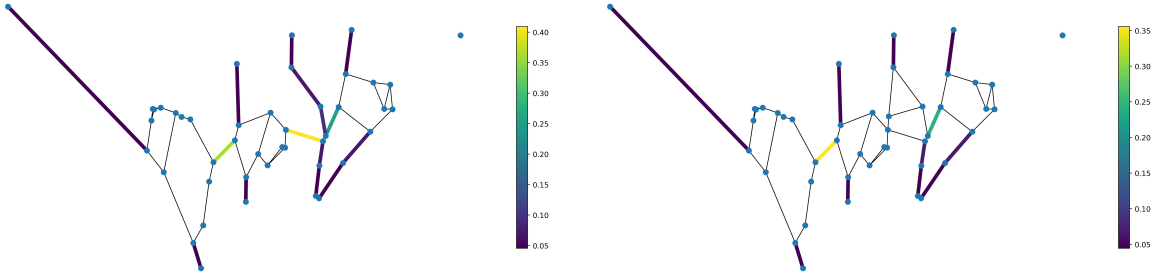

(a) Bridges in the present area.

(b) Bridges after bypass construction.

Figure 5.3: Bridges in the graph of the Sliedrechtse Biesbosch and the relative fragmentation after deletion of each individual bridge, in the present area layout (a) and after a bypass is constructed around the Zoetemelkskil (b).

This measure also results in a different betweenness centrality for the nodes in the centre of the graph. From Figure 5.4b a similar pattern can be observed as to Figure 5.4a, However, at the right side of the Zoetemelkskil, the node's betweenness centrality has decreased. This can be explained by the fact that part of the shortest paths is now directed via the bypass.

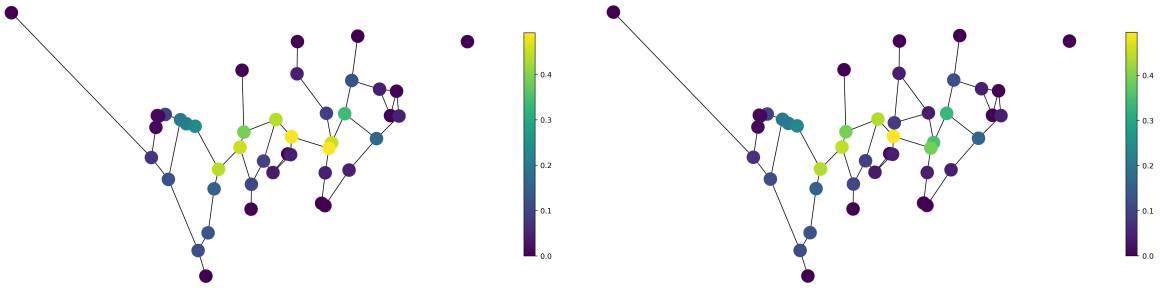

(a) Betweenness centrality in the present area.

(b) Betweenness centrality after bypass construction.

Figure 5.4: Betweenness centrality of the individual nodes in the graph of the Sliedrechtse Biesbosch, in the present area layout (a) and after construction of the bypass around the Zoetemelkskil (b).

The change of the graph in time causes the assessment metrics to vary in time. This can be seen in Figure 5.5. By comparing the metrics in the situation with a bypass with the present area layout (Figure 4.3), the effects of the bypass on the available habitat can be judged. Although the NOC seems relatively unaffected by the bypass, the order and length of connected pathways of the largest component changes significantly. Whereas the available habitat is initially limited to around 14,500 m for five consecutive hours per tidal cycle, the bypass roughly cuts this in half leading to only 2.5 hours of limited habitat per tidal cycle. Also absolute minimum and maximum available habitat is larger for the situation with a bypass. Altogether, the bypass induces an increase in available habitat of 10.04 % per day. The interpretation of the graphs per ten minutes, giving the fragmenting and attaching edges that cause the

evolution of the metrics, is not given here. The corresponding graphs can be found in the Chapter A of the supplementary material.

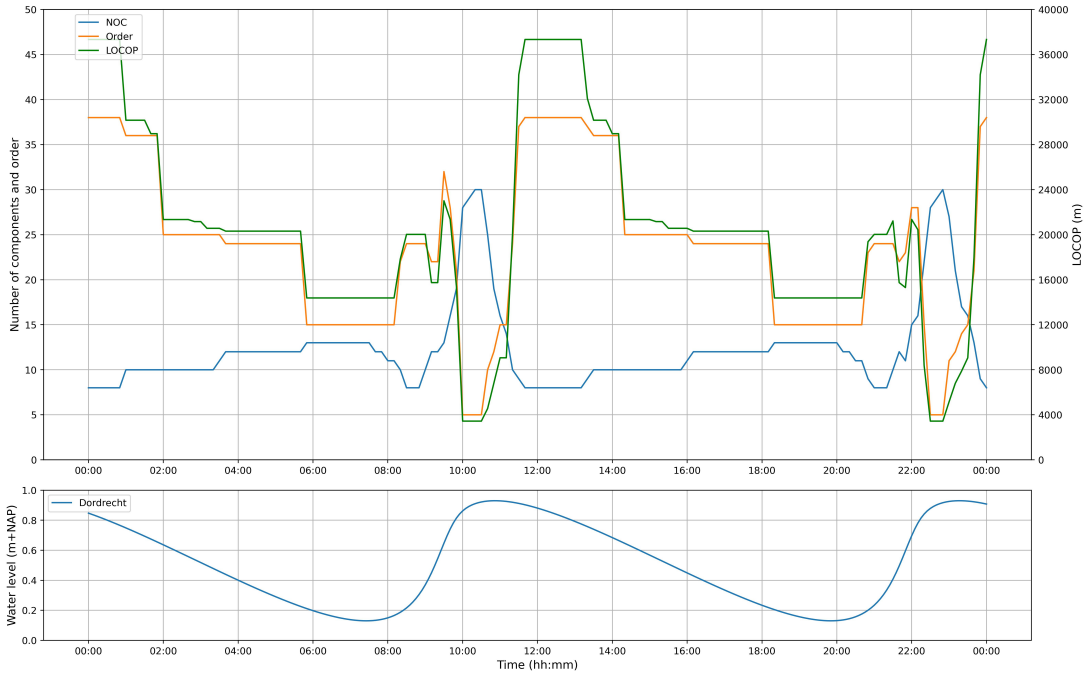

Figure 5.5: Evolution of connectivity of the Sliedrechtse Biesbosch with a bypass around the Zoetemelkskil, during one day and a maximum tolerable flow velocity of $u_{max} = 0.3$ m/s, evaluated by means of three metrics: the NOC in the graph, the order of the largest component, and the length of connected pathways (LOCOP) of the largest component. The bottom figure gives the water level variations in time at the most downstream location of the domain, at Dordrecht.

5.3 Opening the Helsluis

Another possibility to alter the flow conditions in the area is to permanently open the lock located on the north of the Sliedrechtse Biesbosch, the Helsluis. This is an interesting measure as Rijkswaterstaat has already expressed interest in the possibility to take the lock out of service, since operation and maintenance costs are high. Although Sloff and van Zetten (2010) found that permanently opening the lock induces excessive flow velocities for shipping, the measure is still implemented to examine the added value concerning habitat connectivity.

5.3.1 Spatial graph development

Unlike for the construction of the bypass, the graph schematization does not need to be changed. Whereas for the bypass a new edge was created, the Helsluis is situated in a channel already represented as an edge in the original graph. Therefore, the graph is identical to the graph described in section 3.2, and consists of 44 nodes and 64 edges.

5.3.2 Numerical model set-up

The numerical model requires adjustment. In the original model, the lock and corresponding channel were already incorporated. To prevent flow through the channel, two so-called thin dams were created in Delft3D, representing the closed lock. As in this case flow through the channel is possible, the thin dams are removed while the rest of the model settings are unaltered.

5.3.3 Results and interpretation

Since this measures doesn't require any change to the graph with respect to the original graph, the results for the bridges and betweenness centrality is the same as was found in Figure 4.1 and Figure 4.2. The

flow however does change resulting in different results in time. The evolution of the NOC, the order of the largest component and the LOCOP of the largest component can be found in Figure 5.6. Although a new permanent connection of the area with the Beneden Merwede is created, barely any difference is observed comparing with the metric evolution in the original area layout (Figure 4.3). The minimum and maximum habitat length are similar as well as the five hour period of limited LOCOP of 14,500 m. Only the NOC is slightly lower in the case of an open connection, implying a less fragmented network. Although this indicates higher connectivity, the lower fragmentation does not result in a significant change in available habitat of the largest component. Comparing the length of connected pathways of the present situation with that of the bypass, an overall increase of 0.83 % is found. Again, the interpretation of the graphs per ten minutes, giving the fragmenting and attaching edges that cause the evolution of the metrics, is not given here. The reader is referred to Chapter B of the supplementary material for the corresponding graphs.

Furthermore, high flow velocities are observed in the Helsloot and particularly at the lock heads. Because of the cross-sectional constriction flow velocities exceeding 1 m/s are observed during inflow. Further research to the consequences of this flow circumstances should be done to judge the effects on the lock and channel. A feasibility study is not part of this research.

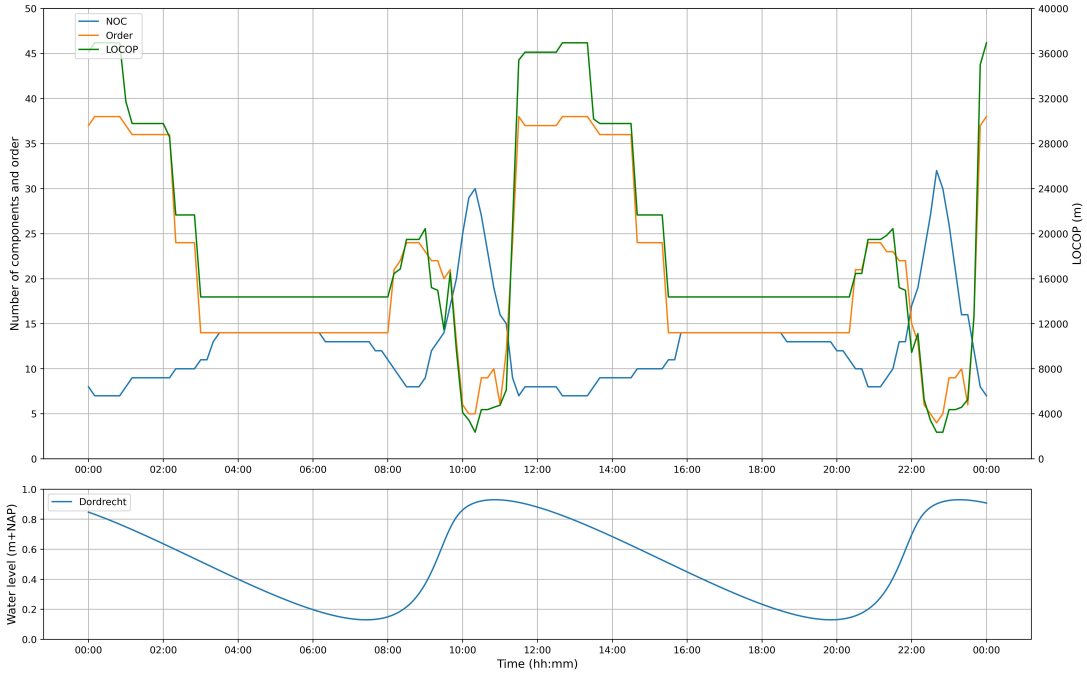

Figure 5.6: Evolution of connectivity of the Sliedrechtse Biesbosch with a permanent connection between the Helsloot and Beneden Merwede (permanently opened Helsluis), during one day and a maximum tolerable flow velocity of $u_{max} = 0.3$ m/s, evaluated by means of three metrics: the NOC in the graph, the number of nodes in the largest component, and the LOCOP of the largest component. The bottom figure gives the water level variations in time at the most downstream location of the domain, at Dordrecht.

5.4 Opening the Ottersluis

Also on the southern side of the Sliedrechtse Biesbosch a lock is situated. The Ottersluis is located between the Wantij and the Nieuwe Merwede. Similarly as to the Helsluis, Rijkswaterstaat is interested in the possibility of a permanent open connection between the Sliedrechtse Biesbosch and the Nieuwe Merwede, replacing the locks. This can be achieved by a bypass around the locks or by permanently opening the locks. In this section, the latter is considered.

5.4.1 Spatial graph development

Like for the opening of the Helsluis (section 5.3), the graph does not need to be changed for opening the Ottersluis. Therefore, the graph is identical to the graph described in section 3.2, and consists of 44 nodes and 64 edges.

5.4.2 Numerical model set-up

Again, the numerical model requires a minor adjustment. The thin dams in Delft3D FM, representing the closed lock, are removed and water can flow freely through the channel.

5.4.3 Results and interpretation

Again, this measures doesn't require any change to the graph with respect to the original graph, so the results for the bridges and betweenness centrality is the same as was found in Figure 4.1 and Figure 4.2. The flow however does change resulting in different results in time. The metric results can be found in Figure 5.7. As can be seen, the results for a permanently opened Ottersluis differ considerably from the present area layout. First of all, the NOC is reduced, implying a higher connectivity. Furthermore, the order of the largest component in the graph is larger during the entire tidal cycle. This implies a more connected channels in the available habitat. Finally, by looking at the length of connected pathways of the largest component, it can be found that the available habitat in the largest component is a lot larger. The minimum LOCOP is increased from roughly 2.5 km to nearly 8 km. The limited habitat length of 14.5 km during five hours is increased noticeably to more than 24 km, almost reaching the maximum LOCOP of nearly 36 km. Permanently opening the Ottersluis results in an increase of 29.58 % of the largest available habitat length per day. The main difference with the results for the present connectivity is the fact that the Zoetemelkskil and Helsloot remain available in the situation with an opened Ottersluis, whereas these channels disappeared and caused fragmentation in the present area layout. The reader is referred to Chapter C of the supplementary material for the corresponding graphs.

It should be mentioned that, since the connection between the Wantij and the Nieuwe Merwede now conveys most of the Wantij flow, high flow velocities occur. Flow velocities exceeding 2 m/s both during inflow and outflow of the Sliedrechtse Biesbosch are found from the model. Again, the flow velocity is highest at the lock heads. Although for habitat connectivity, this measure causes a significant improvement of the area, the solution is less feasible considering shipping. Without additional measures, the flow velocities are too high to ensure safe passage.

5.5 Combination of a bypass around Zoetemelkskil and opening Helsluis and Ottersluis

The final considered case consists of a combination of the three measures treated above. Both a bypass around the Zoetemelkskil is constructed as the two locks are opened permanently. This is the most drastic measure since it contains measures at multiple locations in the area. Also simulating the connectivity for this measure is most extensive since both the graph and the numerical model require adjustments.

5.5.1 Spatial graph development

As was discussed in section 5.2, a new edge is constructed and thus the graph needs to be altered. Since the same bypass design is applied here, the new graph can be found in Figure 5.1 and Figure 5.2. This graph consists of 45 nodes and 66 edges.

5.5.2 Numerical model set-up

The numerical model is adjusted accordingly. The topography is updated for the new channel, similar to section 5.2 and the opening of the locks is incorporated in the model by removing the thin dams, as was elaborated in section 5.3 and section 5.4. Boundary conditions and other parameters are identical to the model used for simulating the present area layout.

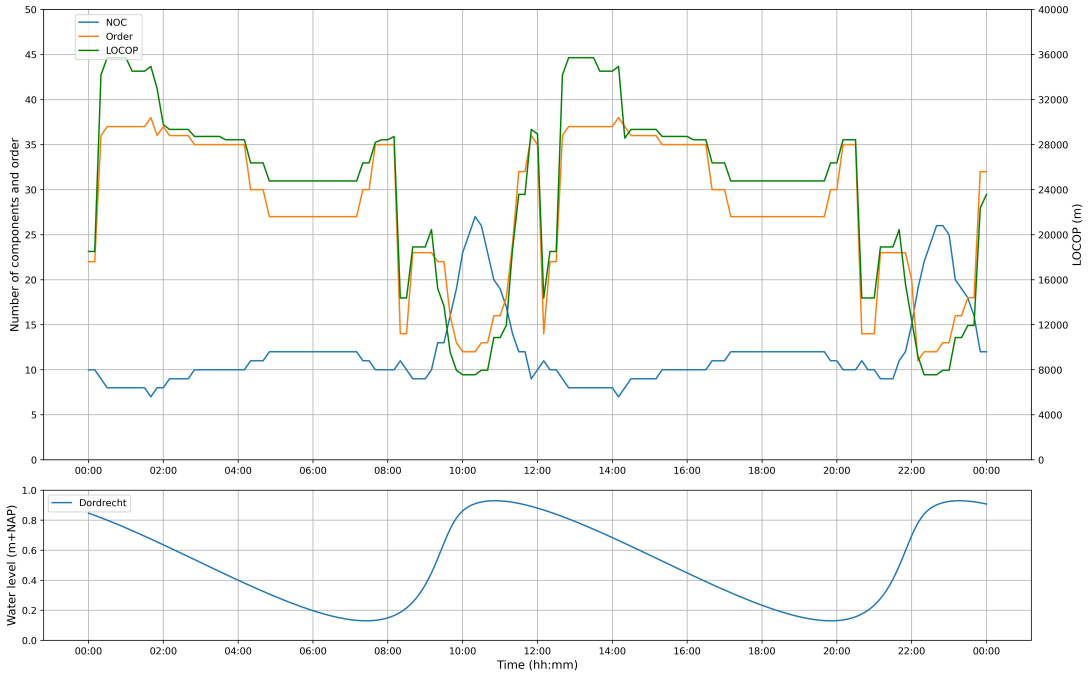

Figure 5.7: Evolution of connectivity of the Sliedrechtse Biesbosch with a permanent connection between the Wantij and Nieuwe Merwede (permanently opened Ottersluis), during one day and a maximum tolerable flow velocity of $u_{max} = 0.3$ m/s, evaluated by means of three metrics: the NOC in the graph, the number of nodes in the largest component, and the LOCOP of the largest component. The bottom figure gives the water level variations in time at the most downstream location of the domain, at Dordrecht.

5.5.3 Results and interpretation

As for this measure the graph requires small adjustments, distinct bridges and betweenness centrality are found. The same graph is used as was applied for the construction of a bypass. The results for the bridges and betweenness centrality can therefore be found in Figure 5.3b and Figure 5.4b. Variation in time does change and the results for this final measure can be found in Figure 5.8. All three metrics change significantly with respect to the present case. During the entire tidal cycle, the NOC is lower and shows less variability. Also the maximum NOC is reduced from 31 to 24. The order and LOCOP of the largest component resemble and are considerably larger than in the present area's connectivity. As was the case for opening the Ottersluis, the five hour period of limited connectivity is increased from 14.5 km to more than 24 km. Only during HW at Dordrecht, when the water level is still rising further upstream and in the Sliedrechtse Biesbosch, flow velocities become so high that sincere fragmentation occurs. The fragmented state takes approximately one hour, after which the edges attach again. Overall, the measure causes an increase of 38.14 % of the LOCOP of the largest component per day. The corresponding graphs can be found in Chapter D of the supplementary material.

As was found for opening the Ottersluis, high flow velocities (> 2 m/s) occur in the corresponding channel. Different from what was found for opening the Helsluis, flow velocities in the Helsloot remain limited.

5.6 Results and interpretation

From the different cases considered in the previous sections, it can be concluded different measures can largely influence the flow within the study area and thus change the suitability of the area as habitat. For comparison of the four cases that were treated, the relative effects of the NOC, order and LOCOP of the largest component are listed in Table 5.1. Furthermore, the evolution of the three distinct metrics for each case is plotted in Figures 5.9 to 5.11, respectively.

Table 5.1 shows that a combination of a bypass around the Zoetemelkskil, opening the Helsluis and open-

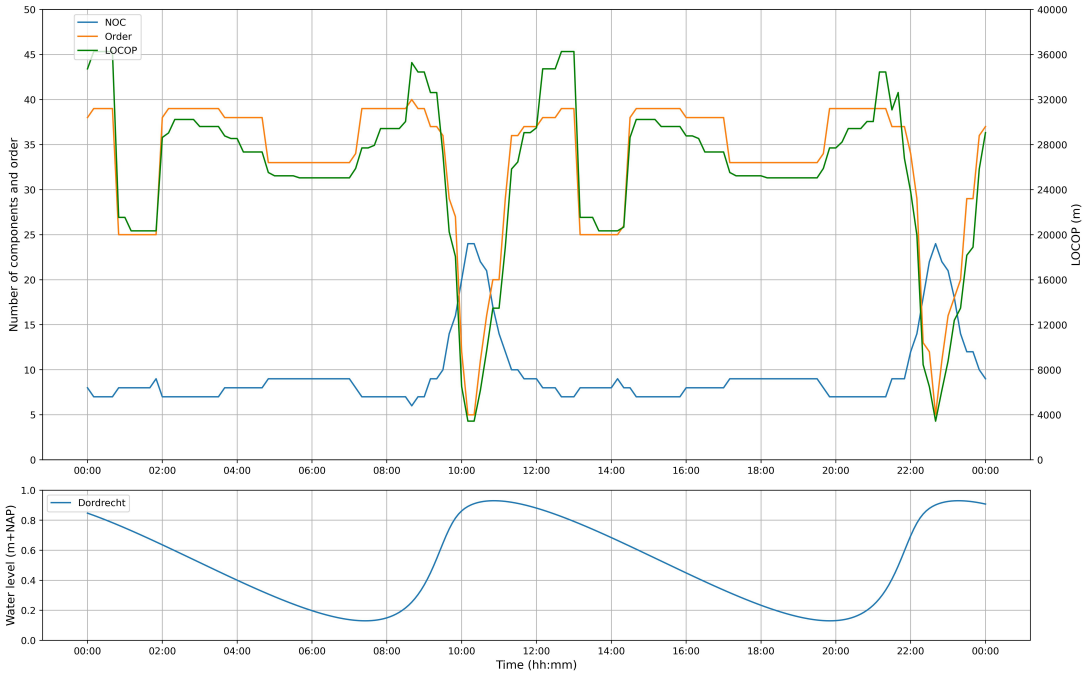

Figure 5.8: Evolution of connectivity of the Sliedrechtse Biesbosch with a bypass around the Zoetemelkskil, a permanent connection between the Helsloot and the Beneden Merwede (permanently opened Helsluis) and a permanent connection between the Wantij and Nieuwe Merwede (permanently opened Ottersluis), during one day and a maximum tolerable flow velocity of $u_{max} = 0.3$ m/s, evaluated by means of three metrics: the NOC in the graph, the number of nodes in the largest component, and the LOCOP of the largest component. The bottom figure gives the water level variations in time at the most downstream location of the domain, at Dordrecht.

Table 5.1: Effect of measures on connectivity metrics.

Measure	Relative effect		
	NOC	Order	LOCOP
Bypass	-7.09 %	13.96 %	10.04 %
Opening Helsluis	-4.95 %	-0.24 %	0.83 %
Opening Ottersluis	-11.02 %	35.99 %	29.58 %
All measures	-29.18 %	59.91 %	38.14 %

ing the Ottersluis gives the most favourable results from a habitat connectivity perspective. Since the number of components is reduced by nearly 30 %, fragmentation occurs considerably less while maintaining a relatively large available habitat (nearly 40 % increase in length of connected pathways). However, this case requires the most measures to be taken which will all lead to new side-effects. Especially at the Ottersluis, high flow velocities occur which might require additional measures to prevent excessive erosion in the channel or scour around the lock heads. Also the importance of shipping through the channel must be questioned, since this would lead to requirements concerning e.g. the maximum flow velocity. Since measures to prevent or limit negative side-effects might introduce construction costs, it is not recommended to implement all three measures.

Only opening the Ottersluis gives the second-best results concerning habitat connectivity. For the high flow velocity, the same applies as discussed above for the implementation of all three measures. However, in this case the permanent opening of the lock is the only measure to be implemented. This makes potential construction costs less important since savings are made on the Helsluis and the bypass.

The construction of a bypass around the Zoetemelkskil also positively affects the habitat connectivity of the Sliedrechtse Biesbosch. A 10 % rise in LOCOP is found. In this research only one bypass layout is

simulated, but various bypass designs could be tested to examine the effect of wider, deeper or longer bypasses.

Permanently opening the Helsluis does not affect the aquatic habitat connectivity as assessed by the metrics in this research. This can also be found by studying Figures 5.9 to 5.11, where the results resemble the results for the present area. Besides, this measure leads to side-effects such as high flow velocities in the Helsloot, particularly through the constricted conveyance area at the lock doors. This might require additional measures to reinforce the channel or lock, which is why this measure is not recommended. However, Stoffers (2022) states lateral connections with the river are crucial elements in habitat connectivity. This could be an argument in favour of the permanent opening of the lock.

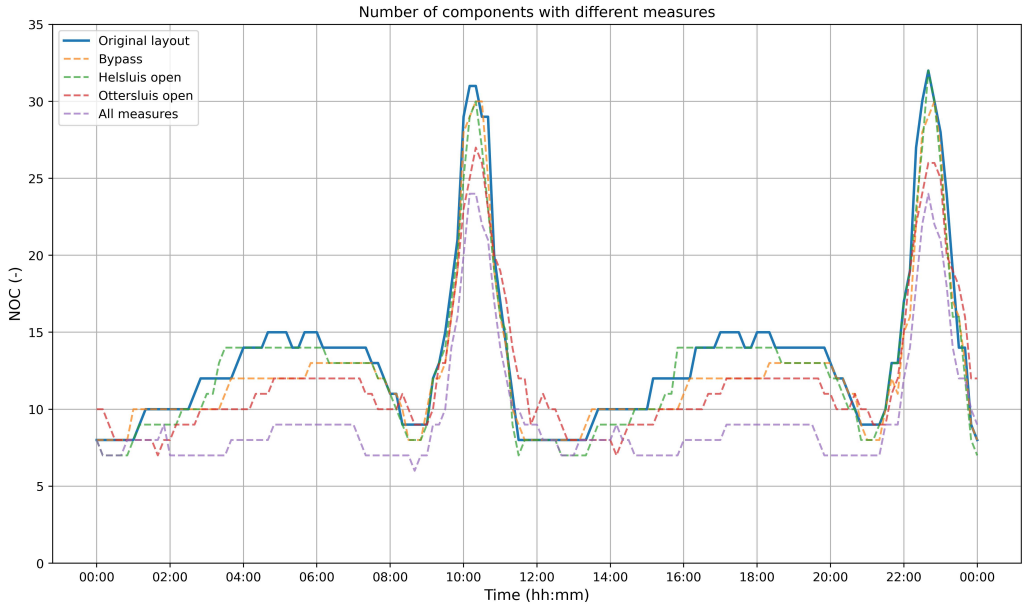

Figure 5.9: The number of components for the present area layout compared to the NOC during one day with various measures.

As is to be expected, the various measures result in different flow patterns through the water system. Particularly the open connection between the Wantij and the Nieuwe Merwede gives an interesting result since this actually forms a bypass around the Sliedrechtse Biesbosch. Where currently the tide only reaches the Nieuwe Merwede by travelling through the Beneden Merwede until the Boven Merwede, tidal influences now enter the Nieuwe Merwede earlier since the tide travels through the Wantij immediately into the Nieuwe Merwede. A possible disadvantage of a permanent open connection between the Wantij and the Nieuwe Merwede could be argued to be a reduced tidal effect. This is undesirable as the previously implemented restoration measures were aimed at increasing tidal movement in the Sliedrechtse Biesbosch. Although reduced tidal movement is suggested, this is not observed in the model output. Likely this is an inaccuracy in the numerical model, since only little tidal dampening is observed. The tidal range at Dordrecht amounts to around 80 cm, while the tidal range in the most upstream part of the Sliedrechtse Biesbosch is found to be 65 cm.

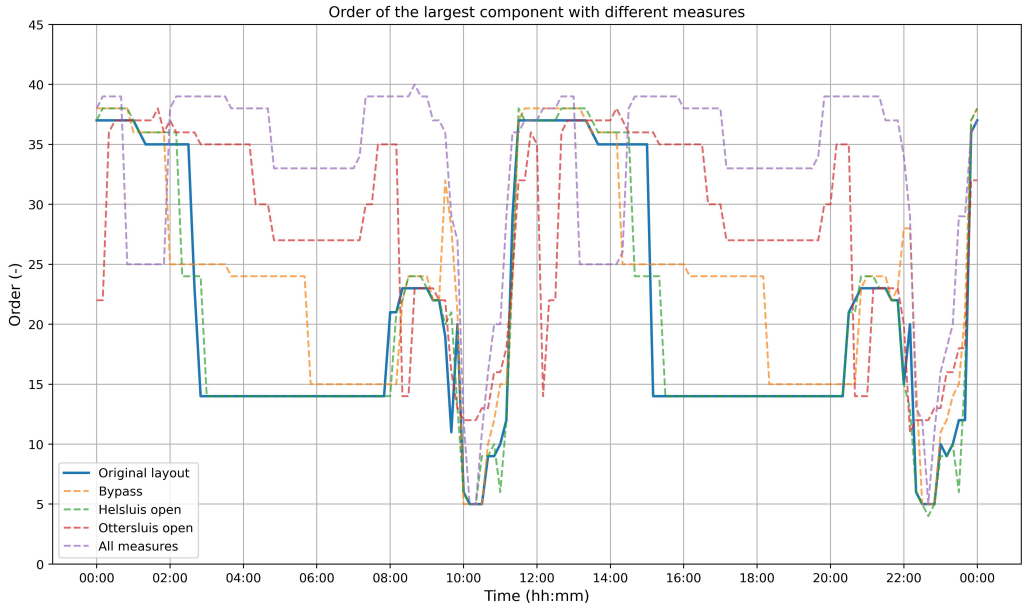

Figure 5.10: The order for the present area layout compared to the order of the largest component during one day with various measures.

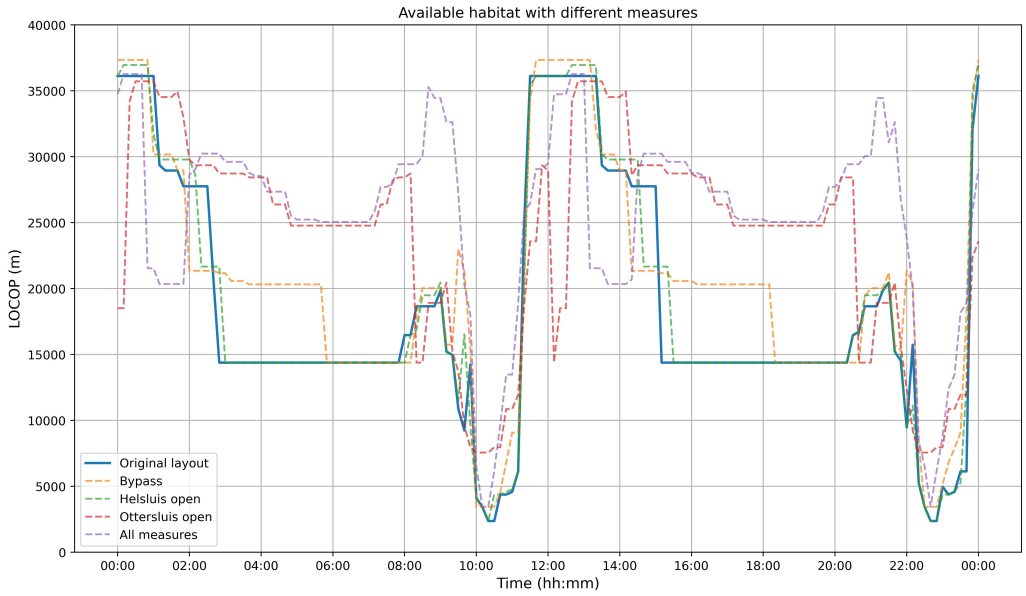

Figure 5.11: The length of connected pathways for the present area layout compared to the LOCOP during one day with various measures.

6

Discussion

This chapter is an analysis of the research. It relates the approach and results of this study to other research in the field and reviews the main similarities and differences. Also, it connects the results to the original research aim and discusses the potential implications of limitations and assumptions that were made.

6.1 Application to aquatic ecology

Nature restoration projects comprise activities that support the recovery of degraded or damaged ecosystems and intend to bring back more nature and biodiversity. Habitat connectivity is a topic that is increasingly considered in such projects as it describes the spatial continuity of habitat patches within an area. For example, Urban and Keitt (2001) studied habitat fragmentation of the Mexican Spotted Owl by means of graph theory and Hou et al. (2017) used several indices to evaluate the habitat connectivity in forests with special consideration of small habitats and barriers. Also habitat connectivity of aquatic areas is receiving increasing attention. The studies concerned vary in specific application and methodology, but often adopt an index approach or a graph-theory approach. Cote et al. (2009) develops an index to quantify longitudinal connectivity of river networks based on the expected probability of an organism being able to move freely between two random points of the network, where freely implies the absence of barriers. The research presented in this report links to all of the above mentioned studies in a certain way, either by studying the same topic or by using similar tools. The added value however is in the specificity with which the habitat of particular aquatic organisms is studied, based on one or more habitat preferences. The combination of numerical modelling and graph theory enables to compare the aquatic habitat connectivity of an area before and after the implementation of restoration measures, such as channel modifications or the construction of bypasses. The resulting hydrodynamics can be observed both on a local level (e.g. investigating extreme flow velocities in a specific channel in the numerical model) and on a holistic system-level by studying the hydrodynamics in the entire area with graph theory. Also the consideration of time-varying flow circumstances, imposed by tidal influences, is new in the field of habitat connectivity research. Whereas former research resulted in connectivity which is constant in time, this study shows that this is not necessarily the case. By selecting appropriate metrics, it can be demonstrated that connectivity varies in time.

However, the approach and application presented in this study also involve a number of limitations and uncertainties. First, while the application used in this study is very practical, it is questionable whether it is realistic and applicable to real nature restoration projects. As stated in section 1.4 and Chapter 3, various limitations, simplifications and assumptions are made. One of these simplifications is to apply a fixed flow velocity threshold that determines if an edge is suitable or not as aquatic habitat. The value for the flow velocity threshold is justifiable but the vulnerability is in the fact that the flow velocity is measured at a point in the middle of the channel width. Therefore flow near the banks or near the bed is not taken into account, where the velocities are likely to be smaller. Especially if riparian vegetation is present at the banks, fish can seek shelter in reed or behind trunks and continue their travel along the channel, escaping the high flow velocities in the centre of the channel. The method is more realistically applicable to birds travelling between habitat patches (Urban & Keitt, 2001), in which the limiting parameter is the distance between the different patches. Here a bird either can or cannot reach a habitat

patch, resulting in a more objective connectivity result.

Also the availability of aquatic habitat is not as unambiguous as is assumed in this study. Based on an excessive flow velocity somewhere along the channel length, an entire channel is categorized as unsuitable habitat. Possibly, this excessive velocity occurs only at one cross-section of a channel, inducing a rejected channel which is actually suitable for the vast majority of its length. This could be solved by a more detailed schematization of the system into a graph. In the presented research, the individual channels are represented by edges while the junctions between these channels are represented by nodes. A more detailed schematization could be obtained by subdividing the channels into multiple edges and nodes, such that a channel can also be partially available as habitat.

As research on the behaviour of fish is lacking, the application of this method on aquatic habitat connectivity should be considered with caution. In other applications which are less dependent of behaviour of species, the method is more suitable. Aquatic habitat connectivity could be investigated more objectively for a river system in which hard barriers such as dams and sluices are located (e.g. as proposed by Cote et al. (2009)). These barriers are blocking the migratory path and limiting the dispersion distance of fish. In such research, the same method can be applied and it could be investigated where the most habitat-limiting barrier is located. Such an application focuses more on habitat quantity, whereas the application in this research has strong relation with habitat quality. On top of that, it is debatable whether larger connectivity is always preferable. Studying the territory of invasive species, for example, might require limitation of the available habitat.

6.2 Numerical model

High level of uncertainty is introduced by the numerical model in Delft3D Flexible Mesh. Since the output of this model is used as the basis of the graph, its uncertainty greatly influences the connectivity results. First of all, a numerical model is, by definition, an approximation of reality. The accuracy of this approximation is dependent on the way the model is set up. A high resolution of the grid results in higher accuracy but leads to longer computation time. A coarse grid on the other hand delivers results quickly but might miss important flow characteristics. In this research a topography resolution of 5 m is applied, which can be considered sufficient for the large rivers, but which is too coarse for the narrow creeks in the Sliedrechtse Biesbosch. Although Delft3D FM offers the possibility to refine the mesh locally, the coarse topography inevitably influences in the flow through the channels.

Regarding the accuracy of the numerical model, calibration and validation play an important role. As hydraulic data is available along the large rivers around the study area, the flow in the river can be approximated relatively well. The flow in the creek network of the Sliedrechtse Biesbosch however cannot be calibrated since no measurements are available. Therefore, the flow conditions that follow from the simulation cannot be verified. This is an important weakness considering the results of this specific research, but in other research where flow data is provided, calibration is possible which results in a more accurate model.

Finally, dampening of tidal signal within the Sliedrechtse Biesbosch is unsure. The tidal range is reduced with 15 cm between the downstream boundary at Dordrecht and the most upstream part of the Sliedrechtse Biesbosch, in the Aart Eloyenbosch polder. At the downstream boundary of the model domain a tidal range of 80 cm is observed while in the Aart Eloyenbosch the tidal range amounts to 65 cm. Information on the actual tidal range in this part of the Sliedrechtse Biesbosch is lacking, such that the modelled tidal range of 65 cm cannot be validated. It could however be argued that this decrease in tidal range is rather small considering the covered distance through all the creeks and channels. The limited dampening could then be attributed to the standard friction formulation that is applied in the model. Calibration of the model resulted in the most accurate approximation of the available data in the Merwede rivers with a Manning friction parameter of $n = 0.023$ s/m$^{1/3}$. In can be questioned however whether this same formulation can be applied for the creeks and channels in the study area, since the channel properties might differ considerably. Factors such as bed and bank vegetation and debris are likely to increase the exerted friction whilst these are not taken into account. Delft3D FM allows location-specific definition of the friction parameter, such that a higher friction value can be taken into

account in more densely vegetated areas. Measurements of hydrodynamics in these creeks and channels are required to calibrate the model and determine a suitable friction parameter.

6.3 Research findings

The three metrics used to assess the connectivity of the study area, i.e. the number of components, the order of the largest component and the length of connected pathways of the largest component (as introduced in section 3.3), are selected as these give a decent indication of the variation of available habitat in time. Especially the LOCOP gives a complete view on the largest available habitat. The LOCOP in combination with the number of components gives an indication of the size of the remaining habitat patches. The order of the largest component resembles very much the LOCOP but is a indispensable in identifying whether relatively short or long edges are part of the largest component. Although many more metrics exist to evaluate a graph, these three prove to be most useful in studying the connectivity of aquatic habitats. Studying e.g. sediment connectivity most likely requires other metrics, since fluxes play an important role. Consequently, node-specific properties such as (betweenness) centrality or strength become more relevant.

Designing nature restoration measures is not as trivial as it might seem. If, e.g. by edge deletion, an edge appears to be lost by an excessive flow velocity, it seems obvious to target the specific channel with restoration measures such that a lower flow velocity occurs. However, it needs to be kept in mind that changing a specific parameter in the channel layout or water system as a whole can change the flow in the entire area. Especially when applying multiple habitat criteria in one analysis, such as minimum flow depth and maximum flow velocity, interdependencies of parameters should be considered while designing measures.

Bridges are vulnerabilities in a graph since these are the only connecting links between two components in a graph. Deletion of such a link, by definition, causes fragmentation of the graph into more components. In studying a network it is therefore always useful to locate the bridges and pay close attention to their role within the network. If a bridge is located in the centre of a graph it can be convenient to create a new edge, strengthening the connection between the two components of the graph coupled by the bridge. The bridge is then downgraded to an ordinary edge since there is an alternative connection. In the application to aquatic habitat connectivity however, creating such a bypass does not necessarily improve the graph's connectivity. This is mainly dependent on the weight of the edges after construction of the bridge. The identification of bridges can therefore be an appropriate instrument in the initial investigation of weak links, but it can be misleading to solely focus restoration projects on the bypassing of bridges. Other measures altering the flow in the area might turn out more useful, as resulted from the connectivity study with a permanent opening of the Ottersluis with respect to the bypass around the Zoetemelkskil.

7

Conclusions and recommendations

This chapter is a summary of the main findings and the final thoughts on the significance of the research. It highlights the key takeaways and provides recommendations for future research or action based on the findings. Also the aim and objectives are reflected upon.

7.1 Conclusions

The aim and objectives formulated in the introduction of this research can now be reflected upon. The aim of the research was to:

> *Apply and evaluate the use of graph theory to objectively identify vulnerable locations in a water channel network that limit the aquatic habitat connectivity of a freshwater tidal area, in order to propose adequate nature restoration measures and preserve or improve the area's ecological value.*

7.1.1 Research objectives

Four objectives were formulated to obtain background information and knowledge to achieve the aim. A summary of the most important findings to the objectives can now be given.

1. Examine the relation between hydrodynamics and ecology in a freshwater tidal wetland.

A highly biodiverse area is home to many species with an equal number of habitat preferences. For fish, Morrow Jr and Fischenich (2000) state that flow velocity, water depth, substrate and turbidity pertain to the most important factors determining the suitability of an area as habitat. There are different types of fish, i.e. reophilic and limnophilic fish preferring flowing water and stagnant water, respectively, while eurytopic fish live in any type of water. Also within the life span of fish, preferred conditions change. Larvae require different circumstances than juveniles and juveniles prefer different conditions than adults (Stoffers, 2022). Therefore it is impossible to create circumstances that fulfill the habitat requirements of all species. However, it is possible to target a specific species and design new habitat based on its preferences. Some of these requirements, such as tolerable flow velocity and water depth, are listed by Marijs et al. (2020) and can be used when designing restoration measures aiming at the re-introduction or population growth of specific species. In this research the flow velocity requirements for different fish species are taken as criteria determining the suitability of habitat.

2. Investigate the different applications of connectivity and discuss the various approaches besides graph theory.

The most general definition of connectivity of a system or object is the state of being (inter)connected. As the concept of connectivity can be applied in many different fields such as computer science, networking, sociology, mathematics and ecology, various specific definitions have been formulated. To illustrate the diversity of applications and definitions, multiple water and ecology-related studies were compared and the applied definitions were gathered in Table 2.1. According to the definition by Wohl (2017), connectivity refers to the degree to which matter and organisms can move among spatially defined units

in a natural system. In aquatic habitat connectivity, this is an appropriate definition since it refers to the spatial continuity of a habitat in which different bodies of water are connected and interact with each other, including connections between rivers, streams and ponds. When habitats are connected, they support a greater diversity of species and provide more opportunities for organisms to interact and thrive, helping to maintain the overall health of the ecosystem and support the survival of a wide range of species. Connectivity can also play a role in the resilience of aquatic ecosystems, allowing them to better adapt to changes and disturbances. Connectivity can be assessed through a wide range of research methods, including graph theory, numerical simulation models, satellite imagery, and the application of connectivity indices. An overview of different approaches and their application is given in Table 2.2.

3. Discuss the various metrics in graph theory and identify the most useful metrics for an aquatic habitat connectivity study.

Graph theory is a mathematical framework used to study the structure, properties, and behavior of complex networks. It provides a wealth of analytical measurements that can be used to examine a network as a whole and its individual nodes and edges. The properties of a graph are characteristics or attributes that are used to describe and analyze its structure and behavior. These properties can be defined in various ways, depending on the specific problem being studied and the goals of the analysis. Numerous metrics exist to study a graph on different levels, such as system level, node level or edge level. As graph theory can be used in such a diverse range of fields and applications, the suitability of individual parameters differs per case. In the application to aquatic habitat connectivity in a water system under tidal influence the number of components (NOC), order and length of connected pathways (LOCOP) proved useful, since with a combination of these three metrics the variation of the available habitat in time can be evaluated accurately and connectivity-limiting locations and conditions can be identified. By using these metrics, researchers and analysts can identify key nodes, edges, and pathways, as well as analyze the connectivity of a network, providing insights into its structure and behavior.

4. Review the added value of graph theory over solely numerical modelling.

Graph theory offers a useful tool for investigating connectivity in a variety of fields, including aquatic habitats. It provides a systematic and mathematical framework to represent and analyze complex relationships between entities, such as nodes and edges in a network. The use of graph theory allows the quantification and analysis of important connectivity metrics, such as centrality and the size of components. These metrics provide valuable information about the structure and function of the network, including the presence of bottlenecks, hubs, and clusters that are critical for the flow of resources and information. Numerical modelling, on the other hand, is a useful method for investigating the behavior and dynamics of physical and biological systems. It provides a powerful tool for simulating the complex interactions between different variables, and can help to predict future trends and outcomes. However, numerical models can be limited in their ability to provide a comprehensive representation of the relationships between entities, and to quantify the complex network structure of an ecosystem. In comparison, graph theory offers an approach that allows the representation and analysis of relationships between entities, and provides a valuable framework for understanding the structure and function of a network. Additional benefit is the relatively large visual accessibility to laypersons or others with no expertise in the interpretation of numerical modelling results.

In summary, the added value of graph theory over solely numerical modelling in studying connectivity is the ability to represent and analyze complex relationships between entities, and to quantify the important connectivity metrics that provide valuable information about the structure and function of the network. Graph theory provides a more holistic view on a system than numerical modelling does, although a combination of the two can provide a more comprehensive understanding of connectivity.

7.1.2 Research aim

With the information gathered from the objectives, the aim can now be reflected upon. Results show that graph theory provides a useful instrument in analyzing the connectivity of the Sliedrechtse Biesbosch. The ease at which key nodes and edges are identified offer great possibilities for the design of nature restoration measures. Various graph-theory metrics can prove useful in the analysis of networks. Bridges

and betweenness centrality can be used to investigate the vulnerable locations of a graph considering only its structure. The NOC, order and LOCOP are useful while looking at fragmentation patterns of a graph including relevant weights, such as a maximum flow velocity. In the present layout of the study area, large variation of aquatic habitat connectivity occurs based on a fragmentation threshold of 0.3 m/s. With a combination of graph theory and numerical modelling, different layouts can be simulated and connectivity can be investigated in potential designs. As results from the case study, more lateral connections between the Sliedrechtse Biesbosch and the surrounding rivers (by permanently opening the Helsluis and Ottersluis) and constructing a bypass around the Zoetemelkskil leads to the highest and most constant habitat connectivity, amounting to an increase of nearly 40 % per day of the largest connected available habitat.

7.2 Recommendations

As is demonstrated in this research, a graph-theory approach to aquatic habitat connectivity is promising for future projects of habitat restoration. The research shows an application of the method to investigate weak spots and efficient restoration measures. A number of recommendations are listed in this section to indicate how this study could be used best by engineers, ecologists or other parties in restoration projects (Section 7.2.1). Also recommendations concerning a connectivity study of the Sliedrechtse Biesbosch (Section 7.2.2) and regarding further development of the of the applied method are made (Section 7.2.3).

7.2.1 Application for stakeholders

The study presents a method to investigate the connectivity of aquatic habitats in an area of interest. The following recommendations are made regarding application by different stakeholders for whom the method might be useful. Different parties may have different interests while considering the same study area. The most important starting points are clear habitat requirements, such as a minimum or maximum flow velocity or water depth, and detailed data on the considered study area, e.g. flow data and bed topography. With this information available, the full connectivity analysis can be carried out following the flow chart given in Figure 1.4 and the different steps presented in Chapter 3 this report.

- **Application for ecologists:** Ecologists can apply the method in issues such as the investigation of available habitat for threatened species. Topics like this can be addressed with the presented method as very specific habitat preferences can be set as boundary conditions, corresponding to the targeted species. Favourable habitats can be identified as graph components which do not show fragmentation in time, while migratory obstacles can be distinguished as frequently fragmenting bridges.
- **Application for engineers:** Engineers are recommended to apply the presented method in investigating the effect of construction measures in the study area on the aquatic habitat connectivity. When the goal for a nature restoration measure is specifically to improve the habitat connectivity for a certain species, the measure should be designed to reach an optimum connectivity. For projects in which habitat restoration is not the main aim, the connectivity results can be considered as added value or downsides of certain measures.
- **Application for nature organisations:** Nature organisations may demand a high biodiversity, requiring water system that hosts many different species. This requires hydrodynamic conditions that fit the preferences of many different species. In this case the method can be applied such that the entire area contains channels and creeks with varying flow conditions. This means that both deep and shallow creeks are present, as well as running and stagnant waters. By implementing various measures and constructing bypasses, these different channels can be tested and the area can be designed such that a great variety of species can settle.

7.2.2 Connectivity in the Sliedrechtse Biesbosch

In this section, recommendations are made concerning the aquatic habitat connectivity of the Sliedrechtse Biesbosch specifically. If a more accurate view of the connectivity in the study area is of interest, it is advised to implement the following remarks.

- **Gather flow data within the study area:** In a connectivity study concerning the aquatic habitat in the Sliedrechtse Biesbosch, it is recommended to gather more data on the hydrodynamic conditions within the area. As was elaborated on in the discussion (Chapter 6), the Delft3d FM model was calibrated solely on available data at the surrounding rivers. For more certain results, physical measurements should be carried out within the area. Flow velocity and water level measurements at multiple locations allow for more extensive calibration, which would lead to more certain results regarding the effect of potential measures.

- **Refinement of the bed topography:** As the many narrow and shallow creeks are characteristic of the Biesbosch, it is recommended to gather more accurate bed topography data. The currently available bed topography has a resolution of 5×5 m, which is too coarse to include these small water bodies. It is therefore advised to include higher resolution bed topography, e.g. 1×1 m resolution. The computational grid should then be refined correspondingly, which is very well possible in Delft3D FM. It is recommended to refine the grid only locally since such refinement increases the computational time noticeably.

- **Validate by measuring populations:** In order to validate the results of the aquatic habitat connectivity study, it is recommended to compare the results to actual populations in the area. As information on fish populations is not available, monitoring of the population size has to be done first. With this data preferred habitat can be identified and it can be compared with the available habitat resulting from the connectivity study.

- **Investigate the effect of the Haringvliet sluices:** Concerning the aquatic habitat connectivity of the Sliedrechtse Biesbosch specifically, special attention goes out to the opening of the downstream located Haringvliet sluices. The so-called Kierbesluit is an agreement that describes the partial opening of the sluices during high tide, allowing for the tide to enter the Haringvliet and travel upstream (Rijkswaterstaat, n.d.-a). This agreement has been topic of discussion as there is a demand, mainly from nature organisations, for the restoration of tidal nature. Although the effects of further or full opening of the sluices on the hydrodynamics in the Sliedrechtse Biesbosch might be small, it is recommended to investigate the effects before actually implementing restoration measures.

- **Consider more connectivity-improving measures:** The final recommendation concerning the Sliedrechtse Biesbosch is that in this study, four connectivity improving measures were simulated. The effects of local measures such as adjusting channel parameters are not examined and only one bypass is investigated. Engineers or others involved in the design of measures in a nature restoration project should investigate more measures and designs and work within the area's constraints such as houses, cables and pipelines. Also, as the area is protected under the Natura2000 legislation, building permits can greatly affect the possibilities within the Sliedrechtse Biesbosch.

7.2.3 Improvement of the method

Finally, recommendations are made concerning the method to investigate aquatic habitat connectivity as described in this study. Although the method is applied in a case study, the method is applicable in any water system. This section includes the recommendations that should be taken into account in further applications of the presented method.

- **Include more habitat requirements:** In future research, a more complete result of aquatic habitat connectivity can be obtained by taking into account additional parameters. Next to a maximum flow velocity, fish can also be susceptible to a minimum or maximum water depth, temperature, oxygen, tidal range or other parameters (Morrow Jr & Fischenich, 2000). Graph theory provides the possibility to create a graph for each parameter individually. By overlaying the results of the respective habitat quality parameters, more detailed insight into the suitability of habitats and vulnerability of channels can be obtained. While including more habitat requirements, the same graph theory metrics can be applied resulting in similar figures as were presented in this report. More accurate results would also be obtained if variation in flow velocity along the channel width and depth are taken into account.

- **Consider varying flow conditions and preferences:** The flow conditions within the area are influenced by the boundary conditions. In this research a representative constant value for the discharge is chosen as the upstream boundary condition. Also downstream, a constant value is chosen for the water level and the amplitude of the tidal forcing. In reality, values for these parameters vary continuously. In more accurate research, this irregularity can be included by for example looking at typical seasonal hydraulic conditions for winter or summer. The results can then be more accurately applied for a specific type of species in a certain life stage. For example a specific type of spawning fish seeks appropriate circumstances in summer. Then the aquatic habitat connectivity for this spawning fish can be investigated more accurately by applying only hydraulic data from summer. Infinite applications of the proposed method are possible to investigate the habitat connectivity for any combination of fish species and life stage.
- **Investigate various applications of the method:** Finally, it should be mentioned that with minor modifications of the graph, many more applications can be found than just aquatic ecology. A relatively simple extension of the model, taking into account flow direction, could be incorporated to study, for example, dispersion patterns. This is more or less equivalent to a tracer study in a numerical model, but numerical modelling is often a time-consuming activity, while analysing a graph is much faster. This can be useful in emergency situations or in studying the dispersal of seed or waste (e.g. plastics).

Bibliography

AHN. (2022). *Actueel Hoogtebestand Nederland.* Author. Retrieved 1 July 2022, from https://www.ahn.nl/

Amoros, C., & Bornette, G. (2002). Connectivity and biocomplexity in waterbodies of riverine floodplains. *Freshwater biology*, *47*(4), 761–776.

Biggs, N., Lloyd, E., & Wilson, R. (1986). *Graph Theory, 1736-1936.* Clarendon Press. Retrieved from https://books.google.nl/books?id=XqYTk0sXmpoC

Bracken, L. J., & Croke, J. (2007). The concept of hydrological connectivity and its contribution to understanding runoff-dominated geomorphic systems. *Hydrological Processes: An International Journal*, *21*(13), 1749–1763.

Bracken, L. J., Wainwright, J., Ali, G., Tetzlaff, D., Smith, M., Reaney, S., & Roy, A. (2013). Concepts of hydrological connectivity: Research approaches, pathways and future agendas. *Earth-Science Reviews*, *119*, 17–34.

Bureau Waardenburg. (2007, June). *Aansluiting polders in de Sliedrechtse Biesbosch op de getijdekreken: habitattoets.* Bureau Waardenburg.

Cavalli, M., Trevisani, S., Comiti, F., & Marchi, L. (2013). Geomorphometric assessment of spatial sediment connectivity in small Alpine catchments. *Geomorphology*, *188*, 31–41.

Cote, D., Kehler, D. G., Bourne, C., & Wiersma, Y. F. (2009). A new measure of longitudinal connectivity for stream networks. *Landscape Ecology*, *24*(1), 101–113.

Deltares. (2022a, October). D-Flow Flexible Mesh, User Manual (2023rd ed.) [Computer software manual].

Deltares. (2022b, August). RGFGRID (7.00 ed.) [Computer software manual]. (Generation and manipulation of structured and unstructured grids, suitable for Delft3D-FLOW, Delft3D-WAVE or D-Flow Flexible Mesh)

Freeman, M. C., Pringle, C. M., & Jackson, C. R. (2007). Hydrologic connectivity and the contribution of stream headwaters to ecological integrity at regional scales 1. *JAWRA Journal of the American Water Resources Association*, *43*(1), 5–14.

Frings, R. M. (2005). Sedimenttransport op de Merwedekop tijdens de hoogwaterperiode van 2004. In *Icg* (Vol. 5, p. 1).

Heckmann, T., & Schwanghart, W. (2013). Geomorphic coupling and sediment connectivity in an alpine catchment—Exploring sediment cascades using graph theory. *Geomorphology*, *182*, 89–103.

Hiatt, M., Addink, E. A., & Kleinhans, M. G. (2022). Connectivity and directionality in estuarine channel networks. *Earth Surface Processes and Landforms*, *47*(3), 807–824.

Hou, W., Neubert, M., & Walz, U. (2017). A simplified econet model for mapping and evaluating structural connectivity with particular attention of ecotones, small habitats, and barriers. *Landscape and Urban Planning*, *160*, 28–37.

Kadaster. (n.d.). *200 Jaar Topografische Kaarten.* Retrieved 16 June 2022, from https://www.topotijdreis.nl/

Lexartza-Artza, I., & Wainwright, J. (2009). Hydrological connectivity: Linking concepts with practical implications. *Catena*, *79*(2), 146–152.

Marijs, L. B., Achterkamp, B., Collas, F. P. L., De la Haye, M., Dorenbosch, M., Liefveld, W. M., ... Van Kessel, N. (2020, November). *KRW Leidraad Rijkswaterstaat.*

Masselink, R. J., Heckmann, T., Temme, A. J., Anders, N. S., Gooren, H. P., & Keesstra, S. D. (2017). A network theory approach for a better understanding of overland flow connectivity. *Hydrological Processes*, *31*(1), 207–220.

McDonald, R. I., Kareiva, P., & Forman, R. T. (2008). The implications of current and future urbanization for global protected areas and biodiversity conservation. *Biological conservation*, *141*(6), 1695–1703.

Melger, E. (2019, Dec). *DSD-INT 2019 - Delft3D FM suite - Key advantages.* Deltares. Retrieved from https://www.slideshare.net/Delft_Software_Days/dsdint-2019-delft3d-fm-suite-key-advantagesmelger

Mohammad, I. H. R., & Saiful, A. A. (2010). Ecological connectivity framework in the state of Selangor,

Peninsular Malaysia: A potential conservation strategy in the rapid changing tropics. *Journal of Ecology and the Natural Environment*, *2*(5), 73–83.

Molinari, B., Stewart-Koster, B., Malthus, T. J., & Bunn, S. E. (2022). Impact of water resource development on connectivity and primary productivity across a tropical river floodplain. *Journal of Applied Ecology*, *59*(4), 1013–1025.

Morrow Jr, J. V., & Fischenich, J. C. (2000). Habitat requirements for freshwater fishes. *EMRRP Technical Notes Collection (ERDC TN-EMRRP-SR-06)*.

Nijhuis, L. (2021). *Tidal parks in the Rhine Meuse estuary: Case study Groene Poort* (Unpublished master's thesis). Delft University of Technology.

Okin, G. S., Parsons, A. J., Wainwright, J., Herrick, J. E., Bestelmeyer, B. T., Peters, D. C., & Fredrickson, E. L. (2009). Do changes in connectivity explain desertification? *BioScience*, *59*(3), 237–244.

OpenStreetMap contributors. (n.d.). *Sliedrechtse Biesbosch.* Retrieved 31 May 2022, from https://umap.openstreetmap.fr/en/map/kaart-zonder-naam_233490#13/51.8101/4.7777

PAGW. (2022, June). *Preverkenning Biesbosch Rijn-Maasmonding krijgt groen licht.* Programmatische Aanpak Grote Wateren (PAGW). Retrieved 20 June 2022, from https://www.pagw.nl/actueel/nieuws/2022/06/10/preverkenning-biesbosch-rijn-maasmonding-groen-licht

Passalacqua, P. (2017). The Delta Connectome: A network-based framework for studying connectivity in river deltas. *Geomorphology*, *277*, 50–62.

Pearson, S. G., van Prooijen, B. C., Elias, E. P., Vitousek, S., & Wang, Z. B. (2020). Sediment connectivity: a framework for analyzing coastal sediment transport pathways. *Journal of Geophysical Research: Earth Surface*, *125*(10), e2020JF005595.

Pringle, C. M. (2001). Hydrologic connectivity and the management of biological reserves: a global perspective. *Ecological Applications*, *11*(4), 981–998.

Pringle, C. M. (2003). What is hydrologic connectivity and why is it ecologically important? *Hydrological Processes*, *17*(13), 2685–2689.

QGIS 3.16. (2020). QGIS 3.16 Hannover [Computer software manual]. Retrieved from https://www.qgis.org

Raap, F. (2021, May). *a) sinusoidal, b) skewed and c) asymmetric wave shape.* Retrieved from https://upload.wikimedia.org/wikipedia/commons/2/2c/Waves111111111111111.png

Rijkswaterstaat. (n.d.-a). *Haringvliet: Haringvlietsluizen op een kier.* Retrieved 16 February 2023, from https://www.rijkswaterstaat.nl/water/projectenoverzicht/haringvliet-haringvlietsluizen-op-een-kier

Rijkswaterstaat. (n.d.-b). *Herstel leefgebied Sliedrechtse Biesbosch (Merwedes).* Retrieved 6 April 2022, from https://www.rijkswaterstaat.nl/water/projectenoverzicht/herstel-leefgebied-sliedrechtse-biesbosch-merwedes

Rijkswaterstaat. (2010, April). *Meetverslag Open Helsluis metingen 1 en 2 maart 2010.*

Rijkswaterstaat. (2021a, May). *Bathymetrie Nederland - binnenwateren 1 mtr. RWS Zuid-Nederland West.* Author. Retrieved from https://maps.rijkswaterstaat.nl/dataregister/srv/dut/catalog.search#/metadata/a17ea8b8-39c2-48eb-a14f-2173ff8adn81?tab=general

Rijkswaterstaat. (2021b, December). *Start zoektocht naar meer intergetijdennatuur langs Boven- en Beneden (Merwede).* Retrieved 30 May 2022, from https://www.rijkswaterstaat.nl/water/projectenoverzicht/herstel-leefgebied-sliedrechtse-biesbosch-merwedes

Schuurman, F. (2012, December). *Onderzoek openingen bij Hel- en Spieringsluis* (Tech. Rep.). The Netherlands: Royal Haskoning DHV.

Sloff, C. J. (2022). Private Communication. Delft, the Netherlands.

Sloff, C. J., & van Zetten, J. W. (2010, May). *SOBEK schematisatie Sliedrechtse Biesbosch* (Tech. Rep.). The Netherlands: Deltares.

Sluiter, H., & Veenhuizen, D. (2008, April). *Als het tij keert, verzet men de bakens.* Stichting Vakblad Natuur Bos Landschap.

Snippen, E., Van der Heijdt, L., & Van Zetten, J. (2002, January). Abiotisch effectenonderzoek Sliedrechtse Biesbosch. *Rijkswaterstaat, RIZA-rapport*.

Stoffers, T. (2022, October 13). *Kraamkamers riviervis.* Wageningen University & Reserch. Retrieved from https://www.stowa.nl/agenda/webinar-cop-beken-en-rivieren-hoe-goed-functioneren-nevengeulen-en-strangen-als-kraamkamer

Stoffers, T., Buijse, A. D., Verreth, J. A., & Nagelkerke, L. A. (2022). Environmental requirements and heterogeneity of rheophilic fish nursery habitats in European lowland rivers: Current insights and

future challenges. *Fish and Fisheries*, *23*(1), 162–182.

Tian, K., Yin, X.-a., Bai, J., Yang, W., & Zhao, Y.-w. (2021). Grading evaluation of the structural connectivity of river system networks based on ecological functions, and a case study of the Baiyangdian wetland, China. *Water*, *13*(13), 1775.

Urban, D. L., & Keitt, T. (2001). Landscape connectivity: a graph-theoretic perspective. *Ecology*, *82*(5), 1205–1218.

Urban, D. L., Minor, E. S., Treml, E. A., & Schick, R. S. (2009). Graph models of habitat mosaics. *Ecology letters*, *12*(3), 260–273.

Vellinga, N., Van der Vegt, M., & Hoitink, T. (2014). *Hydrodynamics of tidal waves in the Rhine-Meuse river delta network.* University of Utrecht.

Visser, A., Snippen, E., & de Gelder, A. (2005, February). Erosie en sedimentatie na sanering Sliedrechtse Biesbosch. *Rijkswaterstaat, RIZA-rapport*.

Ward, J. V., & Stanford, J. (1995). Ecological connectivity in alluvial river ecosystems and its disruption by flow regulation. *Regulated rivers: research & management*, *11*(1), 105–119.

Wohl, E. (2017). Connectivity in rivers. *Progress in Physical Geography*, *41*(3), 345–362.

Wohl, E., Brierley, G., Cadol, D., Coulthard, T. J., Covino, T., Fryirs, K. A., ... others (2019). Connectivity as an emergent property of geomorphic systems. *Earth Surface Processes and Landforms*, *44*(1), 4–26.

Xie, C., Cui, B., Xie, T., Yu, S., Liu, Z., Chen, C., ... Shao, X. (2020). Hydrological connectivity dynamics of tidal flat systems impacted by severe reclamation in the Yellow River Delta. *Science of The Total Environment*, *739*, 139860.

Zhang, Y., Huang, C., Zhang, W., Chen, J., & Wang, L. (2021). The concept, approach, and future research of hydrological connectivity and its assessment at multiscales. *Environmental Science and Pollution Research*, *28*(38), 52724–52743.

A

Bed topography of creeks and polders

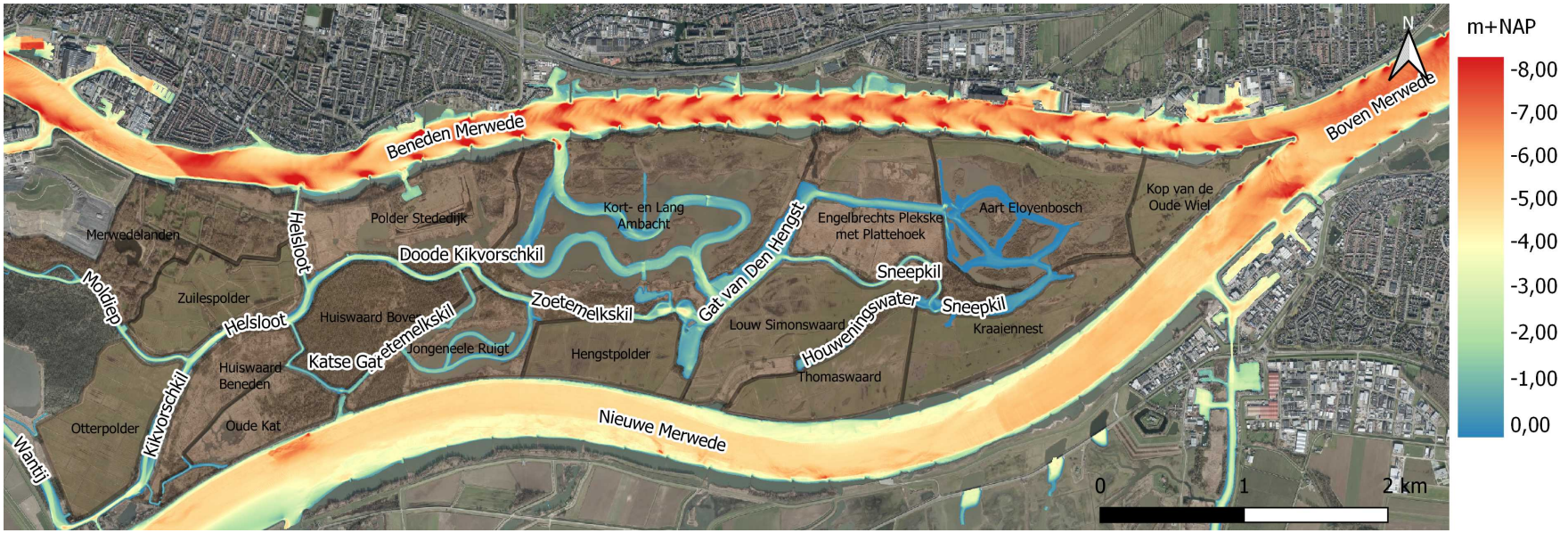

Figure A.1: Most recent bed topography of the creeks and different polders in the Sliedrechtse Biesbosch (Rijkswaterstaat, 2021a).

B

Calibration results

This appendix gives the figures corresponding to the calibration simulations with varying Manning bed friction coefficient n, as was referred to in chapter 3. For clarity only three water level outputs are plotted per figure, corresponding to simulations with friction values $n = 0.020$ s/m$^{1/3}$, $n = 0.023$ s/m$^{1/3}$ and $n = 0.030$ s/m$^{1/3}$ (minimum, most accurate and maximum friction, respectively). Mean deviation, standard deviation, maximum deviation and R^2 are given in Tables 3.5 to 3.8, for Figures B.1 to B.4, respectively.

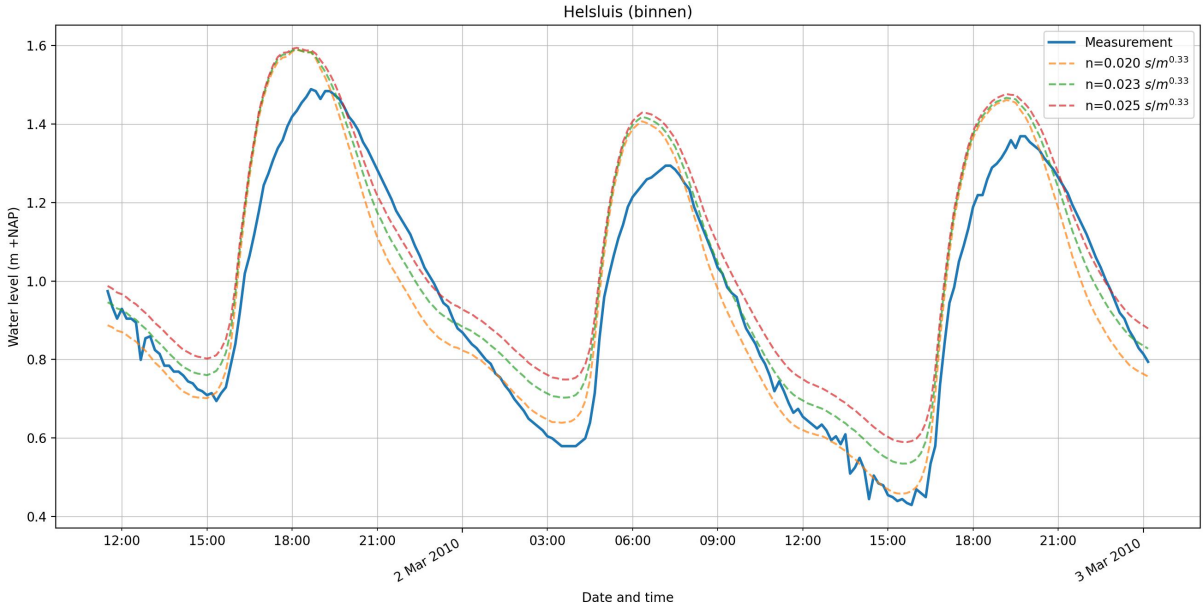

Figure B.1: Real water level measurements and model output for different Manning friction coefficients at the Helsluis (1 March 2010 until 3 March 2010), corresponding to Table 3.5.

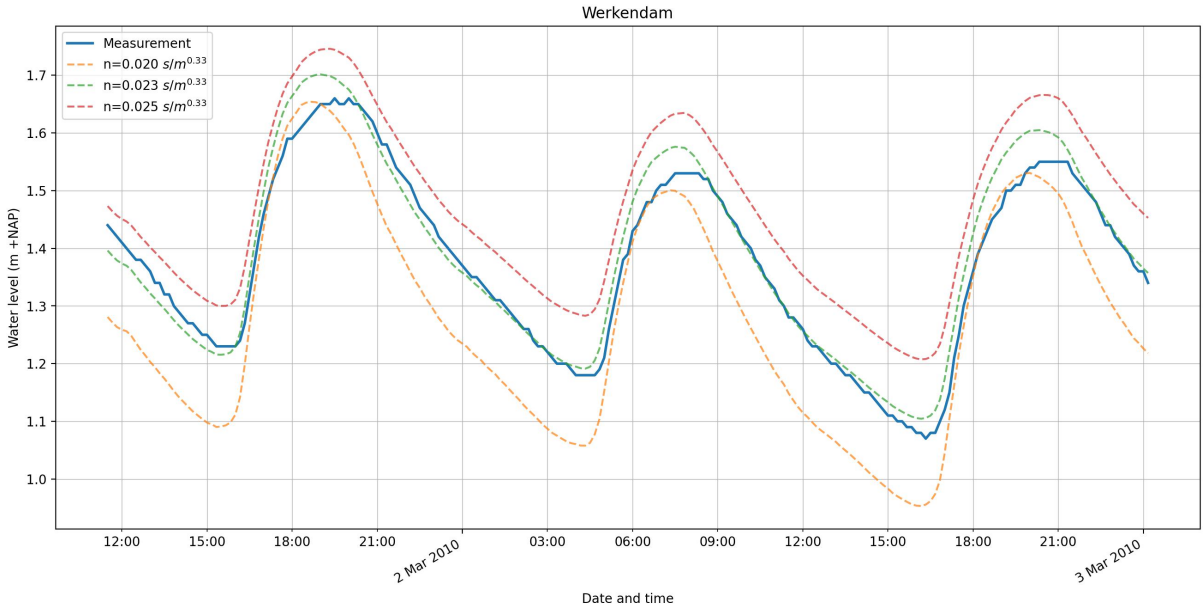

Figure B.2: Real water level measurements and model output for different Manning friction coefficients at Werkendam (1 March 2010 until 3 March 2010), corresponding to Table 3.6.

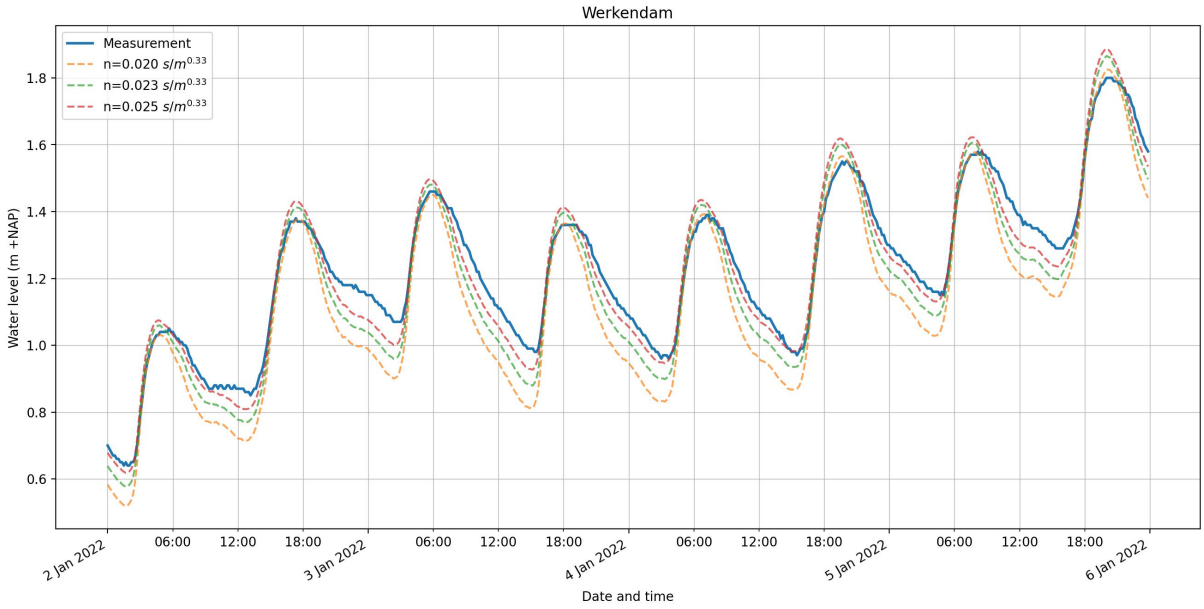

Figure B.3: Real water level measurements and model output for different Manning friction coefficients at Werkendam (1 January 2022 until 5 January 2022), corresponding to Table 3.7.

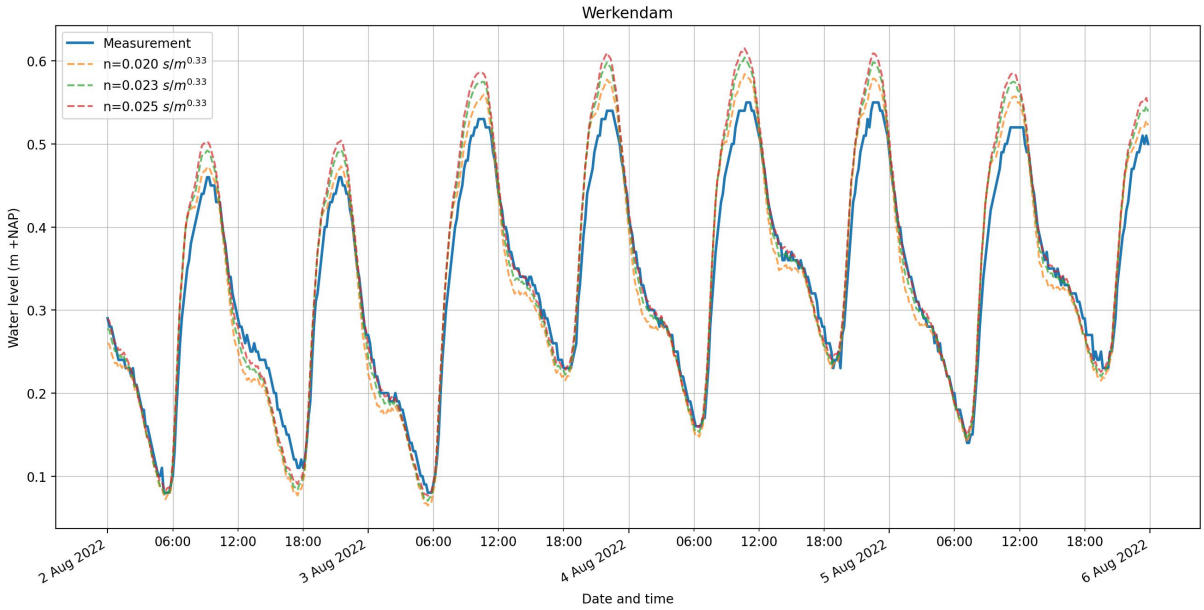

Figure B.4: Real water level measurements and model output for different Manning friction coefficients at Werkendam (1 August 2022 until 5 August 2022), corresponding to Table 3.8.

C

Time varying connectivity

This appendix gives the connectivity results for the present situation in the Sliedrechtse Biesbosch, as is presented in chapter 4. Figure C.1 illustrates the time-varying connectivity metrics, i.e. the number of components (NOC), the order of the largest component and the length of connected pathways (LOCOP) of the largest component. Next are the graphs indicating the available channels in the system and visualizing the largest available habitat on a time interval of 10 minutes.

Note that the results corresponding to the different restoration measures, as discussed in chapter 5, are not included in this appendix. For these results the reader is referred to the supplementary material.

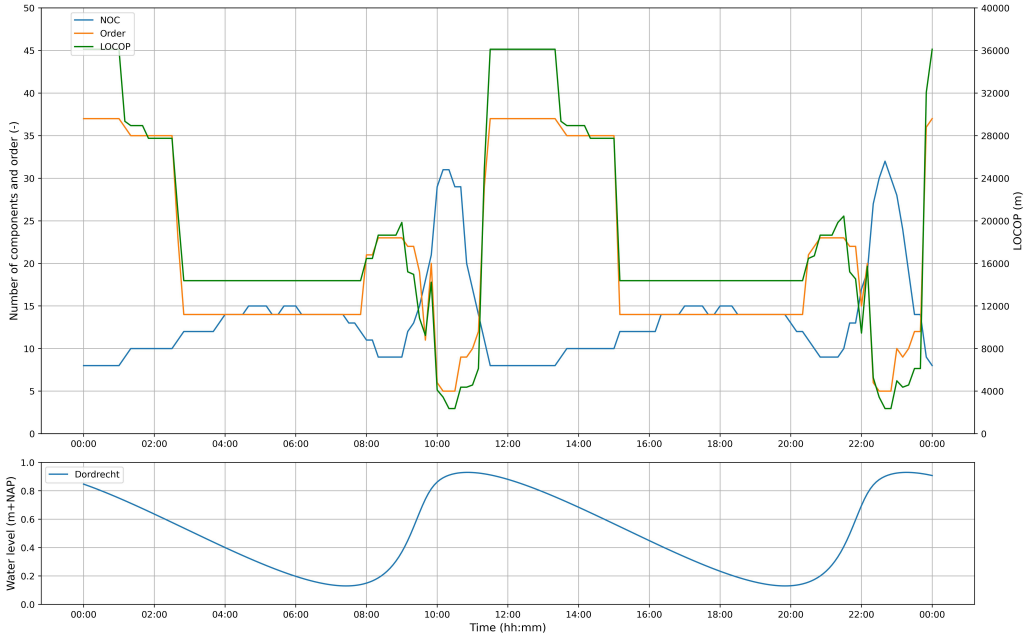

Figure C.1: Evolution of connectivity of the Sliedrechtse Biesbosch during one day and a maximum tolerable flow velocity of $u_{max} = 0.3$ m/s, evaluated by means of three metrics: the number of components in the graph, the number of nodes in the largest component, and the length of connected pathways of the largest component.

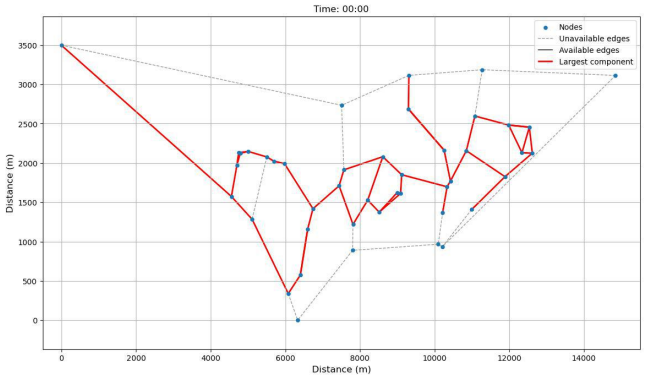
Time: 00:00
Nodes
Unavailable edges
Available edges
Largest component
Distance (m)
Distance (m)

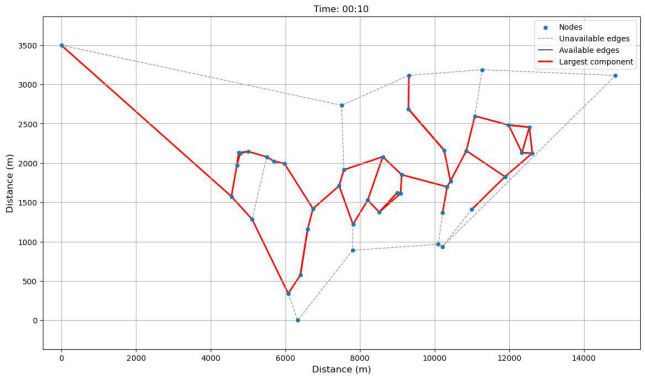
Time: 00:10
Nodes
Unavailable edges
Available edges
Largest component
Distance (m)
Distance (m)

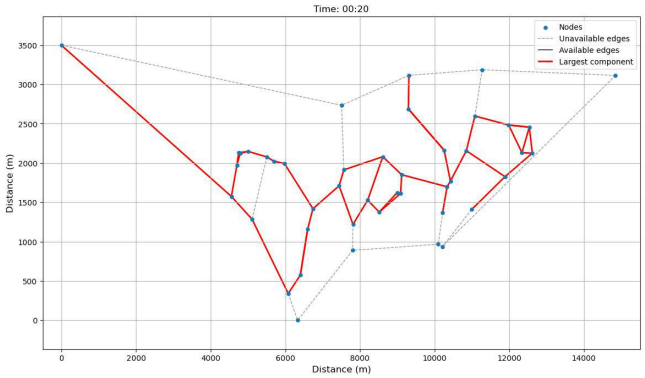
Time: 00:20
Nodes
Unavailable edges
Available edges
Largest component
Distance (m)
Distance (m)

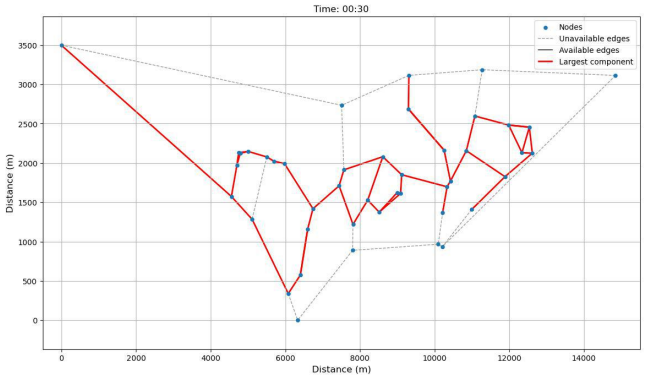
Time: 00:30
Nodes
Unavailable edges
Available edges
Largest component
Distance (m)
Distance (m)

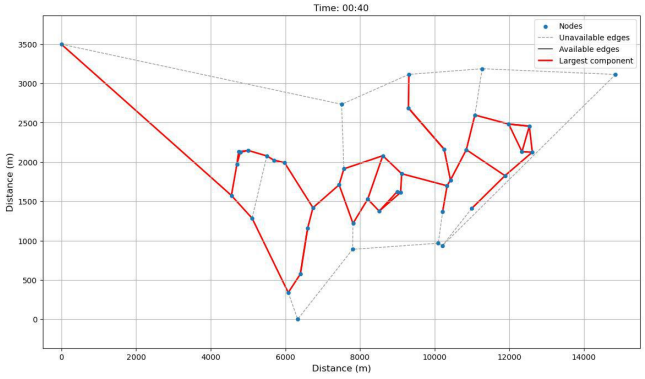
Time: 00:40
Nodes
Unavailable edges
Available edges
Largest component
Distance (m)
Distance (m)

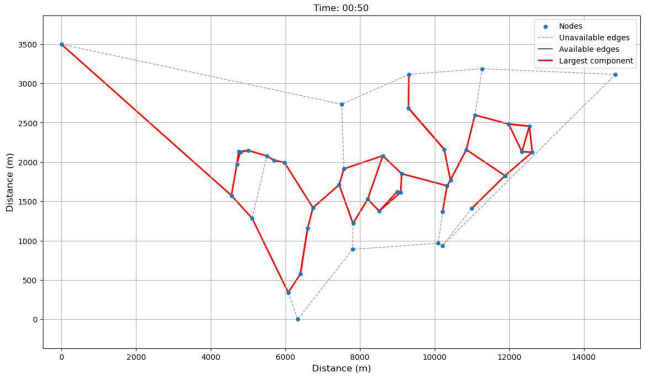
Time: 00:50
Nodes
Unavailable edges
Available edges
Largest component
Distance (m)
Distance (m)

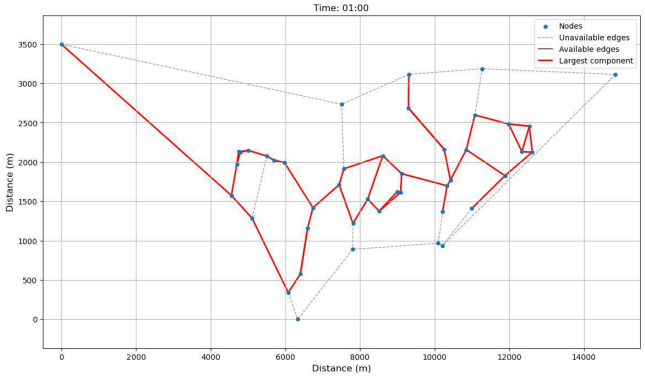
Time: 01:00
Nodes
Unavailable edges
Available edges
Largest component
Distance (m)
Distance (m)

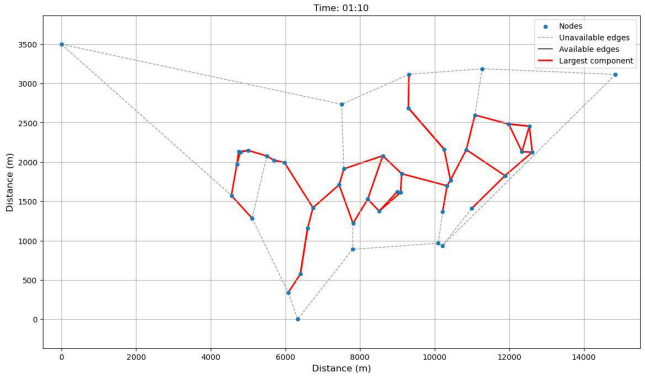
Time: 01:10
Nodes
Unavailable edges
Available edges
Largest component
Distance (m)
Distance (m)

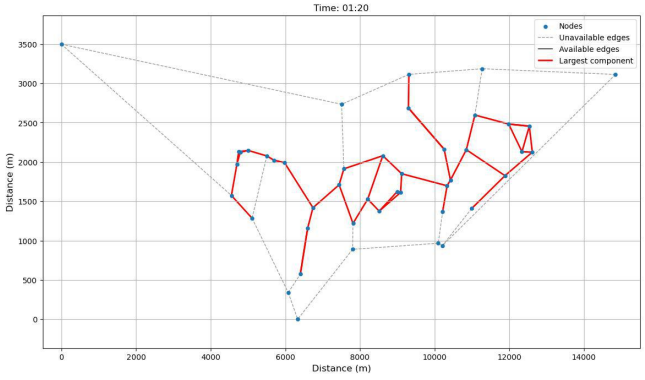
Time: 01:20
Nodes
Unavailable edges
Available edges
Largest component
Distance (m)
Distance (m)

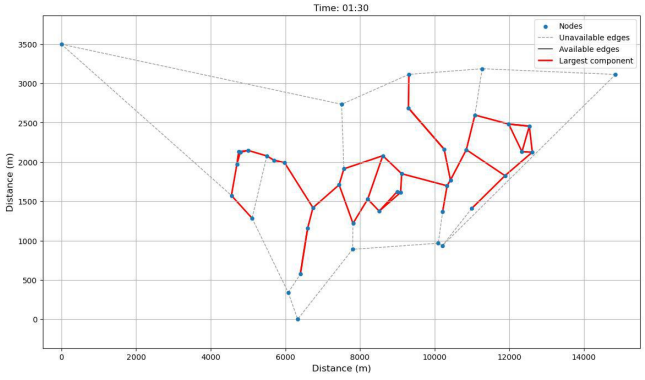
Time: 01:30
Nodes
Unavailable edges
Available edges
Largest component
Distance (m)
Distance (m)

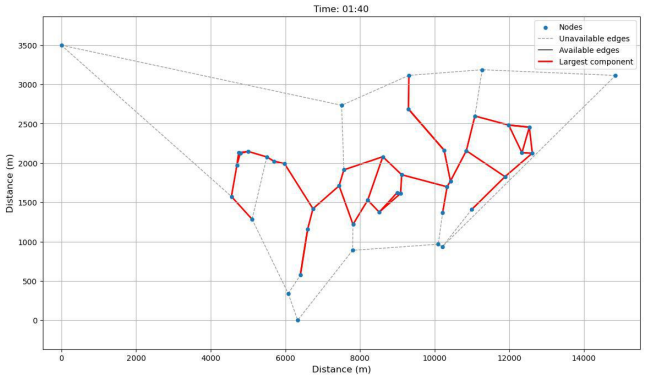
Time: 01:40
Nodes
Unavailable edges
Available edges
Largest component
Distance (m)
Distance (m)

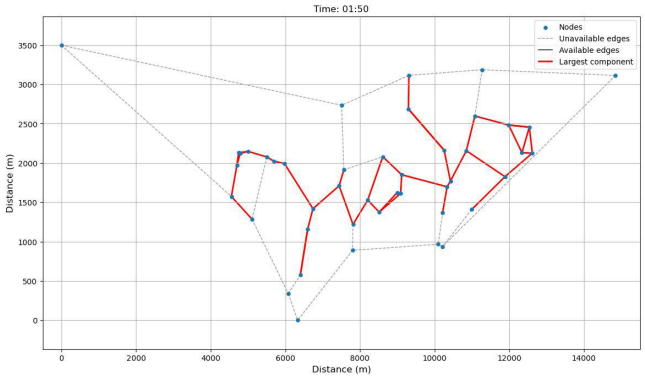
Time: 01:50
Nodes
Unavailable edges
Available edges
Largest component
Distance (m)
Distance (m)

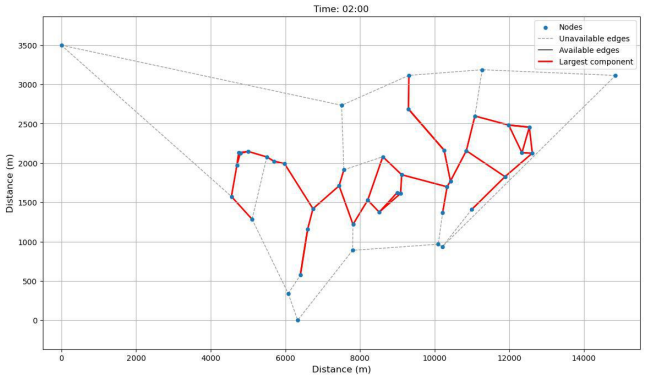
Time: 02:00
Nodes
Unavailable edges
Available edges
Largest component
Distance (m)
Distance (m)

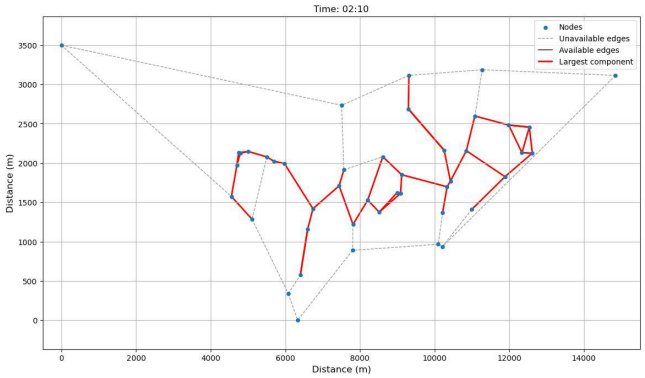
Time: 02:10
Nodes
Unavailable edges
Available edges
Largest component
Distance (m)
Distance (m)

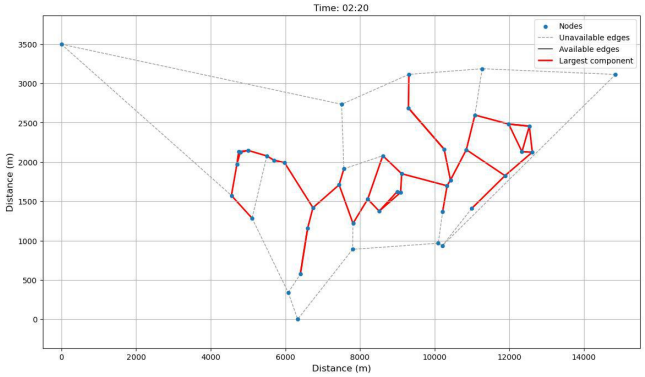
Time: 02:20
Nodes
Unavailable edges
Available edges
Largest component
Distance (m)
Distance (m)

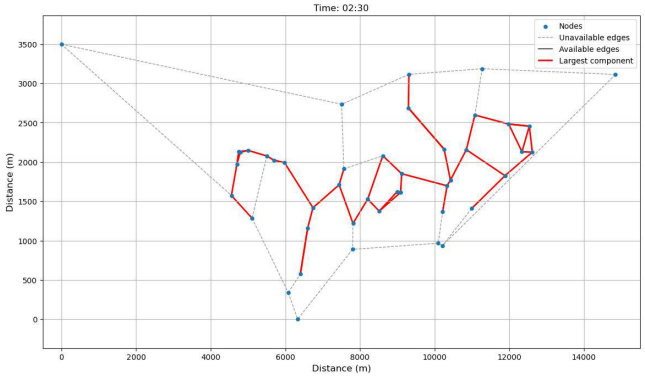
Time: 02:30
Nodes
Unavailable edges
Available edges
Largest component
Distance (m)
Distance (m)

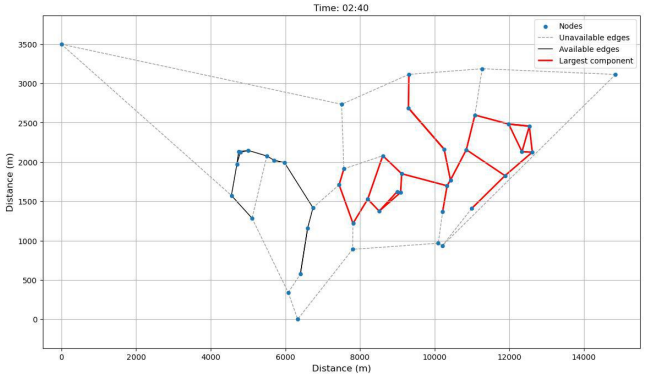
Time: 02:40
Nodes
Unavailable edges
Available edges
Largest component
Distance (m)
Distance (m)

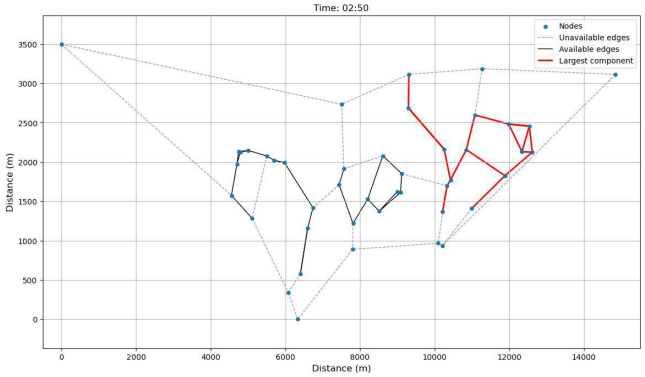
Time: 02:50
Nodes
Unavailable edges
Available edges
Largest component
Distance (m)
Distance (m)

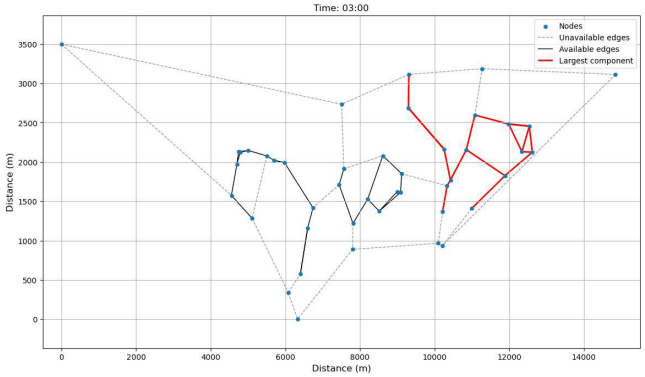
Time: 03:00
Nodes
Unavailable edges
Available edges
Largest component
Distance (m)
Distance (m)

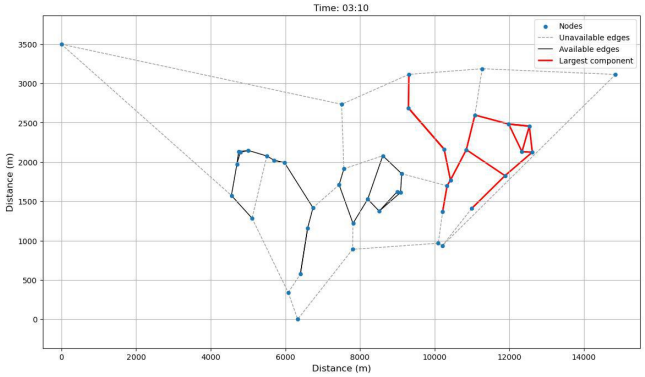
Time: 03:10
Nodes
Unavailable edges
Available edges
Largest component
Distance (m)
Distance (m)

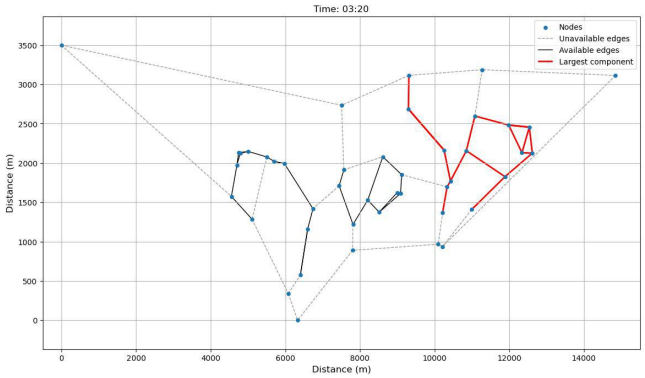
Time: 03:20
Nodes
Unavailable edges
Available edges
Largest component
Distance (m)
Distance (m)

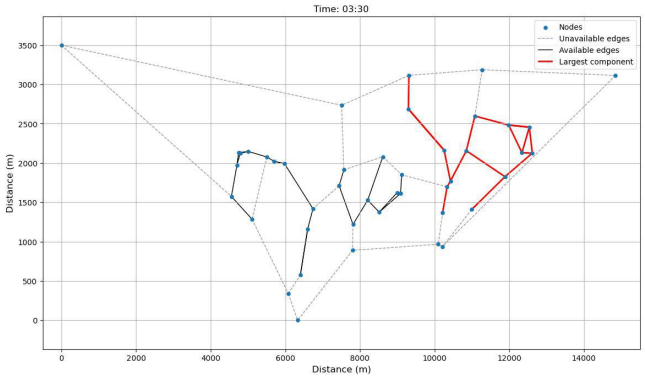
Time: 03:30
Nodes
Unavailable edges
Available edges
Largest component
Distance (m)
Distance (m)

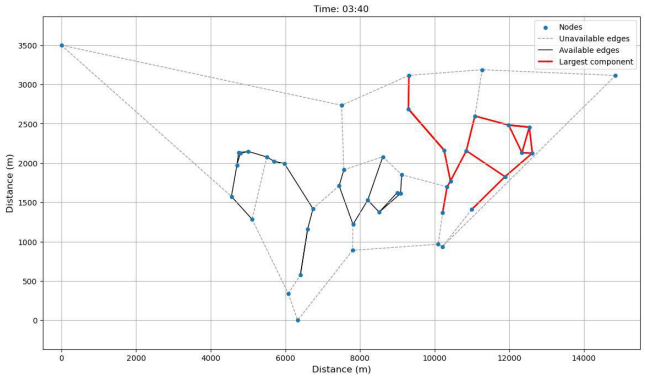
Time: 03:40
Nodes
Unavailable edges
Available edges
Largest component
Distance (m)
Distance (m)

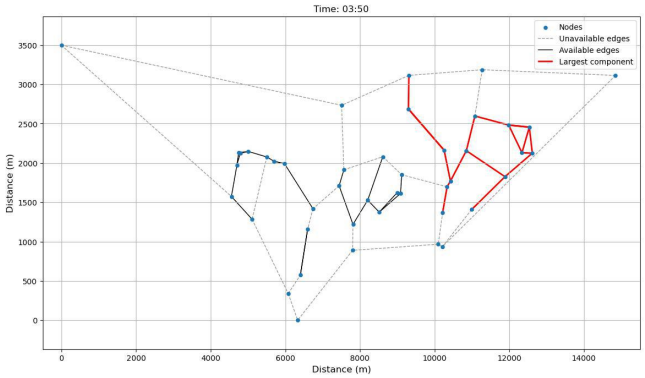
Time: 03:50
Nodes
Unavailable edges
Available edges
Largest component
Distance (m)
Distance (m)

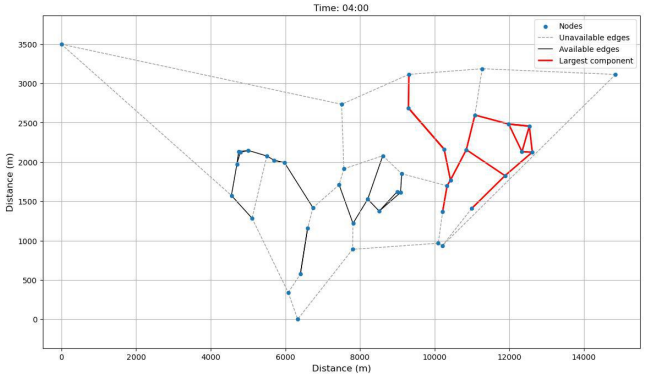
Time: 04:00
Nodes
Unavailable edges
Available edges
Largest component
Distance (m)
Distance (m)

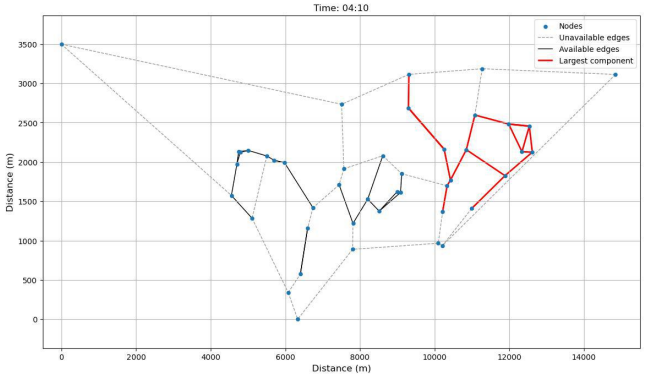
Time: 04:10
Nodes
Unavailable edges
Available edges
Largest component
Distance (m)
Distance (m)

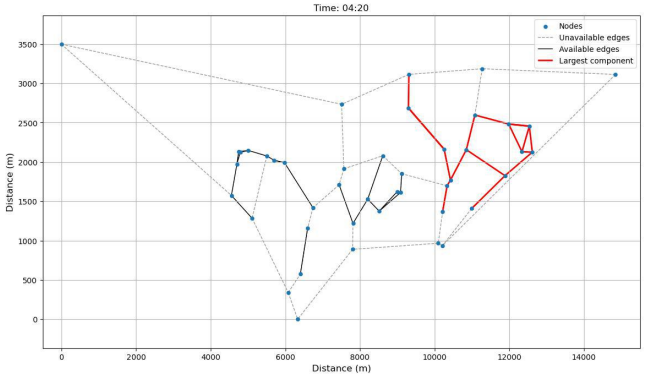
Time: 04:20
Nodes
Unavailable edges
Available edges
Largest component
Distance (m)
Distance (m)

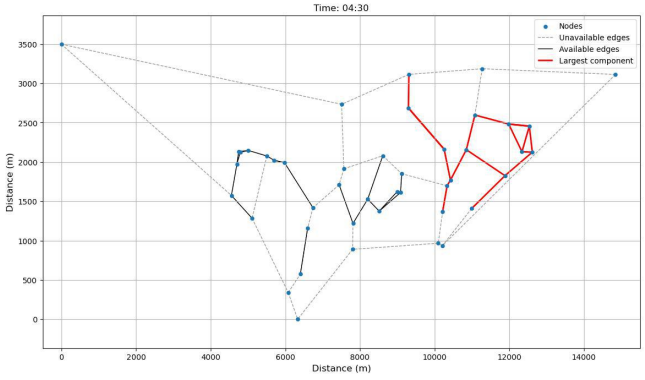
Time: 04:30
Nodes
Unavailable edges
Available edges
Largest component
Distance (m)
Distance (m)

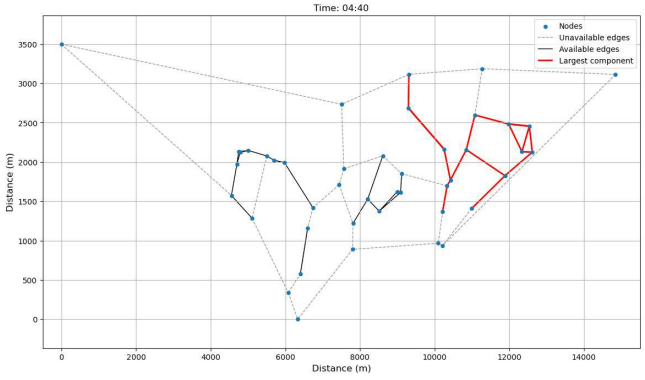
Time: 04:40
Nodes
Unavailable edges
Available edges
Largest component
Distance (m)
Distance (m)

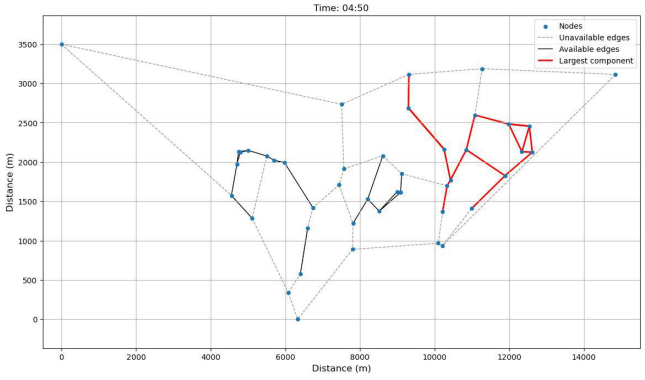
Time: 04:50
Nodes
Unavailable edges
Available edges
Largest component
Distance (m)
Distance (m)

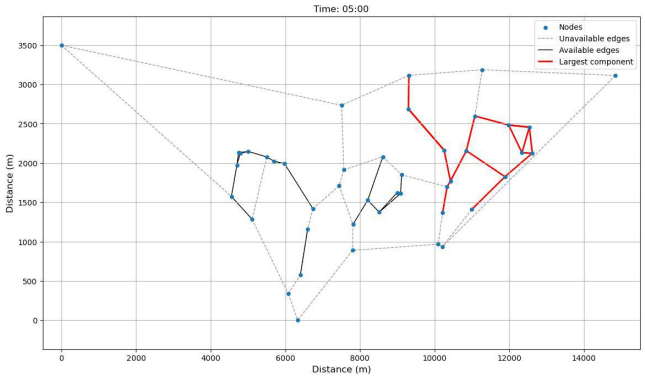
Time: 05:00
Nodes
Unavailable edges
Available edges
Largest component
Distance (m)
Distance (m)

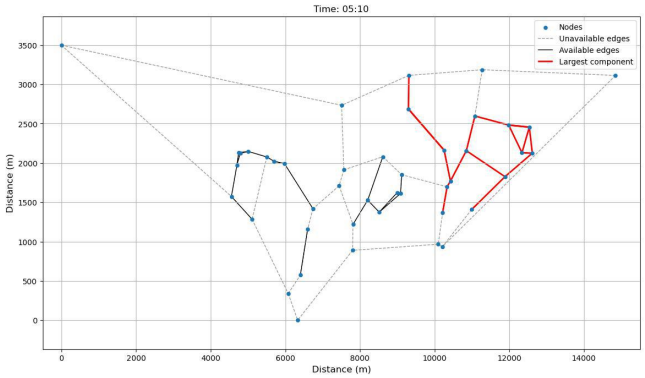
Time: 05:10
Nodes
Unavailable edges
Available edges
Largest component
Distance (m)
Distance (m)

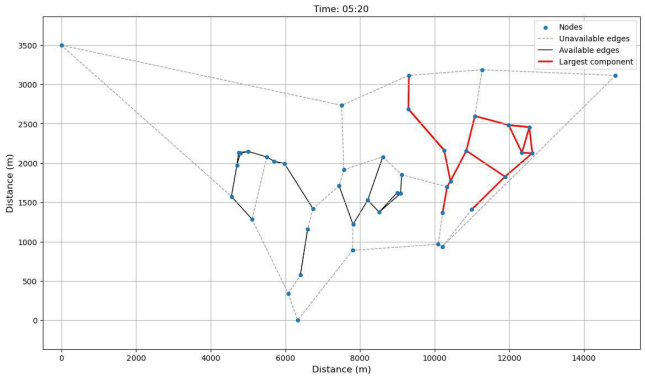
Time: 05:20
Nodes
Unavailable edges
Available edges
Largest component
Distance (m)
Distance (m)

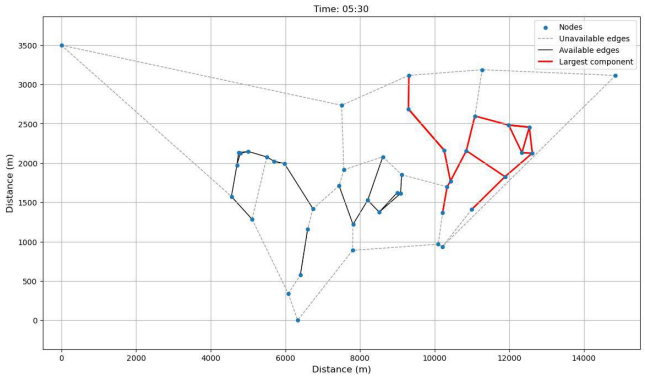
Time: 05:30
Nodes
Unavailable edges
Available edges
Largest component
Distance (m)
Distance (m)

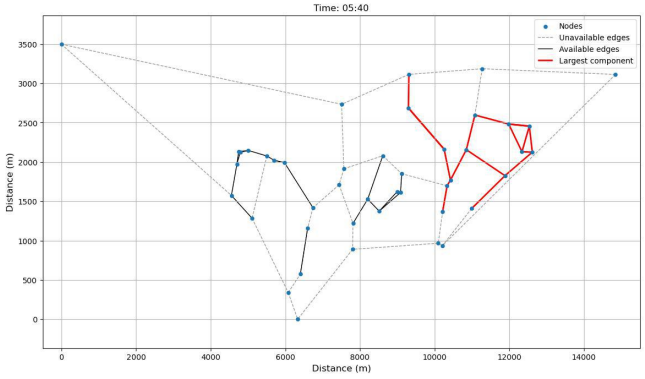
Time: 05:40
Nodes
Unavailable edges
Available edges
Largest component
Distance (m)
Distance (m)

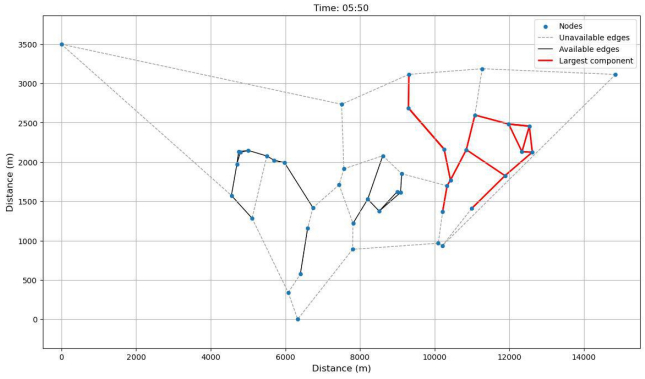
Time: 05:50
Nodes
Unavailable edges
Available edges
Largest component
Distance (m)
Distance (m)

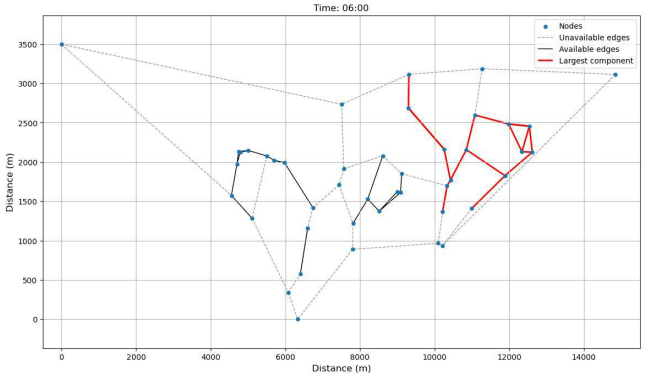
Time: 06:00
Nodes
Unavailable edges
Available edges
Largest component
Distance (m)
Distance (m)

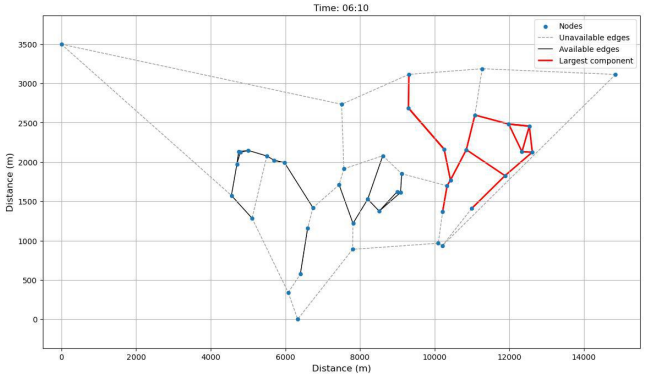
Time: 06:10
Nodes
Unavailable edges
Available edges
Largest component
Distance (m)
Distance (m)

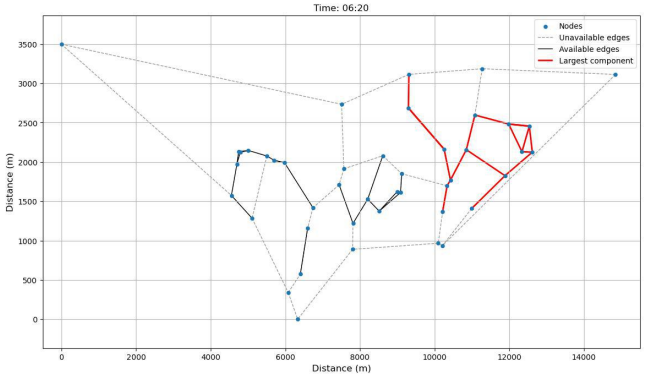
Time: 06:20
Nodes
Unavailable edges
Available edges
Largest component
Distance (m)
Distance (m)

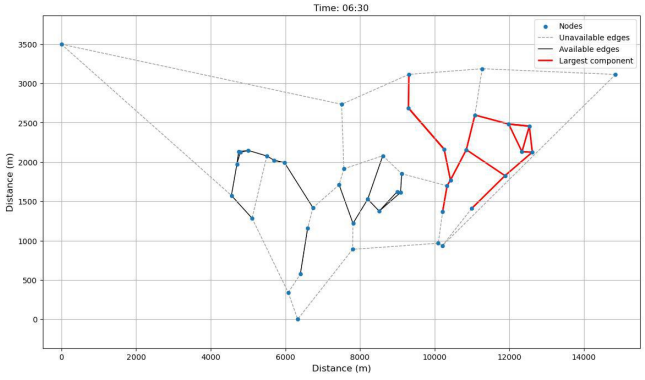
Time: 06:30
Nodes
Unavailable edges
Available edges
Largest component
Distance (m)
Distance (m)

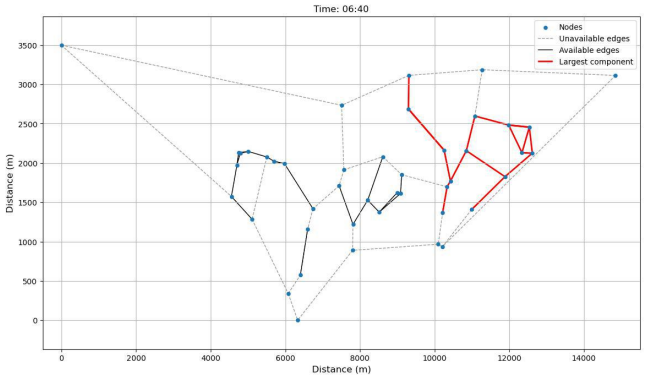
Time: 06:40
Nodes
Unavailable edges
Available edges
Largest component
Distance (m)
Distance (m)

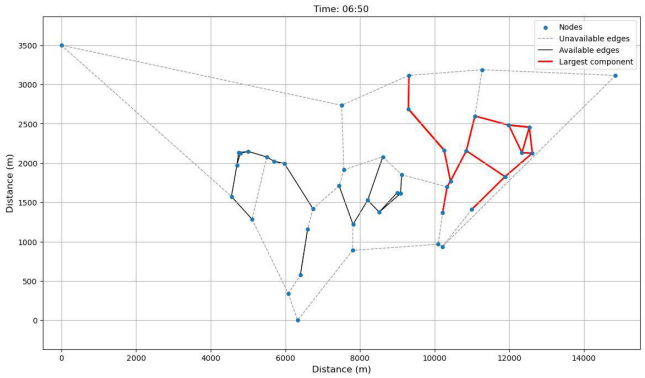
Time: 06:50
Nodes
Unavailable edges
Available edges
Largest component
Distance (m)
Distance (m)

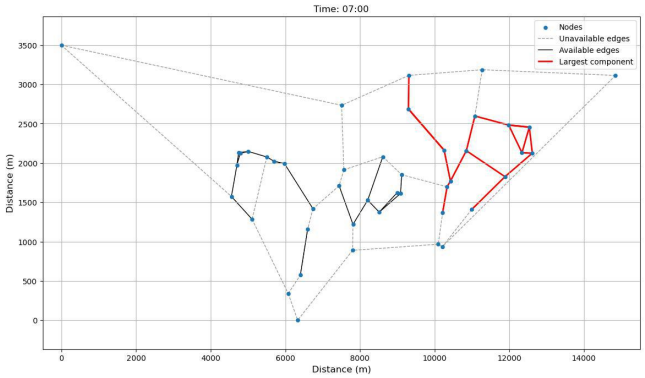
Time: 07:00
Nodes
Unavailable edges
Available edges
Largest component
Distance (m)
Distance (m)

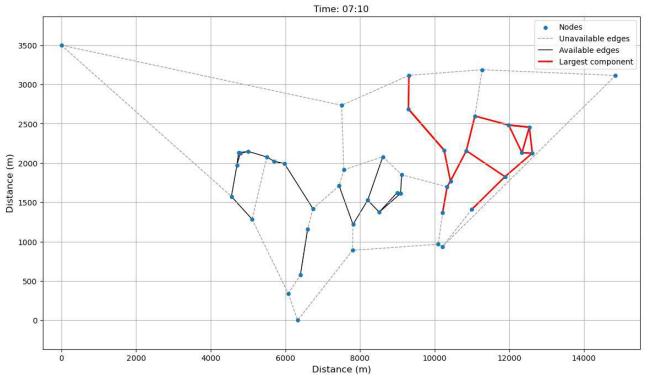
Time: 07:10
Nodes
Unavailable edges
Available edges
Largest component
Distance (m)
Distance (m)

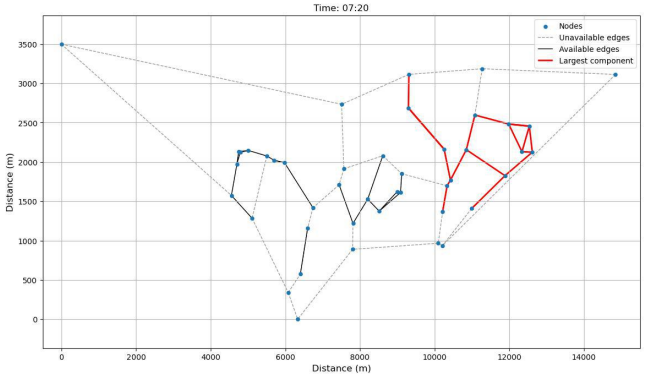
Time: 07:20
Nodes
Unavailable edges
Available edges
Largest component
Distance (m)
Distance (m)

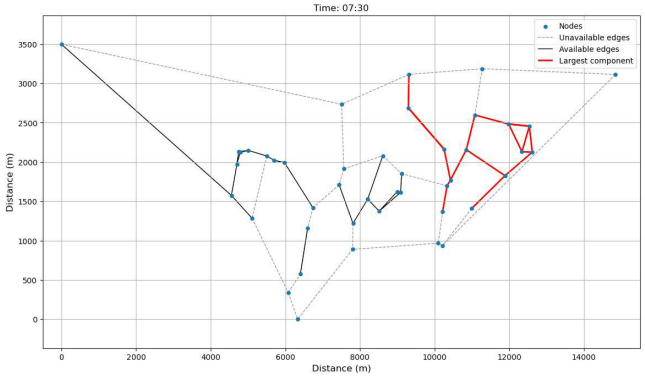
Time: 07:30
Nodes
Unavailable edges
Available edges
Largest component
Distance (m)
Distance (m)

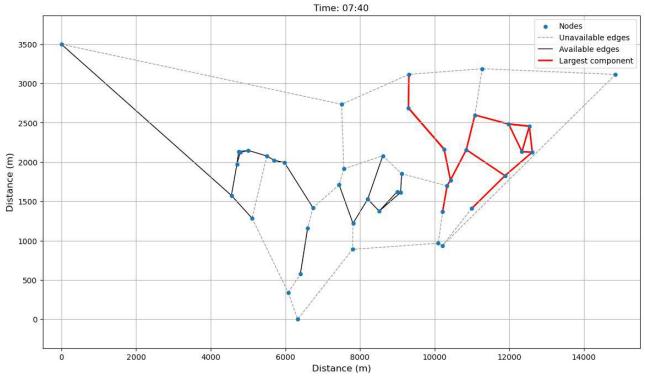
Time: 07:40
Nodes
Unavailable edges
Available edges
Largest component
Distance (m)
Distance (m)

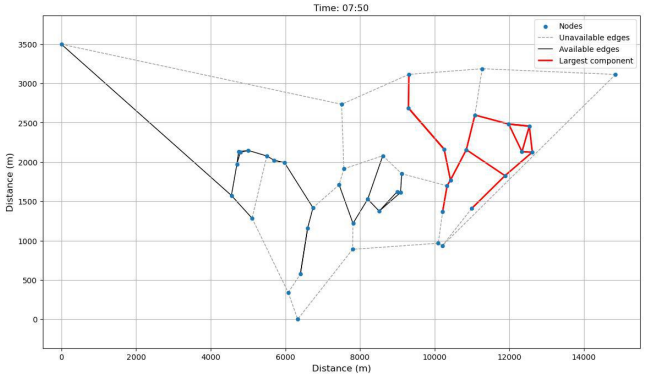
Time: 07:50
Nodes
Unavailable edges
Available edges
Largest component
Distance (m)
Distance (m)

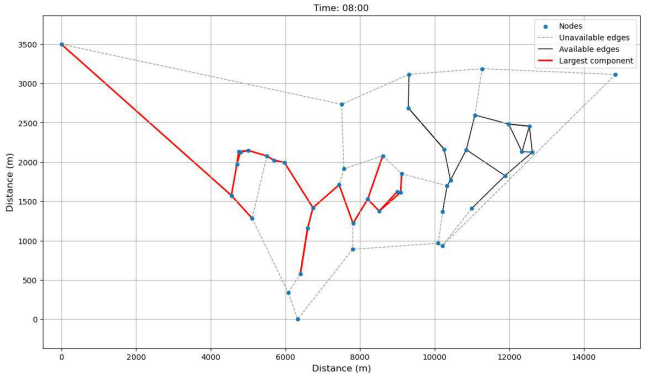
Time: 08:00
Nodes
Unavailable edges
Available edges
Largest component
Distance (m)
Distance (m)

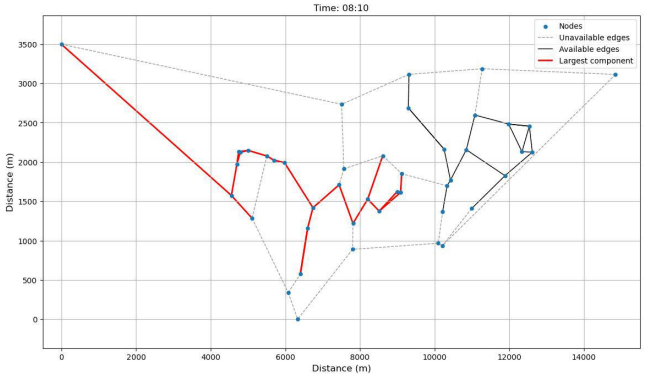
Time: 08:10
Nodes
Unavailable edges
Available edges
Largest component
Distance (m)
Distance (m)

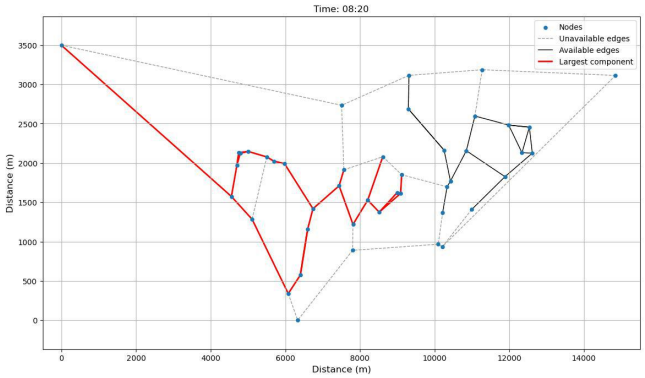
Time: 08:20
Nodes
Unavailable edges
Available edges
Largest component
Distance (m)
Distance (m)

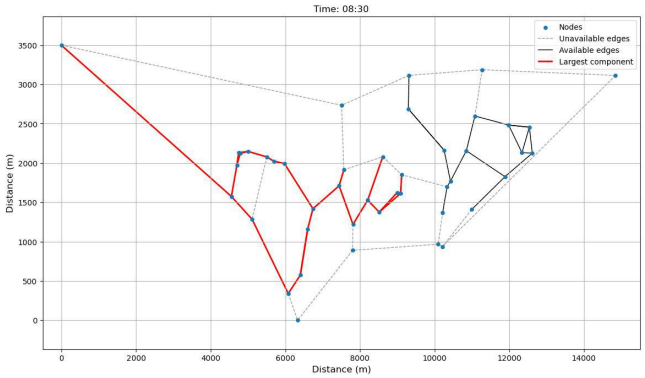
Time: 08:30
Nodes
Unavailable edges
Available edges
Largest component
Distance (m)
Distance (m)

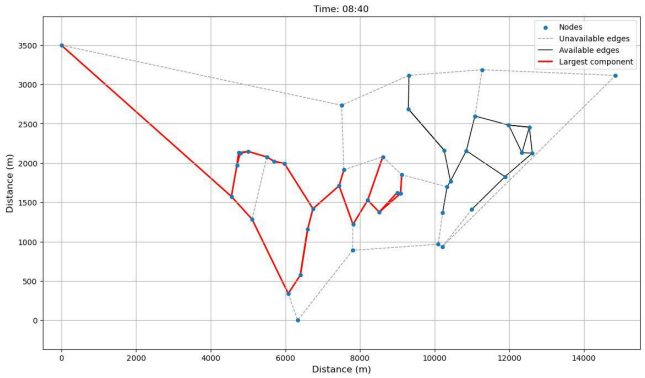
Time: 08:40
Nodes
Unavailable edges
Available edges
Largest component
Distance (m)
Distance (m)

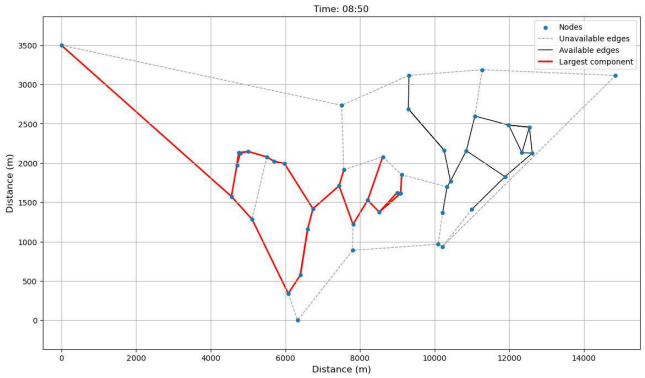
Time: 08:50
Nodes
Unavailable edges
Available edges
Largest component
Distance (m)
Distance (m)

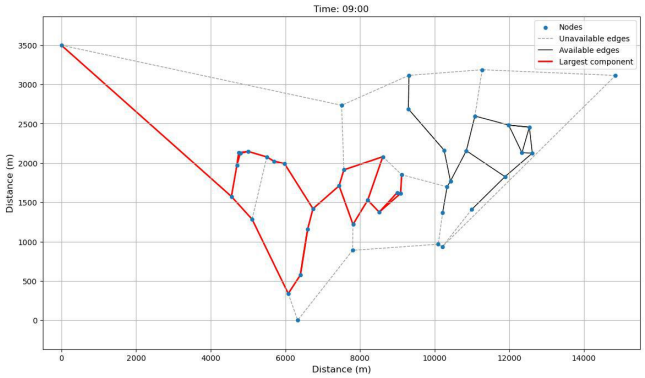
Time: 09:00
Nodes
Unavailable edges
Available edges
Largest component
Distance (m)
Distance (m)

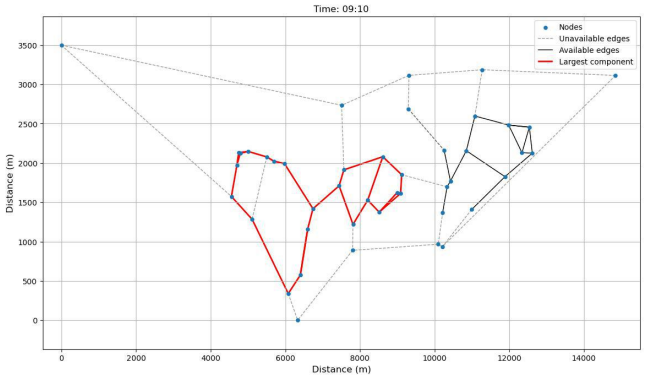
Time: 09:10
Nodes
Unavailable edges
Available edges
Largest component
Distance (m)
Distance (m)

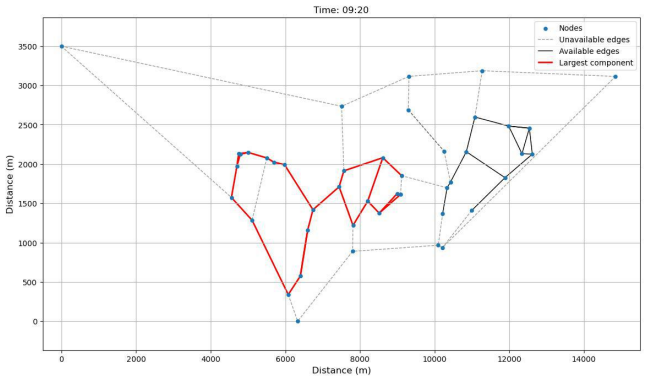
Time: 09:20
Nodes
Unavailable edges
Available edges
Largest component
Distance (m)
Distance (m)

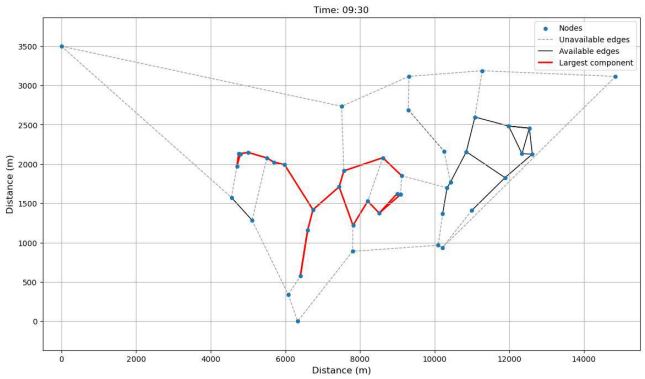
Time: 09:30
Nodes
Unavailable edges
Available edges
Largest component
Distance (m)
Distance (m)

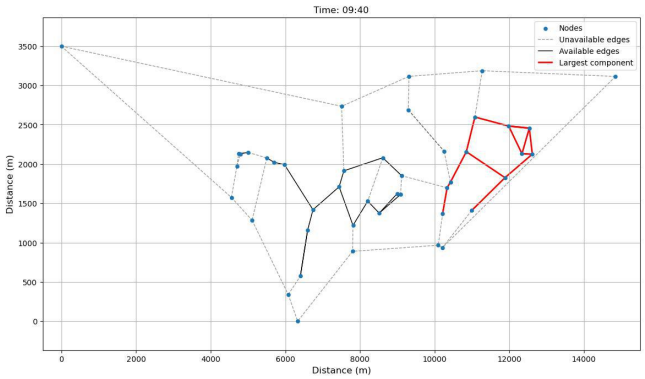
Time: 09:40
Nodes
Unavailable edges
Available edges
Largest component
Distance (m)
Distance (m)

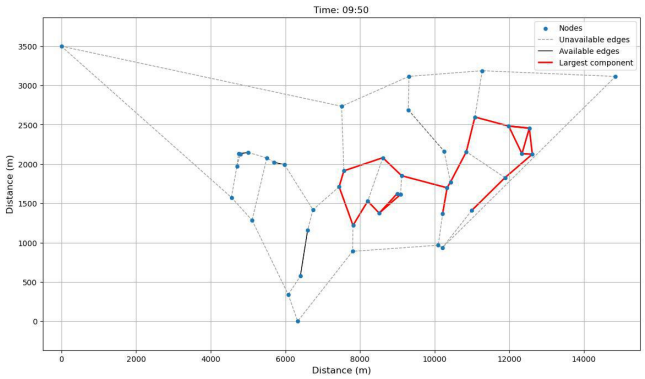
Time: 09:50
Nodes
Unavailable edges
Available edges
Largest component
Distance (m)
Distance (m)

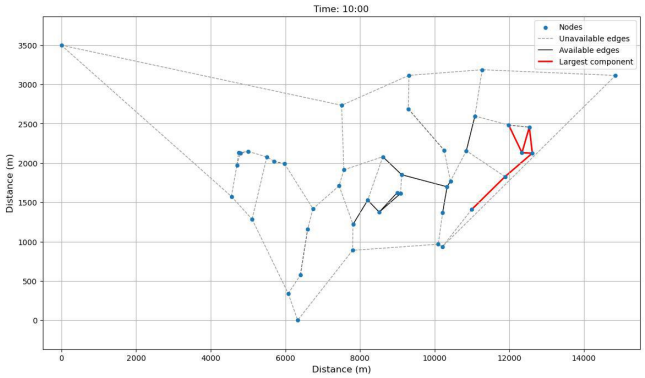
Time: 10:00
Nodes
Unavailable edges
Available edges
Largest component
Distance (m)
Distance (m)

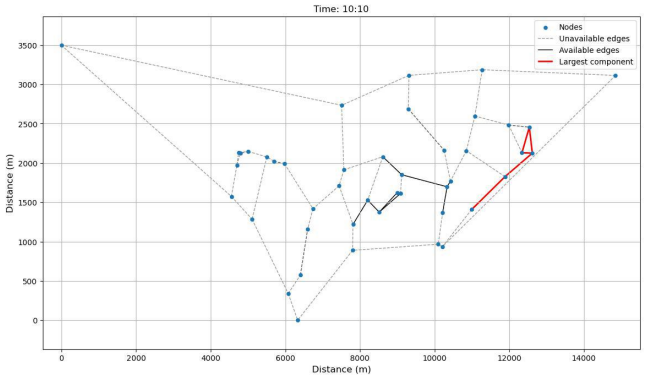
Time: 10:10
Nodes
Unavailable edges
Available edges
Largest component
Distance (m)
Distance (m)

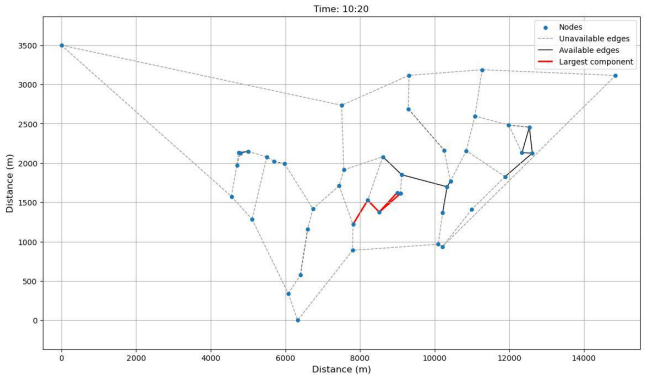
Time: 10:20
Nodes
Unavailable edges
Available edges
Largest component
Distance (m)
Distance (m)

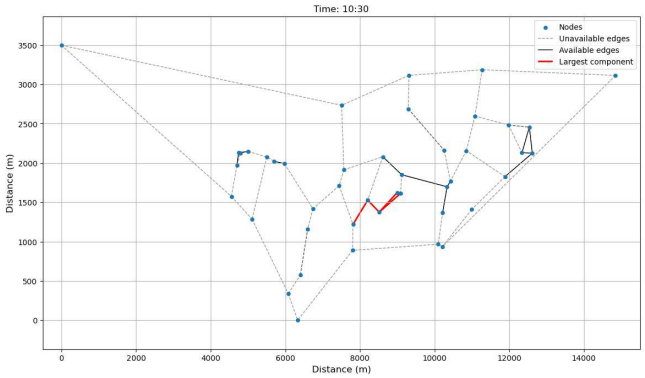
Time: 10:30
Nodes
Unavailable edges
Available edges
Largest component
Distance (m)
Distance (m)

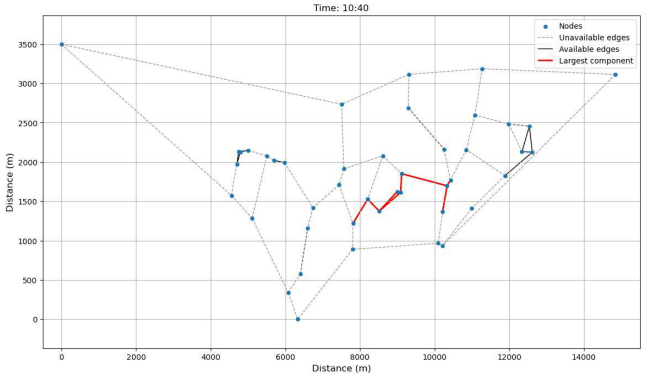
Time: 10:40
Nodes
Unavailable edges
Available edges
Largest component
Distance (m)
Distance (m)

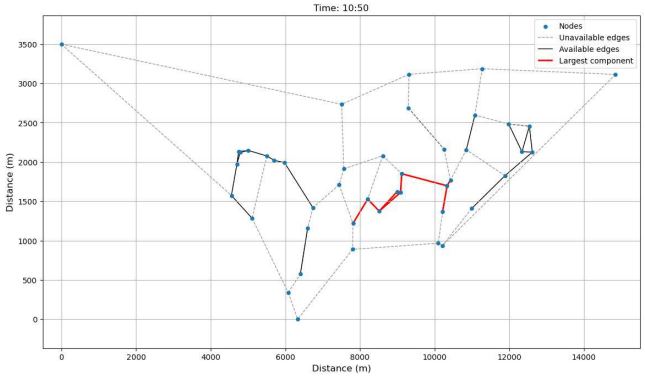
Time: 10:50
Nodes
Unavailable edges
Available edges
Largest component
Distance (m)
Distance (m)

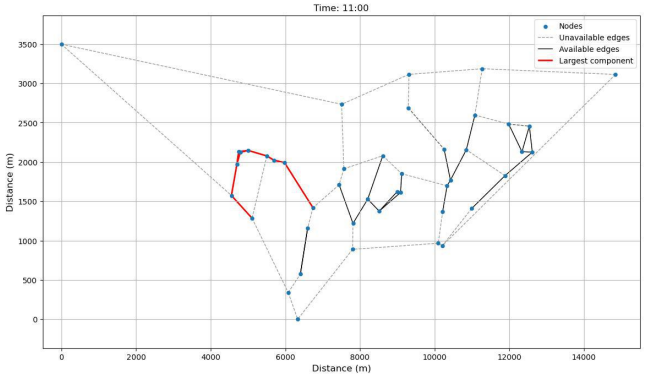
Time: 11:00
Nodes
Unavailable edges
Available edges
Largest component
Distance (m)
Distance (m)

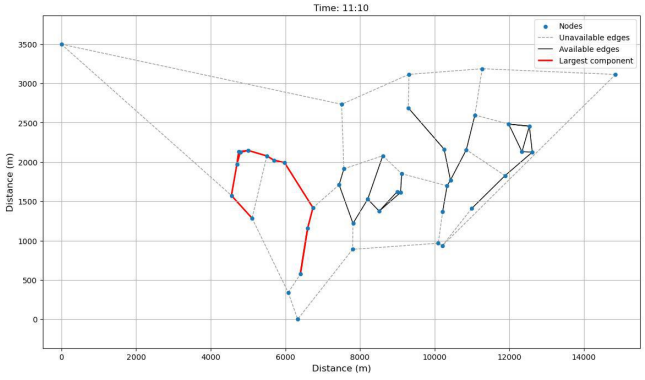
Time: 11:10
Nodes
Unavailable edges
Available edges
Largest component
Distance (m)
Distance (m)

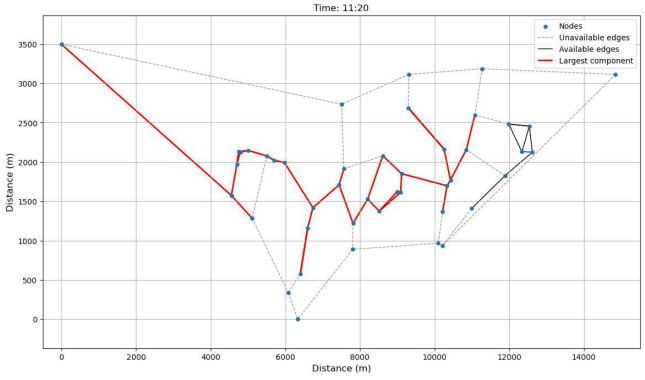
Time: 11:20
Nodes
Unavailable edges
Available edges
Largest component
Distance (m)
Distance (m)

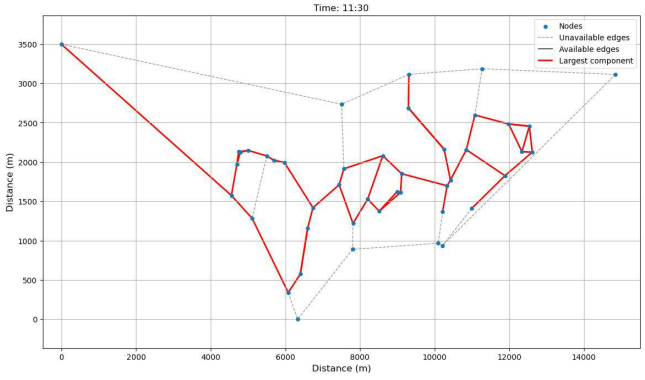
Time: 11:30
Nodes
Unavailable edges
Available edges
Largest component
Distance (m)
Distance (m)

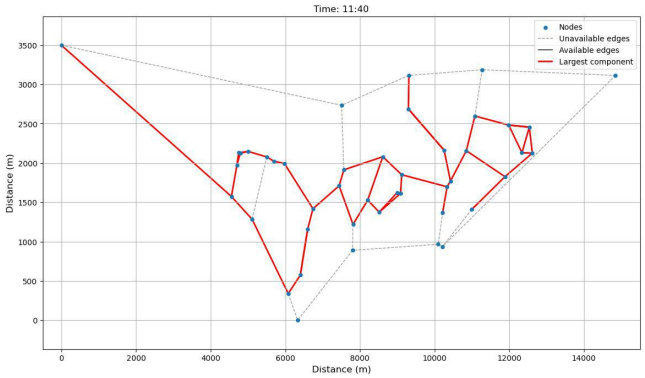
Time: 11:40
Nodes
Unavailable edges
Available edges
Largest component
Distance (m)
Distance (m)

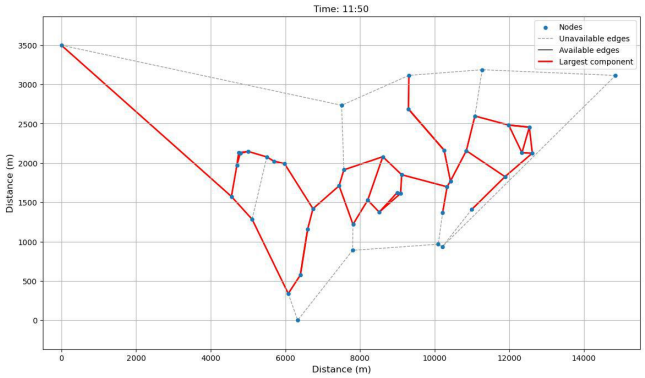
Time: 11:50
Nodes
Unavailable edges
Available edges
Largest component
Distance (m)
Distance (m)

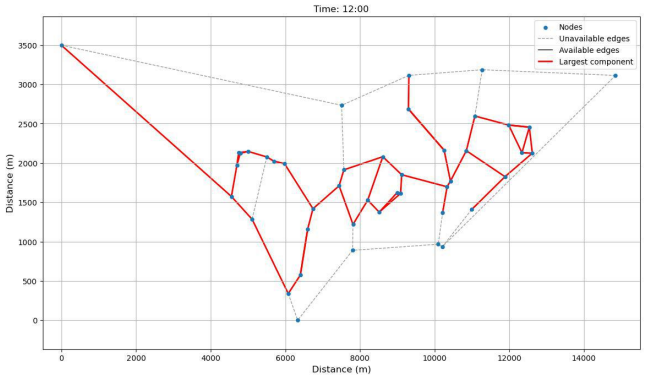
Time: 12:00
Nodes
Unavailable edges
Available edges
Largest component
Distance (m)
Distance (m)

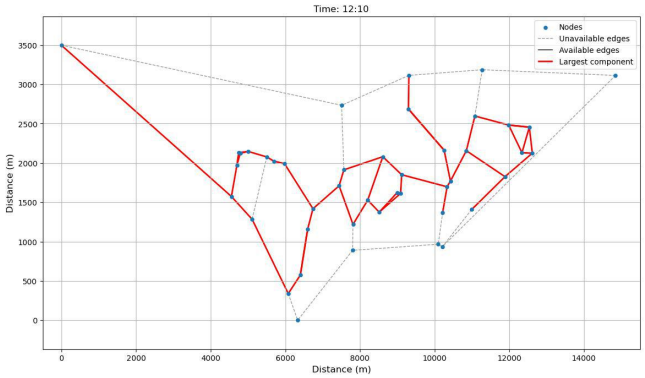
Time: 12:10
Nodes
Unavailable edges
Available edges
Largest component
Distance (m)
Distance (m)

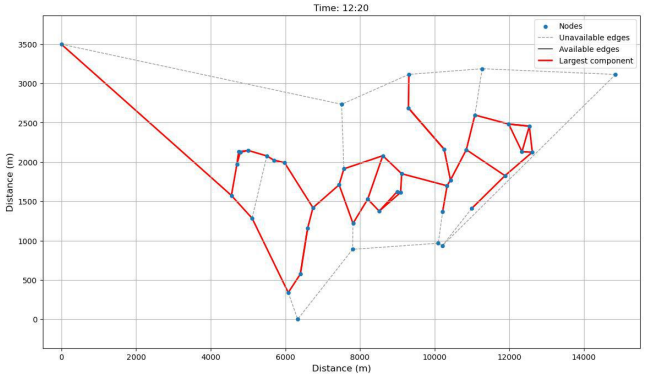
Time: 12:20
Nodes
Unavailable edges
Available edges
Largest component
Distance (m)
Distance (m)

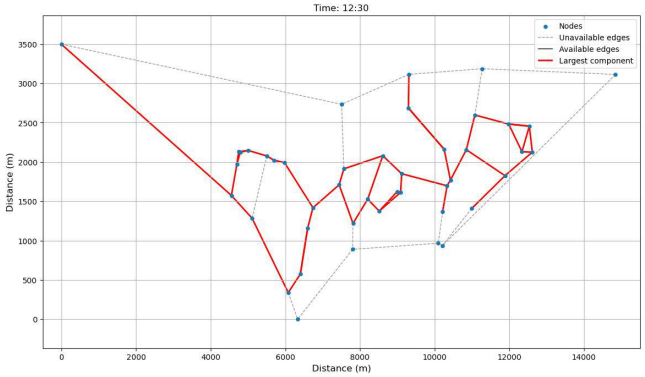
Time: 12:30
Nodes
Unavailable edges
Available edges
Largest component
Distance (m)
Distance (m)

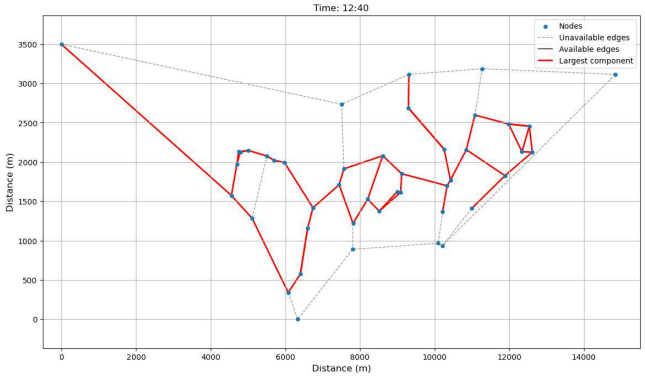
Time: 12:40
Nodes
Unavailable edges
Available edges
Largest component
Distance (m)
Distance (m)

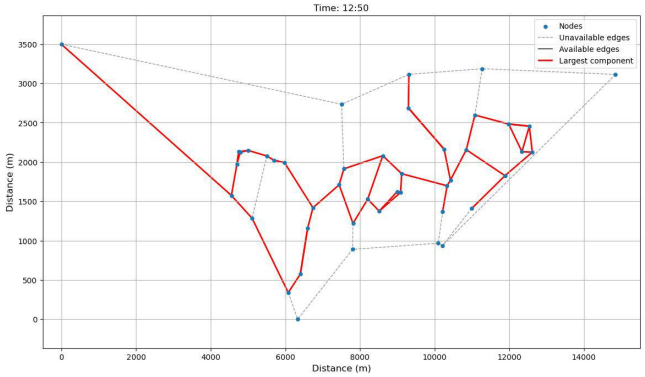
Time: 12:50
Nodes
Unavailable edges
Available edges
Largest component
Distance (m)
Distance (m)

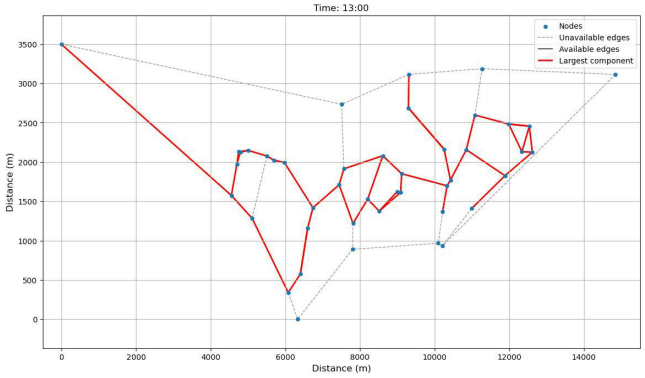
Time: 13:00
Nodes
Unavailable edges
Available edges
Largest component
Distance (m)
Distance (m)

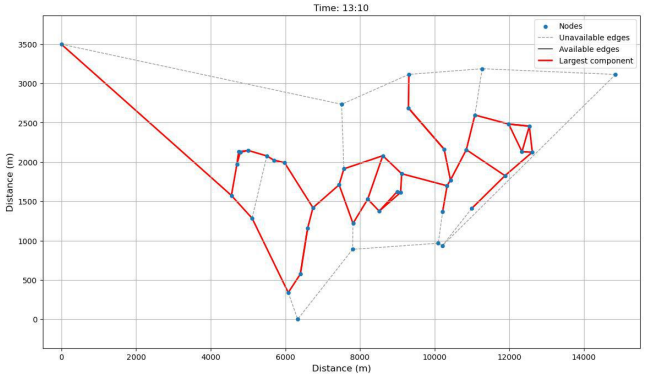
Time: 13:10
Nodes
Unavailable edges
Available edges
Largest component
Distance (m)
Distance (m)

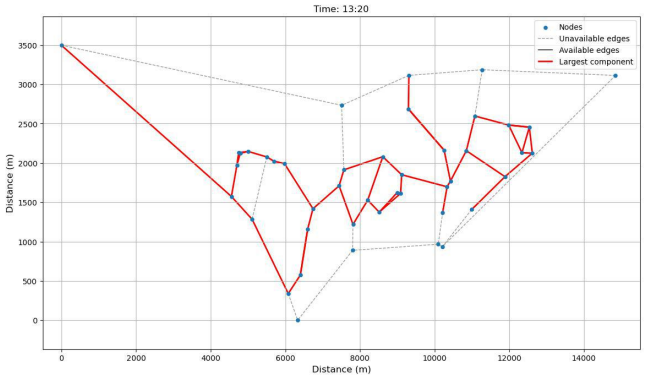
Time: 13:20
Nodes
Unavailable edges
Available edges
Largest component
Distance (m)
Distance (m)

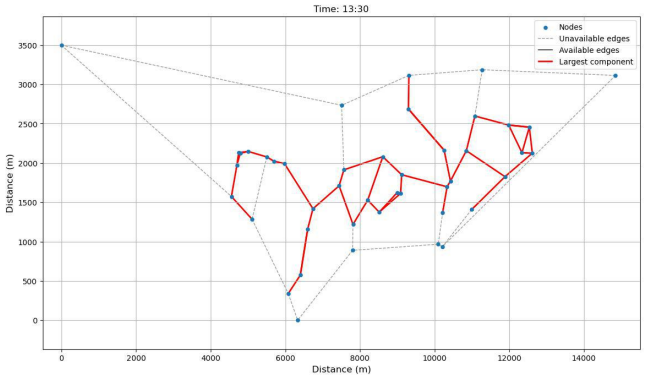
Time: 13:30
Nodes
Unavailable edges
Available edges
Largest component
Distance (m)
Distance (m)

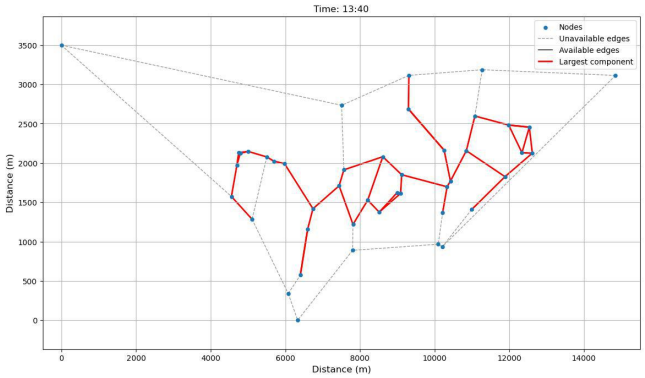
Time: 13:40
Nodes
Unavailable edges
Available edges
Largest component
Distance (m)
Distance (m)

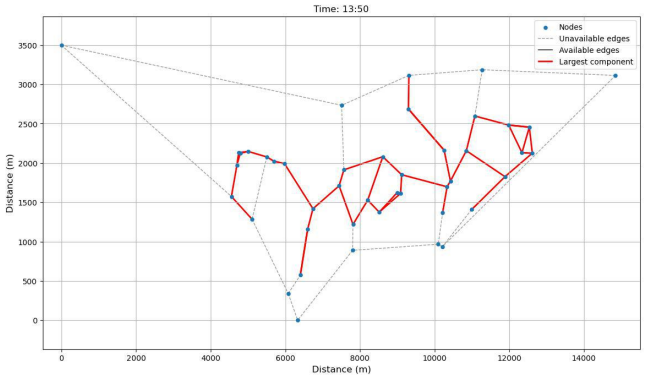
Time: 13:50
Nodes
Unavailable edges
Available edges
Largest component
Distance (m)
Distance (m)

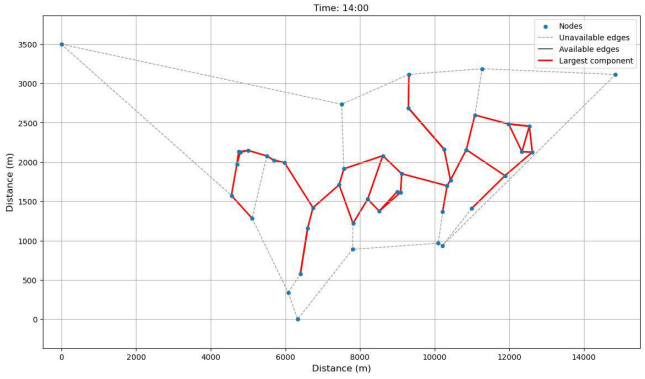
Time: 14:00
Nodes
Unavailable edges
Available edges
Largest component
Distance (m)
Distance (m)

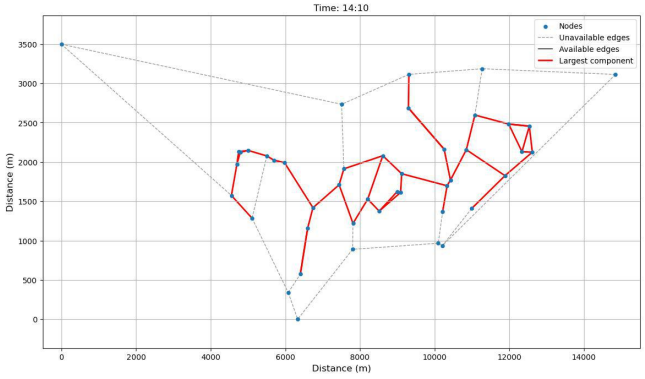
Time: 14:10
Nodes
Unavailable edges
Available edges
Largest component
Distance (m)
Distance (m)

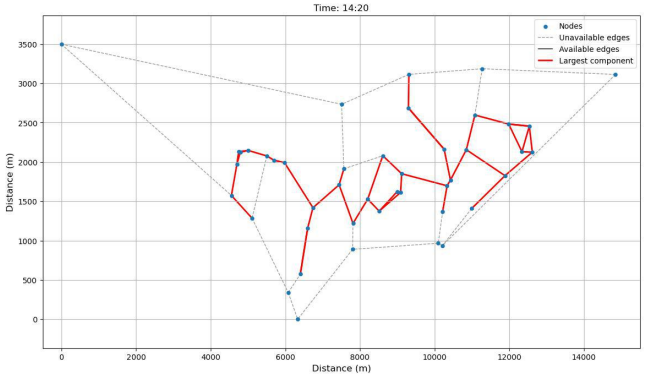
Time: 14:20
Nodes
Unavailable edges
Available edges
Largest component
Distance (m)
Distance (m)

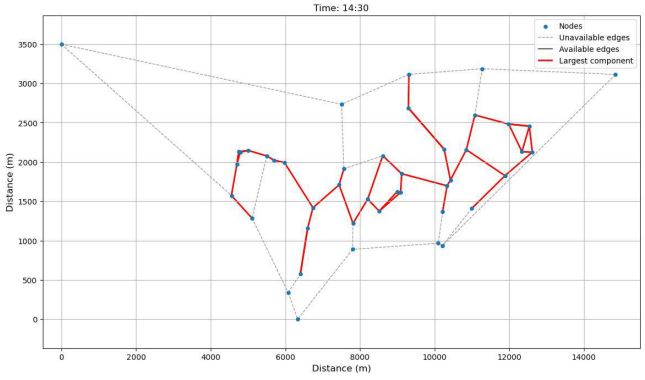
Time: 14:30
Nodes
Unavailable edges
Available edges
Largest component
Distance (m)
Distance (m)

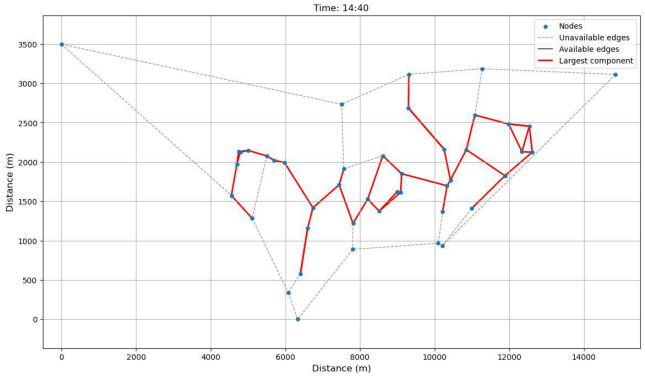
Time: 14:40
Nodes
Unavailable edges
Available edges
Largest component
Distance (m)
Distance (m)

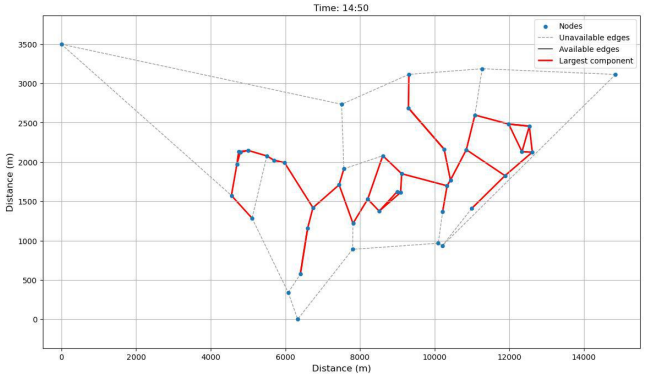
Time: 14:50
Nodes
Unavailable edges
Available edges
Largest component
Distance (m)
Distance (m)

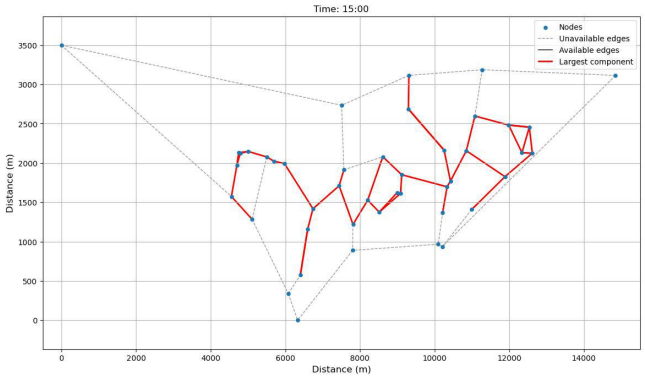
Time: 15:00
Nodes
Unavailable edges
Available edges
Largest component
Distance (m)
Distance (m)

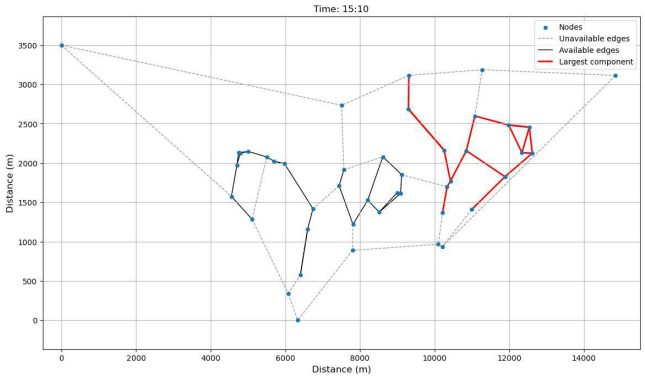
Time: 15:10
Nodes
Unavailable edges
Available edges
Largest component
Distance (m)
Distance (m)

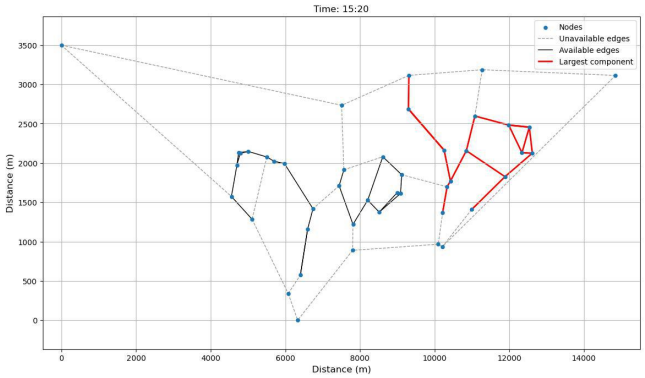
Time: 15:20
Nodes
Unavailable edges
Available edges
Largest component
Distance (m)
Distance (m)

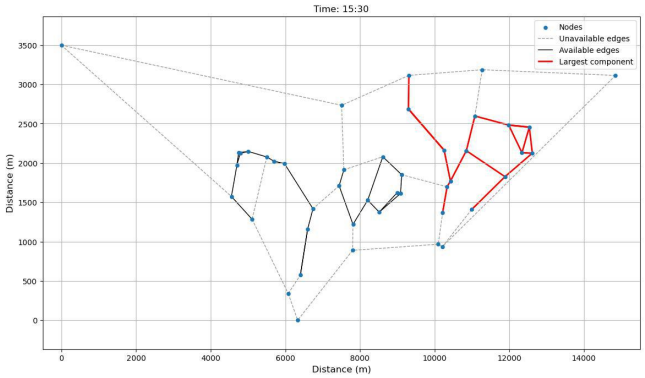
Time: 15:30
Nodes
Unavailable edges
Available edges
Largest component
Distance (m)
Distance (m)

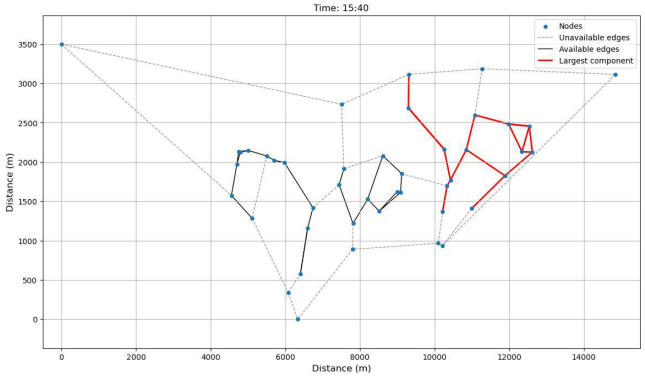
Time: 15:40
Nodes
Unavailable edges
Available edges
Largest component
Distance (m)
Distance (m)

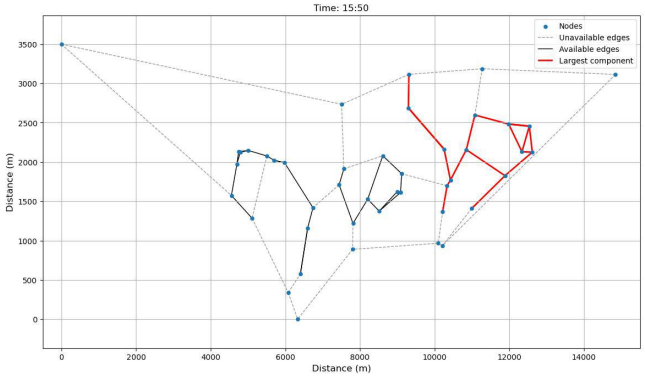
Time: 15:50
Nodes
Unavailable edges
Available edges
Largest component
Distance (m)
Distance (m)

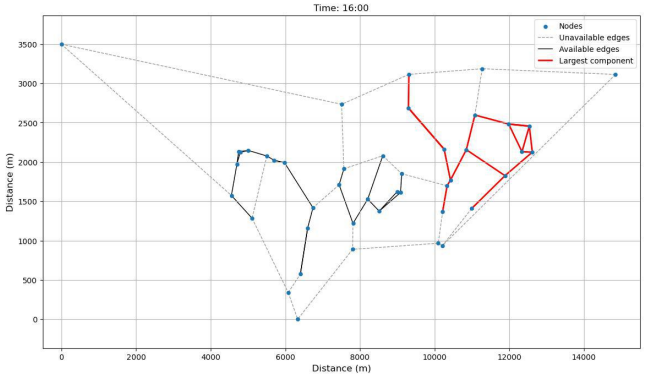
Time: 16:00
Nodes
Unavailable edges
Available edges
Largest component
Distance (m)
Distance (m)

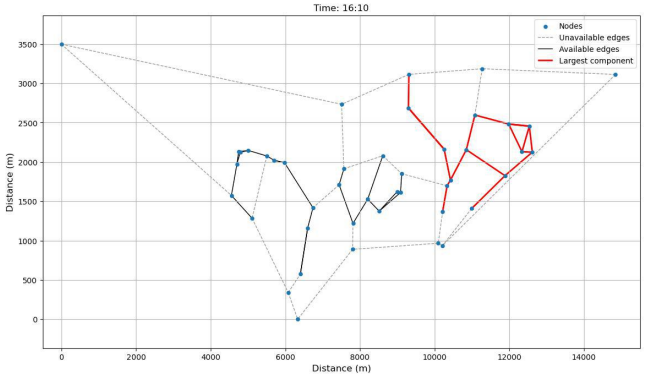
Time: 16:10
Nodes
Unavailable edges
Available edges
Largest component
Distance (m)
Distance (m)

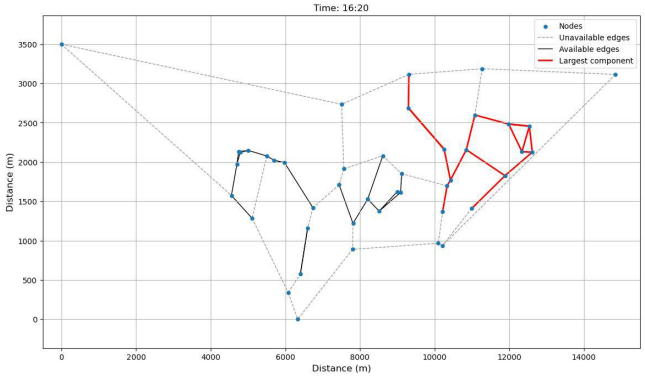
Time: 16:20
Nodes
Unavailable edges
Available edges
Largest component
Distance (m)
Distance (m)

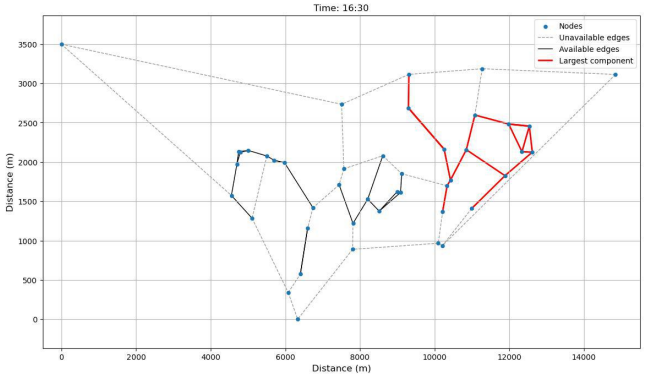
Time: 16:30
Nodes
Unavailable edges
Available edges
Largest component
Distance (m)
Distance (m)

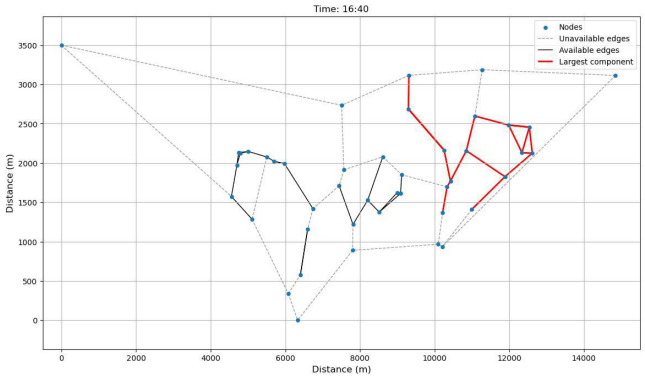
Time: 16:40
Nodes
Unavailable edges
Available edges
Largest component
Distance (m)
Distance (m)

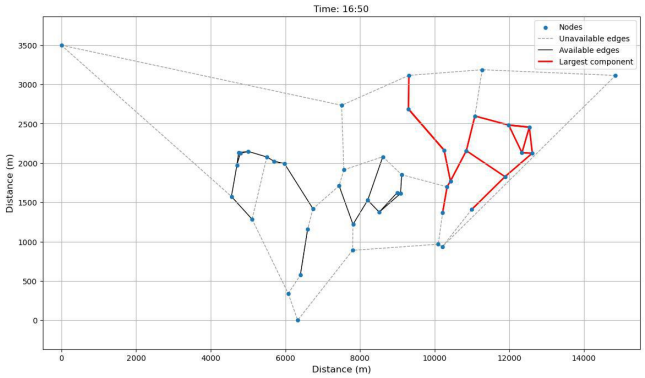
Time: 16:50
Nodes
Unavailable edges
Available edges
Largest component
Distance (m)
Distance (m)

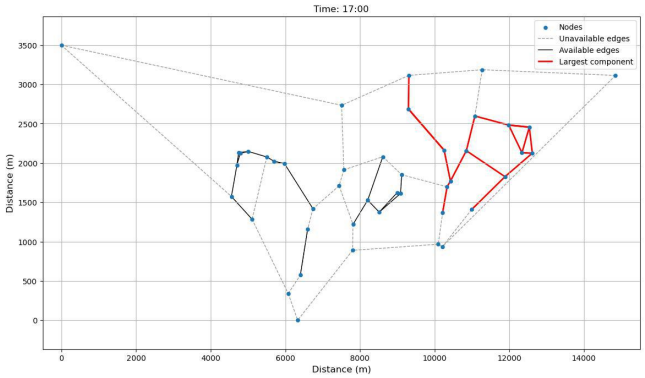
Time: 17:00
Nodes
Unavailable edges
Available edges
Largest component
Distance (m)
Distance (m)

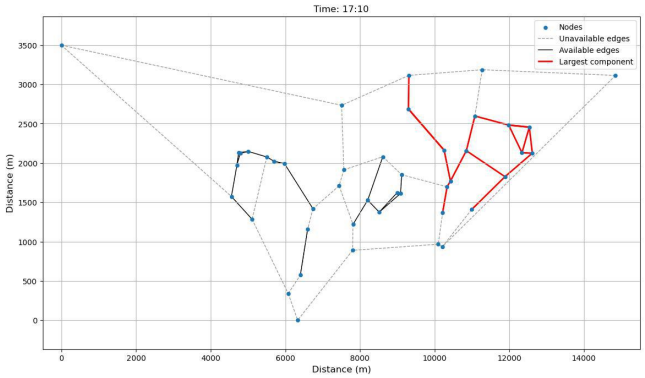
Time: 17:10
Nodes
Unavailable edges
Available edges
Largest component
Distance (m)
Distance (m)

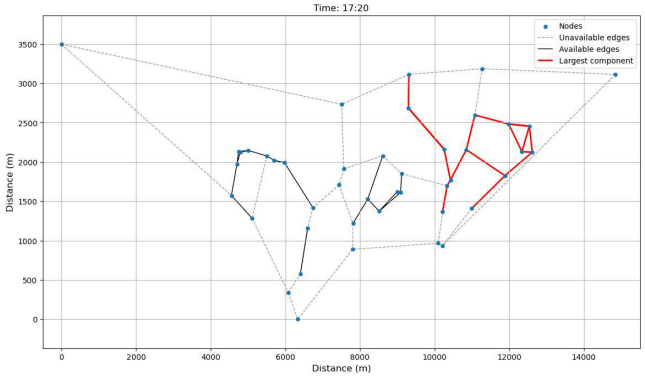
Time: 17:20
Nodes
Unavailable edges
Available edges
Largest component
Distance (m)
Distance (m)

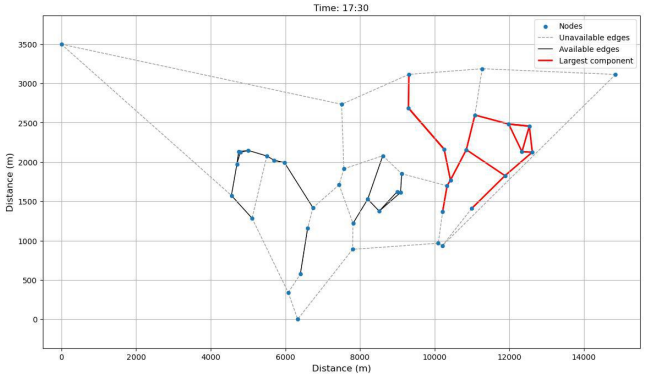
Time: 17:30
Nodes
Unavailable edges
Available edges
Largest component
Distance (m)
Distance (m)

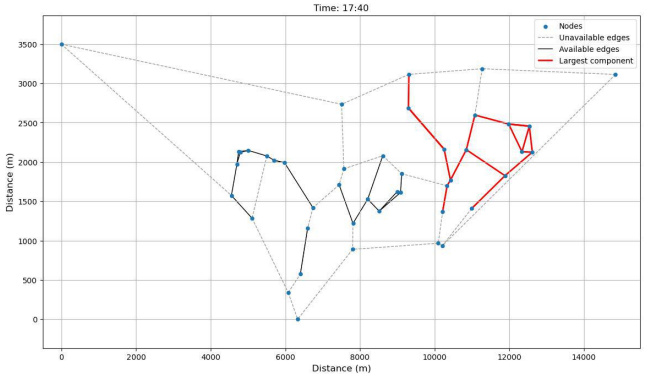
Time: 17:40
Nodes
Unavailable edges
Available edges
Largest component
Distance (m)
Distance (m)

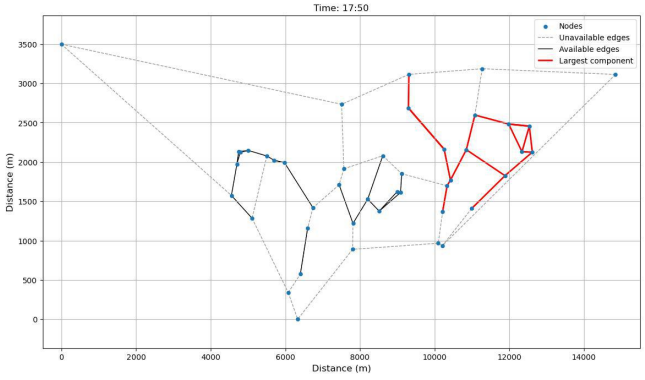
Time: 17:50
Nodes
Unavailable edges
Available edges
Largest component
Distance (m)
Distance (m)

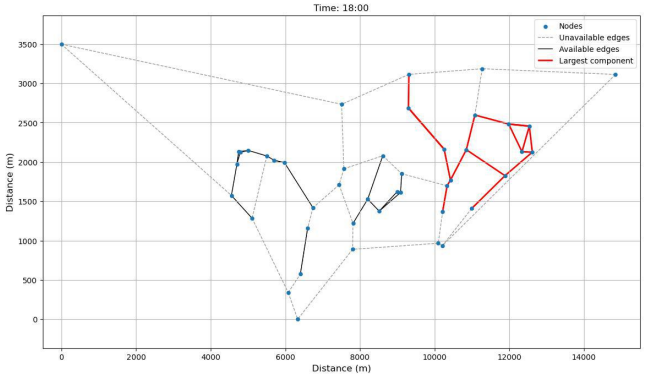
Time: 18:00
Nodes
Unavailable edges
Available edges
Largest component
Distance (m)
Distance (m)

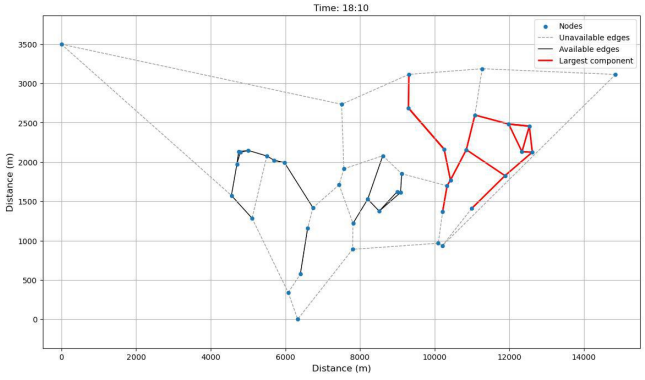
Time: 18:10
Nodes
Unavailable edges
Available edges
Largest component
Distance (m)
Distance (m)

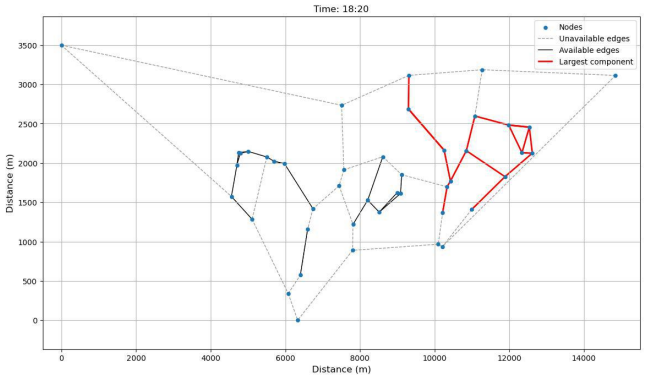
Time: 18:20
Nodes
Unavailable edges
Available edges
Largest component
Distance (m)
Distance (m)

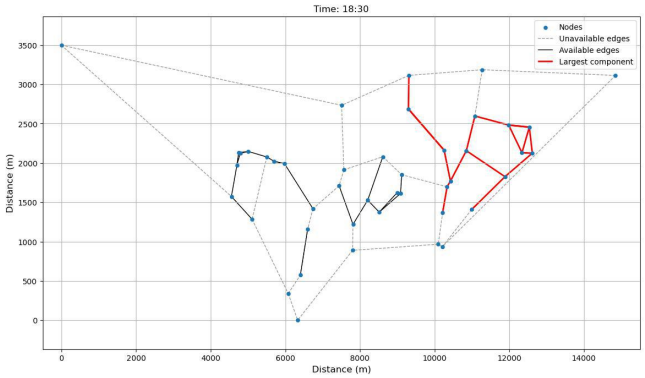
Time: 18:30
Nodes
Unavailable edges
Available edges
Largest component
Distance (m)
Distance (m)

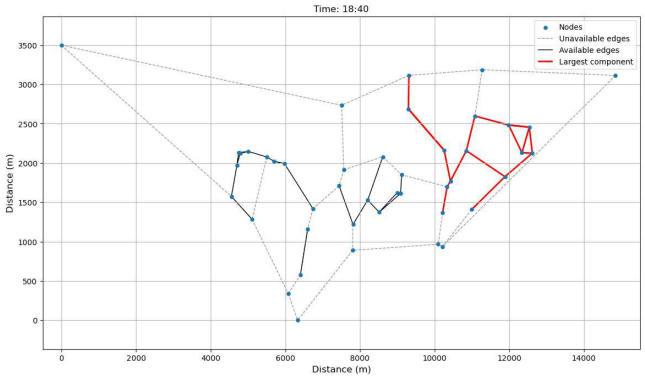
Time: 18:40
Nodes
Unavailable edges
Available edges
Largest component
Distance (m)
Distance (m)

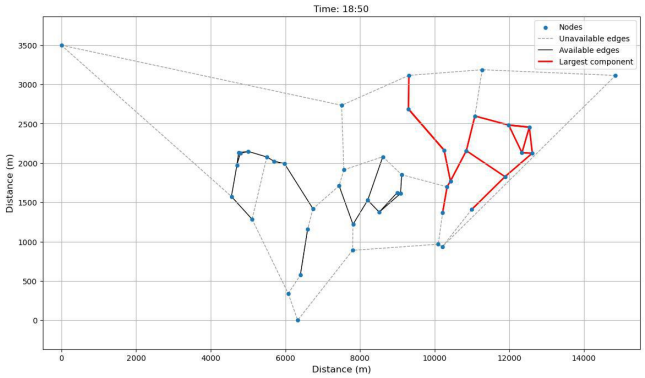
Time: 18:50
Nodes
Unavailable edges
Available edges
Largest component
Distance (m)
Distance (m)

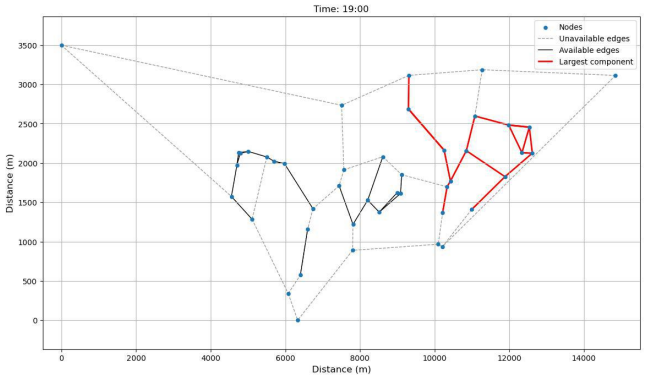
Time: 19:00
Nodes
Unavailable edges
Available edges
Largest component
Distance (m)
Distance (m)

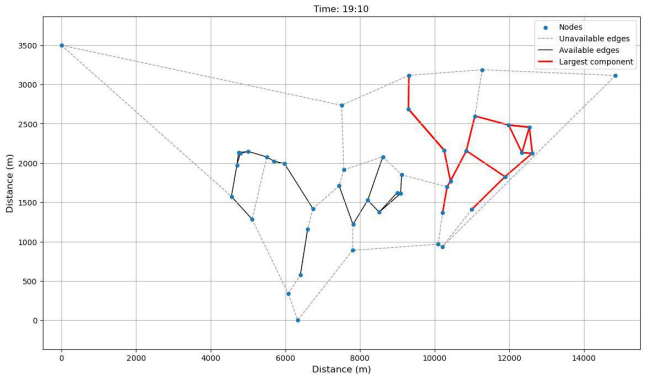
Time: 19:10
Nodes
Unavailable edges
Available edges
Largest component
Distance (m)
Distance (m)

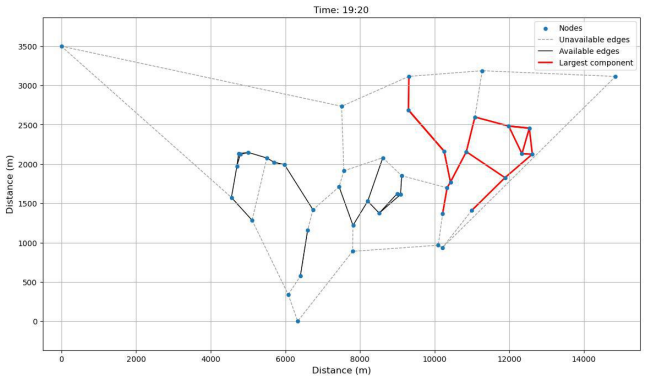
Time: 19:20
Nodes
Unavailable edges
Available edges
Largest component
Distance (m)
Distance (m)

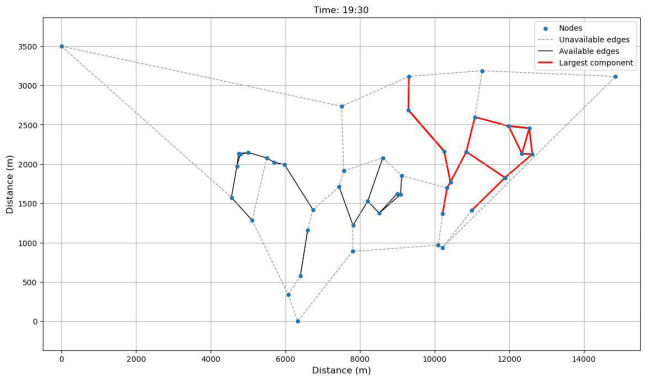
Time: 19:30
Nodes
Unavailable edges
Available edges
Largest component
Distance (m)
Distance (m)

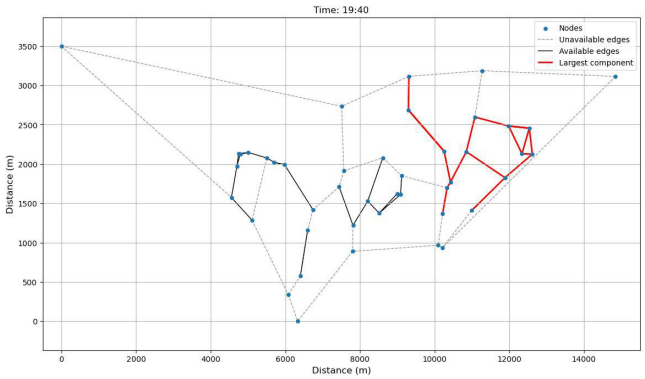
Time: 19:40
Nodes
Unavailable edges
Available edges
Largest component
Distance (m)
Distance (m)

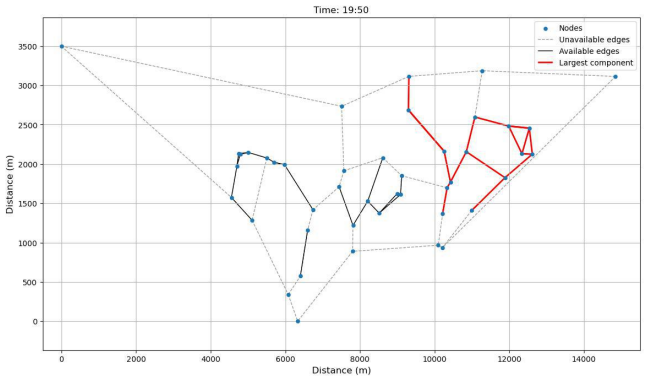
Time: 19:50
Nodes
Unavailable edges
Available edges
Largest component
Distance (m)
Distance (m)

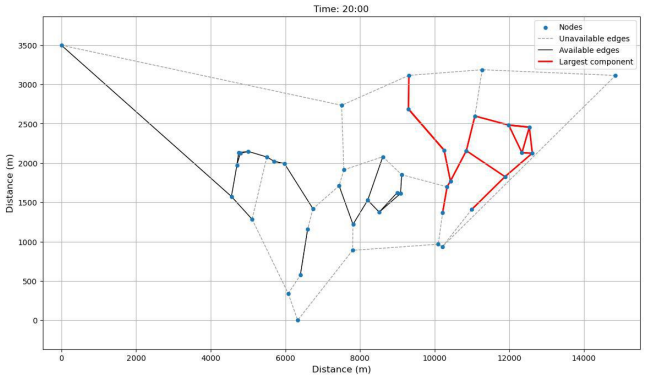
Time: 20:00
Nodes
Unavailable edges
Available edges
Largest component
Distance (m)
Distance (m)

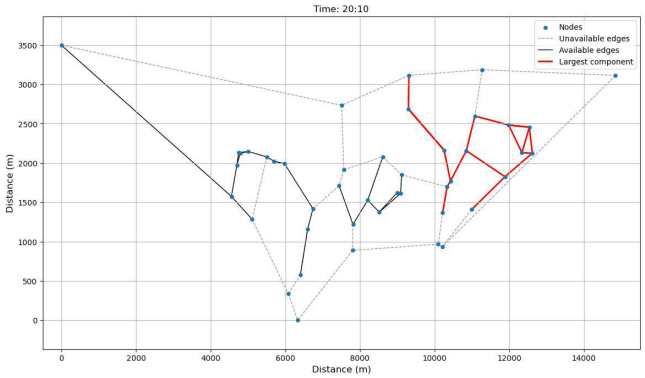
Time: 20:10
Nodes
Unavailable edges
Available edges
Largest component
Distance (m)
Distance (m)

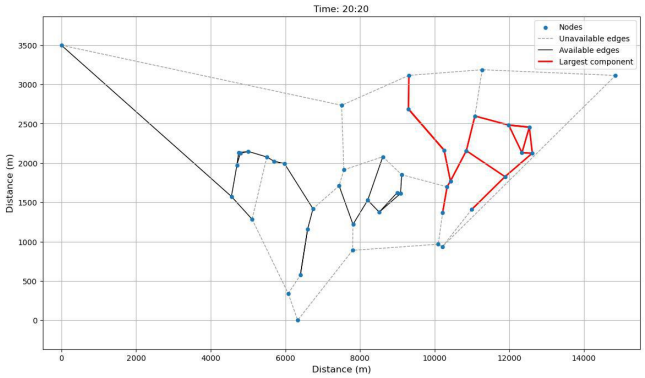
Time: 20:20
Nodes
Unavailable edges
Available edges
Largest component
Distance (m)
Distance (m)

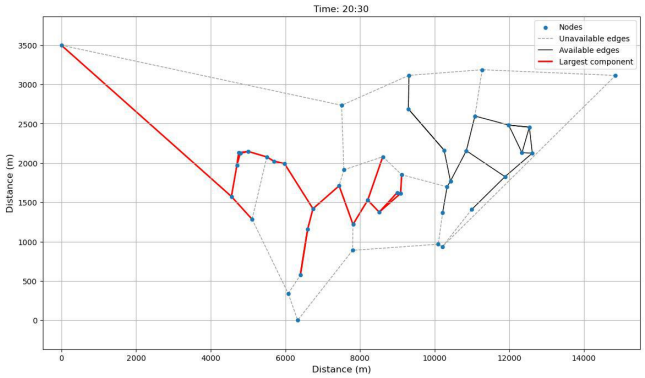
Time: 20:30
Nodes
Unavailable edges
Available edges
Largest component
Distance (m)
Distance (m)

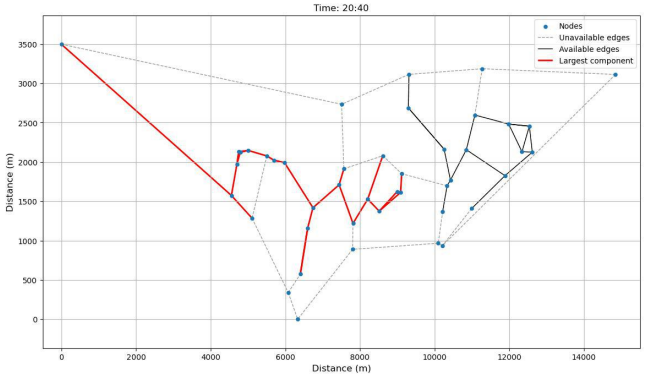
Time: 20:40
Nodes
Unavailable edges
Available edges
Largest component
Distance (m)
Distance (m)

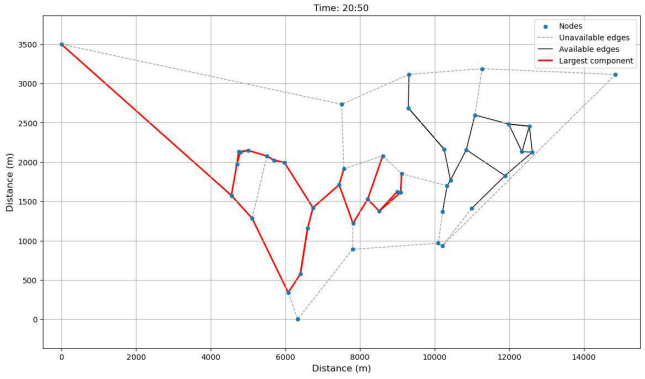
Time: 20:50
Nodes
Unavailable edges
Available edges
Largest component
Distance (m)
Distance (m)

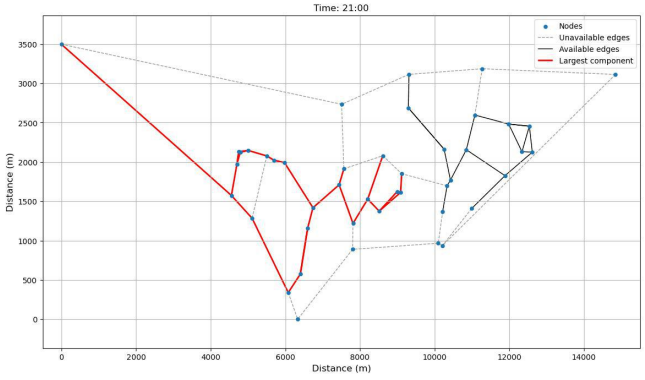
Time: 21:00
Nodes
Unavailable edges
Available edges
Largest component
Distance (m)
Distance (m)

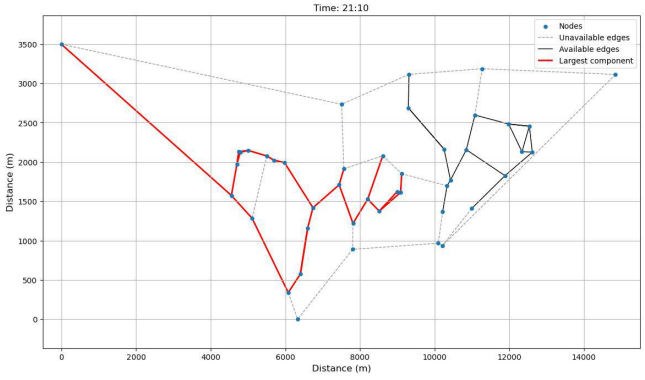
Time: 21:10
Nodes
Unavailable edges
Available edges
Largest component
Distance (m)
Distance (m)

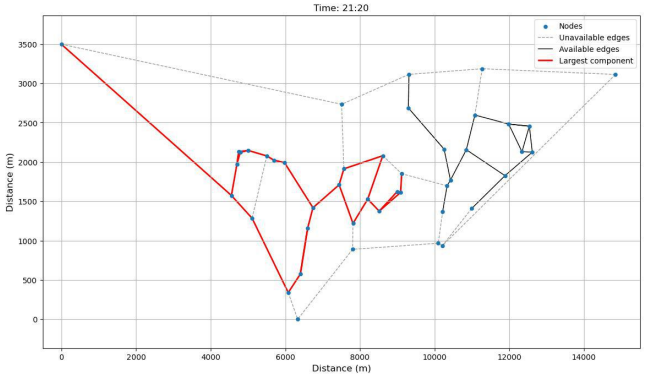
Time: 21:20
Nodes
Unavailable edges
Available edges
Largest component
Distance (m)
Distance (m)

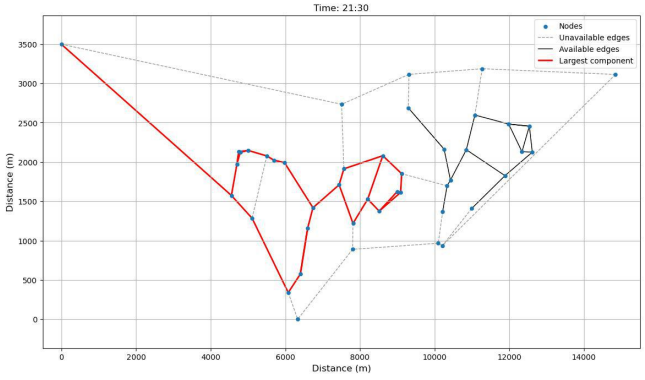
Time: 21:30
Nodes
Unavailable edges
Available edges
Largest component
Distance (m)
Distance (m)

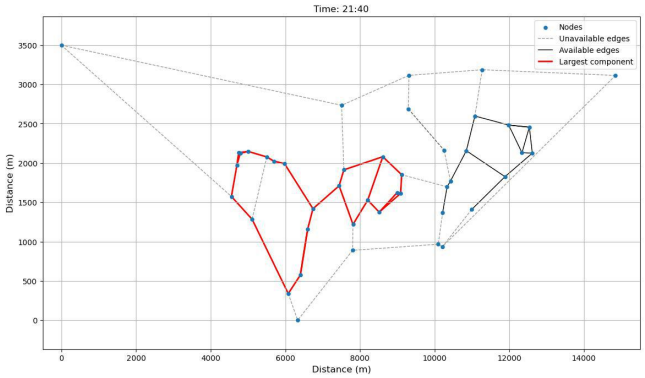
Time: 21:40
Nodes
Unavailable edges
Available edges
Largest component
Distance (m)
Distance (m)

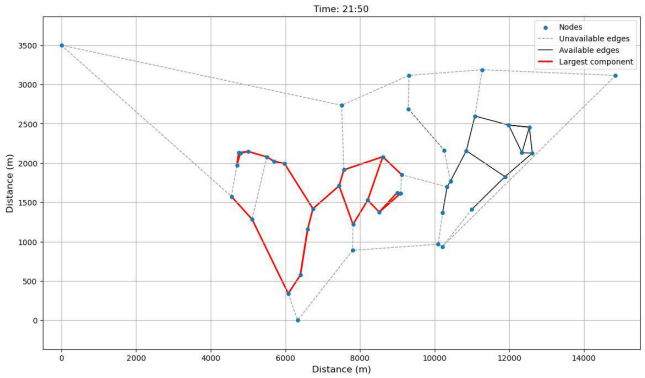
Time: 21:50
Nodes
Unavailable edges
Available edges
Largest component
Distance (m)
Distance (m)

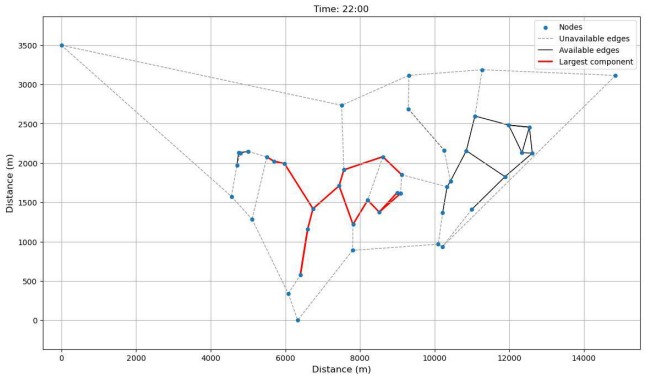
Time: 22:00
Nodes
Unavailable edges
Available edges
Largest component
Distance (m)
Distance (m)

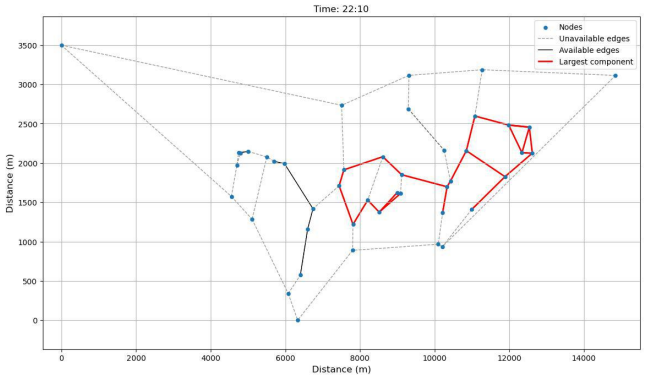
Time: 22:10
Nodes
Unavailable edges
Available edges
Largest component
Distance (m)
Distance (m)

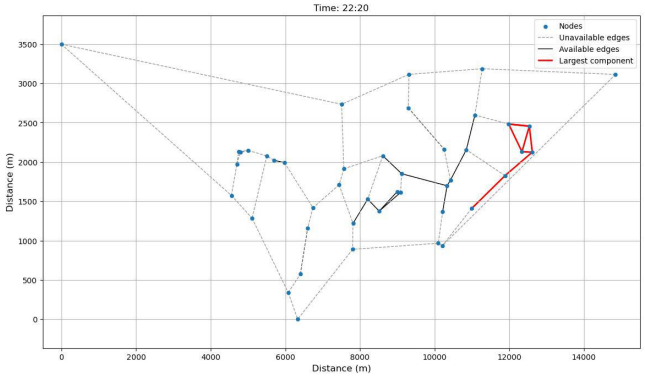
Time: 22:20
Nodes
Unavailable edges
Available edges
Largest component
Distance (m)
Distance (m)

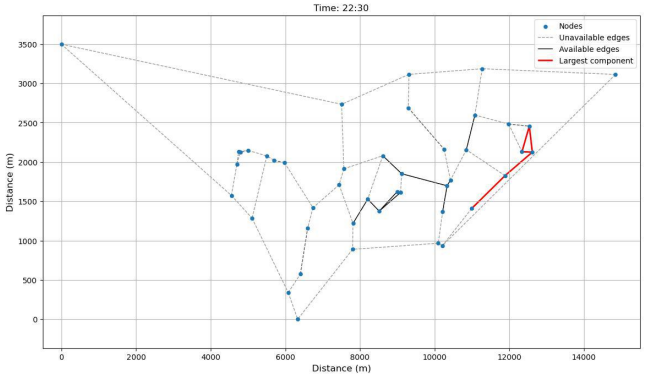
Time: 22:30
Nodes
Unavailable edges
Available edges
Largest component
Distance (m)
Distance (m)

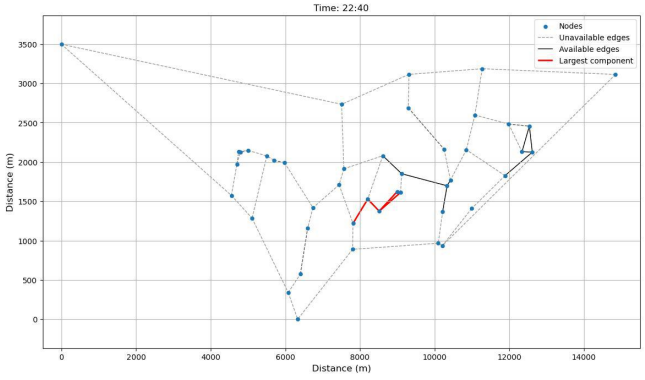
Time: 22:40
Nodes
Unavailable edges
Available edges
Largest component
Distance (m)
Distance (m)

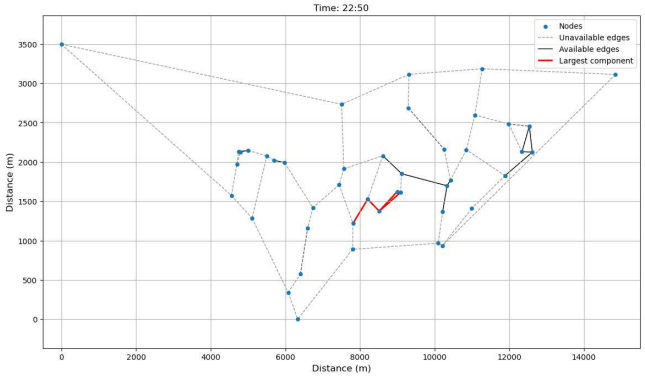
Time: 22:50
Nodes
Unavailable edges
Available edges
Largest component
Distance (m)
Distance (m)

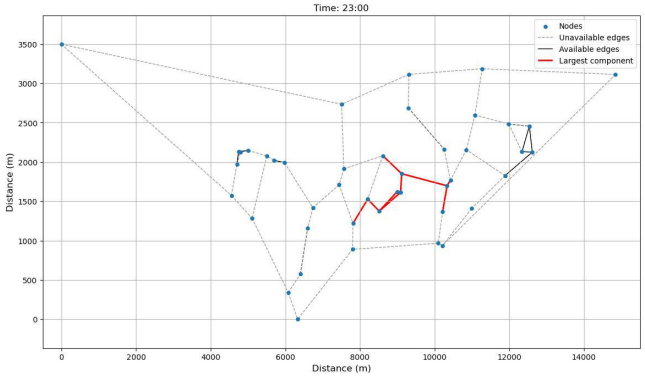
Time: 23:00
Nodes
Unavailable edges
Available edges
Largest component
Distance (m)
Distance (m)

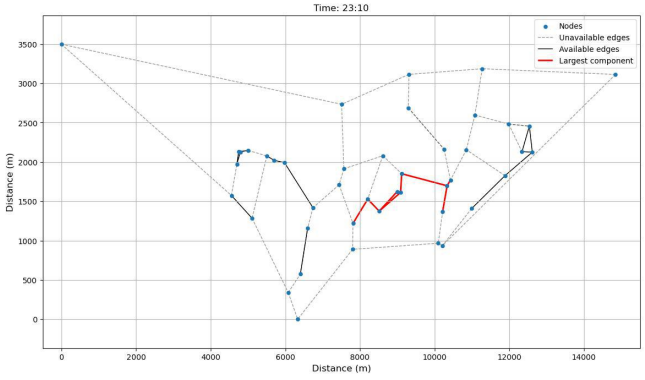
Time: 23:10
Nodes
Unavailable edges
Available edges
Largest component
Distance (m)
Distance (m)

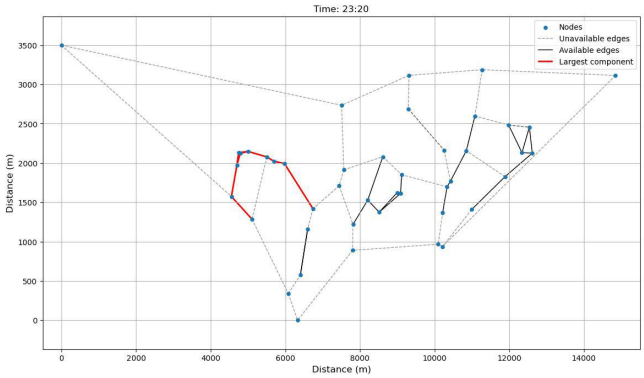
Time: 23:20
Nodes
Unavailable edges
Available edges
Largest component
Distance (m)
Distance (m)

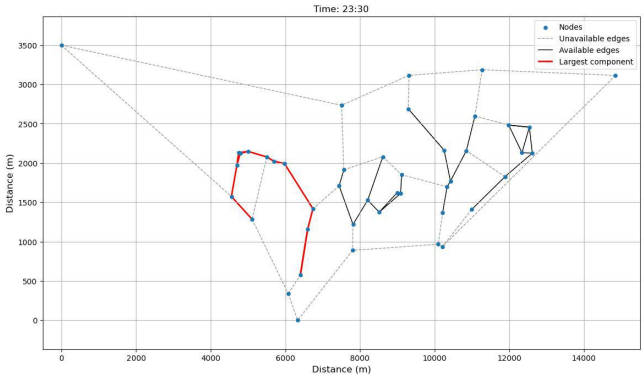
Time: 23:30
Nodes
Unavailable edges
Available edges
Largest component
Distance (m)
Distance (m)

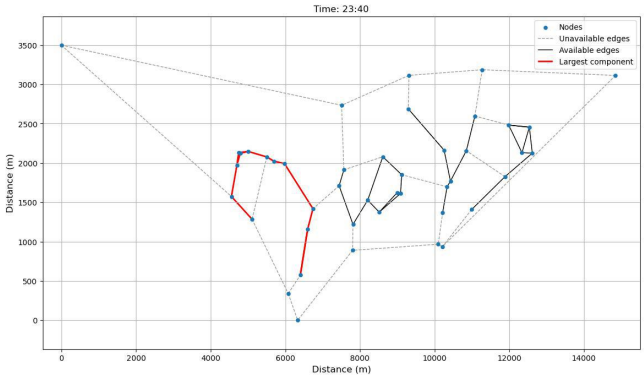
Time: 23:40
Nodes
Unavailable edges
Available edges
Largest component
Distance (m)
Distance (m)

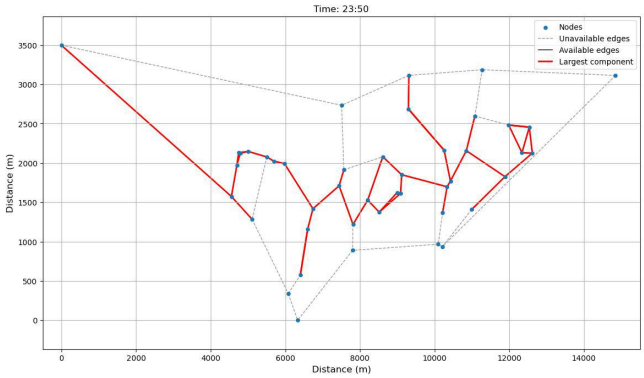
Time: 23:50
Nodes
Unavailable edges
Available edges
Largest component
Distance (m)
Distance (m)